Controlling Lead Release To Drinking Water: Impacts Of Iron Oxides, Complexing Species, Orthophosphate, And Lead Pipe Replacement

by

Benjamin F Trueman

Submitted in partial fulfilment of the requirements
for the degree of Doctor of Philosophy

at

Dalhousie University
Halifax, Nova Scotia
December 2017

Table of Contents

List Of Tables

List Of Figures

Abstract

This work explored various approaches to controlling lead exposure via drinking water: orthophosphate treatment, limiting complexing or adsorbing species in distributed water, and lead service line replacement (LSLR). As determined by residential sampling, full LSLR reduced water lead levels by 35 – 87% within one month, while partial LSLR was associated with a greater frequency of elevated lead even after six months (27% of 1st draw samples > 15 μg L^{-1} vs. 13% pre-replacement). Upstream iron corrosion was a significant factor in these observations: compared with lined distribution mains, lead levels 6 mo. post-replacement were higher by factors of 1.9 (full LSLR) and 4.8 (partial LSLR) at sites supplied by unlined (corroded) iron pipe. Upstream iron corrosion also accompanied an average increase in lead release of 96 μg L^{-1} from a model system. This effect may explain particularly elevated lead levels after partial LSLR and it may be attributed to adsorptive and electrochemical phenomena. Size-exclusion chromatography (SEC) data were consistent with mobilization of lead via adsorption to suspended iron (oxyhydr)oxides: colloidal/nanosize iron and lead were strongly correlated in point-of-use samples ($R^2_{average}$ = 0.96). Galvanic corrosion of lead by iron oxide minerals also increased lead release by a factor of 9.0 compared with uniform corrosion in the absence of iron. Orthophosphate immobilized lead oxidized in galvanic cells as insoluble hydroxypyromorphite ($Pb_5(PO_4)_3OH$) and in field studies, increasing the orthophosphate concentration from 0.5 to 1.0 mg PO_4 L^{-1} reduced lead release by 38% within 8 months. Humic acid, by contrast, mobilized lead oxidized in galvanic cells, increasing lead release by a factor of 9.3 compared with an organic-free electrolyte. This was attributed largely to complexation: SEC data were consistent with formation of a soluble lead-humate species. Polyphosphates may also increase lead solubility via complexation, and SEC may aid in understanding this phenomenon in the field. In a water system dosing polyphosphate, lead was present in a soluble SEC fraction strongly associated with phosphorus. In field samples collected from a separate system—where polyphosphate reverted almost entirely to orthophosphate—lead was instead present in a colloidal fraction associated with iron and natural organic matter.

List Of Abbreviations Used

LSL Lead service line

LSLR Lead service line replacement

NOM Natural organic matter

TOC Total organic carbon

SEC Size-exclusion chromatography

HPLC High-performance liquid chromatography

ICP-MS Inductively coupled plasma mass spectrometry

UV_{254} Ultraviolet absorbance at 254 nm

EPA Environmental Protection Agency

SD Standard deviation

IQR Interquartile range

cps counts per second

ppb parts per billion

AU Absorption unit

SNR Signal-to-noise ratio

HDPE High-density polyethylene

Acknowledgements

This thesis was written with help from colleagues, professors, and several organizations. First, I acknowledge the financial support provided by NSERC through the post-graduate scholarship program, through the CREATE: STEWARD scholarship program, and through the Industrial Research Chair in Water Quality and Treatment. My studies were also supported by a Nova Scotia graduate scholarship.

Second, I thank fellow students who have assisted me in completing the requirements of this degree. These include undergraduate students Dallys Serracin, Kyle Rauch, Everett Sneider, Hayden Estabrook, Reese Williams, Brett Penney, and Javier Locsin. Fellow graduate students Yamuna Vadasarukkai, Jordan Schmidt, and Dave Redden provided important feedback on manuscript drafts, and Greg Sweet and Matthew Harding supplied technical input to the work described in Chapters 4 and 5. Michael Brophy assisted with sampling described in Chapter 6.

Third, I recognize the technical and administrative support provided by post-doctoral fellows Drs. Yuri Park and Allison Mackie; lab technicians Heather Daurie, Elliott Wright, and Nicole Allward; Centre for Water Resources Studies staff Dr. Wendy Krkošek and Tarra Chartrand; Halifax Water employees Adam McKnight and Beth Lowe; and Dr. Paul Bishop in the mechanical engineering department at Dalhousie. My advisor, Dr. Graham Gagnon, provided guidance and encouragement at every stage, and my supervisory committee—Drs. Jennie Rand, Margaret Walsh, and George Jarjoura—supplied important feedback at committee meetings.

Finally, and more personally, Kelly Cameron has been a continued source of support and Dr. Lise Manchester of inspiration. A great deal of this work I owe to them.

Chapter 1 Introduction

1.1 Research Rationale And Objective

1.1.1 Health Effects Of Lead Exposure

Lead is a potent neurotoxin. Even at contemporary exposure levels, childhood exposure is associated with attention disorders[1] and life-long cognitive deficits.[2] Adult exposure is linked with hypertension,[3] renal dysfunction,[4] and cognitive decline.[5]

1.1.2 Lead Exposure Via Drinking Water

Lead in drinking water is correlated with lead in blood,[6] and drinking water sometimes represents the dominant exposure pathway.[7] The most important sources of lead are plumbing components: lead pipe,[8] galvanized iron pipe,[9] lead solder,[10] and brass fittings.[11]

1.1.3 Regulatory Environment

Due to human health risks, lead is regulated as a drinking water contaminant in many jurisdictions. In the U.S., the Lead and Copper Rule specifies an action level of 15 $\mu g\ L^{-1}$.[12] This threshold applies to first-draw regulatory compliance samples collected at the point of use following overnight stagnation. Health Canada has recently proposed a Maximum Acceptable Concentration of 5 $\mu g\ Pb\ L^{-1}$, applying either to 30-minute stagnant or random daytime samples collected from drinking water outlets.[13]

1.1.4 Controlling Lead Solubility With Orthophosphate

Lead forms several orthophosphate compounds with low solubility under typical distributed water conditions. Possibilities include hydroxypyromorphite ($Pb_5(PO_4)_3OH$), chloropyromorphite ($Pb_5(PO_4)_3Cl$), and tertiary lead phosphate ($Pb_3(PO_4)_2$).[14,15] Pyromorphites (hydroxyl- and chloro-) have been identified in lead pipe corrosion scale extracted from systems distributing phosphate-treated water.[14,15] Orthophosphate dosing has been effective in controlling lead solubility under some conditions (e.g., at low alkalinity) and less effective in other cases (e.g., at higher alkalinity and pH).[16]

1.1.5 Lead Service Line Replacement

Lead service lines—pipes linking distribution mains with premises plumbing—represent the most important source of lead in drinking water.[8] Replacing them is crucial to reducing lead levels. But joint ownership can impede full replacement, because lead service lines typically span the property line: often, the publicly owned section is replaced with copper and joined to the privately owned lead pipe left in place. Partial replacement of lead service lines can destabilize lead corrosion scale and can dramatically increase lead levels due to galvanic corrosion at the lead-copper junction.[17,18]

1.1.6 Potential Impacts Of Iron (Oxyhydr)Oxides On Lead Release

Corroded iron distribution mains represent a significant fraction of total pipe length within North American water systems.[19] Iron main corrosion scale is typically composed of magnetite (Fe_3O_4) and goethite (α-FeOOH) along with a wide range of secondary crystalline phases.[20] Iron scale releases iron (oxyhydr)oxide particles to distributed water, and these particles are detectable at the point of use.[21] Lead adsorbs readily to both magnetite and goethite;[22,23] during stagnation within a lead pipe, this may promote dissolution of the solubility-controlling lead phase by supressing activity of the lead cation in solution. Provided (oxyhydr)oxide particles remain in suspension—or are resuspended—adsorption of lead to iron mineral surfaces could increase total lead at the point of use.[24] Iron (oxyhydr)oxides may also corrode lead galvanically upon deposition within lead service lines. Although this phenomenon has not been confirmed in the field, several iron phases have been shown to support oxygen reduction.[25]

1.1.7 The Effect Of Complexing Species On Lead Solubility

Chemical species that form soluble complexes with lead may promote lead release from corrosion scale by maintaining undersaturated conditions.[26] Natural organic matter and polyphosphate represent two classes of complexing species that may be present in distributed water. When they are poorly removed during treatment, naturally occurring humic and fulvic acids may increase lead solubility.[27] Polyphosphate is used to control precipitation of iron and calcium, but polyphosphate may also increase lead release due to complexation.[26]

1.1.8 Thesis Objective

The objective of this thesis was to explore three primary strategies for controlling lead release to drinking water: (1) lead service line replacement, (2) orthophosphate treatment, (3) limiting the concentrations of complexing and adsorbing species in distributed water.

1.2 Organization Of Thesis

Chapters 2 – 6 were prepared as manuscripts for publication in peer-reviewed journals. They retain individual introduction and reference sections that provide a review of relevant literature. Chapter 7 contains the concluding remarks of the thesis. Supplementary information is included as a set of appendices. Routine water quality data (e.g., pH, temperature, alkalinity, turbidity) are included/summarized in the body of the thesis or in the appendices when they have direct relevance to the discussion but have otherwise been omitted.

1.3 References

(1) Nigg, J. T.; Knottnerus, G. M.; Martel, M. M.; Nikolas, M.; Cavanagh, K.; Karmaus, W.; Rappley, M. D. Low blood lead levels associated with clinically diagnosed attention-deficit/hyperactivity disorder and mediated by weak cognitive control. *Biol. Psychiatry* **2008**, *63* (3), 325-331.
(2) Reuben, A.; Caspi, A.; Belsky, D. W.; Broadbent, J.; Harrington, H.; Sugden, K.; Houts, R. M.; Ramrakha, S.; Poulton, R.; Moffitt, T. E. Association of Childhood Blood Lead Levels With Cognitive Function and Socioeconomic Status at Age 38 Years and With IQ Change and Socioeconomic Mobility Between Childhood and Adulthood. *J. Am. Med. Assoc.* **2017**, *317* (12), 1244-1251.
(3) Navas-Acien, A.; Guallar, E.; Silbergeld, E. K.; Rothenberg, S. J. Lead exposure and cardiovascular disease—a systematic review. *Environ. Health Perspect.* **2007**, *115* (3), 472-482.
(4) Loghman-Adham, M. Renal effects of environmental and occupational lead exposure. *Environ. Health Perspect.* **1997**, *105* (9), 928-938.
(5) Shih, R. A.; Hu, H.; Weisskopf, M. G.; Schwartz, B. S. Cumulative lead dose and cognitive function in adults: a review of studies that measured both blood lead and bone lead. *Environ. Health Perspect.* **2007**, *115* (3), 483-492.
(6) Fertmann, R.; Hentschel, S.; Dengler, D.; Janßen, U.; Lommel, A. Lead exposure by drinking water: an epidemiologial study in Hamburg, Germany. *Int. J. Hyg. Environ. Health* **2004**, *207* (3), 235−244.
(7) Edwards, M.; Triantafyllidou, S.; Best, D. Elevated blood lead in young children due to lead-contaminated drinking water: Washington, DC, 2001− 2004. *Environ. Sci. Technol.* **2009**, *43* (5), 1618−1623.
(8) Sandvig, A.; Kwan, P.; Kirmeyer, G.; Maynard, B.; Mast, D.; Trussell, R.; Trussell, S.; Cantor, A. F.; Prescott, A. *Contribution of Service Line and Plumbing Fixtures to Lead and Copper Rule Compliance Issues, 91229*; American Water Works Association Research Foundation and U.S. Environmental Protection Agency: Denver, CO, 2008.
(9) McFadden, M.; Giani, R.; Kwan, P.; Reiber, S. H. Contributions to drinking water lead from galvanized iron corrosion scales. *J. Am. Water Works Assoc.* **2011**, *103* (4), 76−89.
(10) Nguyen, C. K.; Stone, K. R.; Dudi, A.; Edwards, M. A. Corrosive microenvironments at lead solder surfaces arising from galvanic corrosion with copper pipe. *Environ. Sci. Technol.* **2010**, *44* (18), 7076-7081.

(11) Schock, M. R.; Neff, C. H. Trace metal contamination from brass fittings. *J. Am. Water Works Assoc.* **1988**, *80* (11), 47-56.
(12) Maximum contaminant level goals and national primary drinking water regulations for lead and copper. Final rule *Fed. Regist.*, **1991**, *56*, 26460.
(13) *Lead in Drinking Water*; Health Canada: Ottawa, Canada, 2016; http://www.healthycanadians.gc.ca/health-system-systeme-sante/consultations/lead-drinking-water-plomb-eau-potable/document-eng.php#purpose
(14) Schock, M. R.; Wagner, I.; Oliphant, R. J. Corrosion and Solubility of Lead in Drinking Water. In *Internal Corrosion of Water Distribution Systems*; AWWA Research Foundation: Denver, CO, 1996; pp 131−230.
(15) Schock, M. R.; Lytle, D. A.; Sandvig, A. M.; Clement, J.; Harmon, S. M. Replacing polyphosphate with silicate to solve lead, copper, and source water iron problems. *J. Am. Water Works Assoc.* **2005**, *97* (11), 84-93.
(16) Dodrill, D. M.; Edwards, M. Corrosion control on the basis of utility experience. *J. Am. Water Works Assoc.* **1995**, *87* (7), 74-85.
(17) Triantafyllidou, S.; Edwards, M. Galvanic corrosion after simulated small-scale partial lead service line replacements. *J. Am. Water Works Assoc.* **2011**, *103* (9), 85−99.
(18) Cartier, C.; Doré, E.; Laroche, L.; Nour, S.; Edwards, M.; Prévost, M. Impact of treatment on Pb release from full and partially replaced harvested lead service lines (LSLs). *Water Res.* **2013**, *47* (2), 661−671.
(19) McNeill, L. S.; Edwards, M. Iron pipe corrosion in distribution systems. *J. Am. Water Works Assoc.* **2001**, *93* (7), 88-100.
(20) Peng, C. Y., Korshin, G. V., Valentine, R. L., Hill, A. S., Friedman, M. J., Reiber, S. H. Characterization of elemental and structural composition of corrosion scales and deposits formed in drinking water distribution systems. *Water Res.* **2010**, *44* (15), 4570-4580.
(21) Senftle, F. E.; Thorpe, A. N.; Grant, J. R.; Barkatt, A. Superparamagnetic nanoparticles in tap water. *Water Res.* **2007**, *41* (13), 3005−3011.
(22) Eick, M. J.; Peak, J. D.; Brady, P. V.; Pesek, J. D. Kinetics of lead adsorption/desorption on goethite: residence time effect. *Soil Sci.* **1999**, *164* (1), 28-39.
(23) Liu, J. F.; Zhao, Z. S.; Jiang, G. B. Coating Fe_3O_4 magnetic nanoparticles with humic acid for high efficient removal of heavy metals in water. *Environ. Sci. Technol.* **2008**, *42* (18), 6949−6954.
(24) Masters, S.; Edwards, M. Increased lead in water associated with iron corrosion. *Environ. Eng. Sci.* **2015**, *32* (5), 361−369.
(25) Vago, E. R.; Calvo, E. J.; Stratmann, M. Electrocatalysis of oxygen reduction at well-defined iron oxide electrodes. *Electrochim. Acta* **1994**, *39* (11), 1655−1659.
(26) Holm, T. R.; Schock, M. R. Potential effects of polyphosphate products on lead solubility in plumbing systems. *J. Am. Water Works Assoc.* **1991**, 83 (7), 76-82.
(26) Korshin, G. V.; Ferguson, J. F.; Lancaster, A. N. Influence of natural organic matter on the morphology of corroding lead surfaces and behavior of lead-containing particles. *Water Res.* **2005**, *39*, 811−818.

Chapter 2 Evaluating The Effects Of Full And Partial Lead Service Line Replacement On Lead Levels In Drinking Water

This chapter is reprinted with permission from the following:

Trueman, B. F.; Camara, E.; Gagnon, G. A. Evaluating the effects of full and partial lead service line replacement on lead levels in drinking water. *Environ. Sci. Technol.* **2016**, *50* (14), 7389-7396. http://pubs.acs.org/doi/abs/10.1021/acs.est.6b01912

B.F.T. coordinated data collection, analyzed the data, wrote the paper, and prepared the figures.

2.1 Abstract

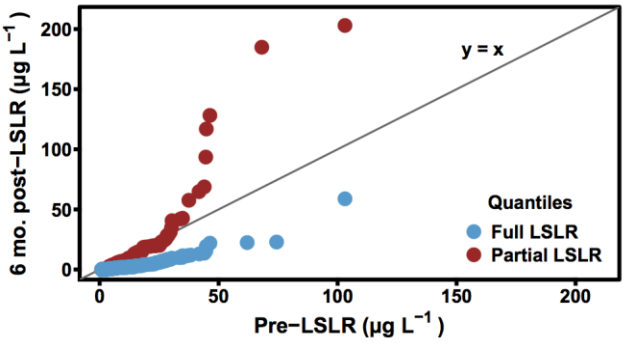

Figure 1 Full LSLR accompanied substantial reductions in lead levels while partial LSLR did not. Quantiles represent the distribution of lead levels before and 6 months after LSLR, separated according to replacement type (full or partial LSLR).

Lead service line replacement (LSLR) is an important strategy for reducing lead exposure via drinking water, but jurisdictional issues can sometimes interfere with full replacement of the lead line. The effects of full and partial LSLR on lead levels were assessed using 5 × 1-L sample profiles collected at more than 100 single-unit residences. Profiles comprised four sequential standing samples (L1− L4) and a free-flowing sample (L5) drawn after a 5 min flush of the outlet. At 45 sites with full lead service lines, 90th percentile lead levels in standing samples ranged from 16.4 to 44.5 µg L^{-1} (L1 and L4, respectively). In the free-flowing sample (L5), 90th percentile lead was 9.8 µg L^{-1}. Within 3 days, full LSLR had reduced L3−L5 lead levels by more than 50%, and within 1 month, lead levels were significantly lower in every liter of the sample profile. Conversely, partial LSLR more than doubled lead release from premises plumbing (L1, L2) in the

short term and did not consistently reduce it in the long term. Even 6 months after partial LSLR, 27% of first-draw lead levels were greater than 15 μg L^{-1} (the U.S. EPA action level), compared with 13% pre-replacement. (Graphical abstract provided as Figure 1.)

2.2 Introduction

Lead service lines (LSLs)—pipes connecting distribution mains to premises plumbing—were installed widely throughout the first half of the 20th century in North America and even occasionally up until the U.S. congressional ban in 1986.[1] In Canada, the National Plumbing Code permitted installation of LSLs until 1975.[2] At sites where they were installed, 50−75% of drinking water lead may be attributable to the LSL.[3]

Elevated lead in drinking water is a significant public health concern because water lead levels have been shown to correlate positively with blood lead levels.[4−7] Childhood blood lead levels below 10 μg dL^{-1}—and early childhood levels as low as 2 μg dL^{-1}—are linked with deficits in cognitive and academic skills.[8−10] Chronic lead exposure in adults is associated with renal dysfunction[11] and hypertension,[12] and lead is a known abortifacient.[13] Lead in U.S. drinking water is regulated under the Lead and Copper Rule,[14] which specifies an action level of 15 μg L^{-1} for the 90th percentile first-draw lead level. In Canada, the maximum acceptable concentration in a free-flowing sample is 10 μg L^{-1}, a benchmark that serves as the current Nova Scotia regulation.[15] Health Canada also recommends corrective action when the 90th percentile first-draw lead level exceeds 15 μg L^{-1}.[2,16]

Lead service line replacement (LSLR) is an important strategy for reducing lead exposure via drinking water, but joint (public−private) ownership can interfere with full replacement of the LSL. Typically, partial LSLR occurs when the public LSL is replaced with copper and joined to the private LSL left in place.[1] Partial LSLR can cause elevated lead in drinking water; disturbance of LSL corrosion scale during replacement may release high levels of lead for an extended period post-replacement. The lead−copper junction is a specific concern due to the potential for galvanic corrosion.[3,17] Elevated lead release owing to a galvanic lead−copper couple has been demonstrated in laboratory and pilot studies and is a likely factor in persistent high lead levels following partial LSLR.[18−21] Mineralogical evidence of galvanic corrosion in lead−copper and lead−brass

joints excavated from several distribution systems has also been reported, although when lead(IV) oxides were present lead was sometimes cathodic to brass and copper.[22]

Limited residential data suggest that partial LSLR may be associated—at best—with insignificant decreases in lead exposure risk. Partial LSLR did not reduce the risk of elevated blood lead among children in Washington, DC, and children living in homes with partial LSLs were more than three times as likely to have elevated blood lead (≥ 10 μg dL^{-1}) compared to those in homes constructed without LSLs.[23] Other residential studies—on five or fewer sites—have reported lead spikes following partial LSLR and modest or minimal subsequent reductions in lead release.[3,24,25] Camara *et al.*[26] reported greater lead release following partial LSLR relative to full LSLR but did not provide detailed pre- and post-replacement comparisons.

In 2011, an advisory board to the U.S. EPA concluded that existing data were inadequate to fully assess the effect of partial LSLR on drinking water lead levels.[27] The board found that the few studies available had limitations—including small sample sizes and limited follow-up sampling—but did conclude that partial LSLR could not be relied upon to reduce lead levels in the short term.[27]

The objective of this work was to estimate changes in lead exposure due to full and partial LSLR via a standardized profile sampling protocol. This protocol was implemented within a water system where Pb(II) compounds—in contrast to highly insoluble Pb(IV) oxides[28]—were presumed to dominate on the basis of distributed water quality and consistent observation of peak lead levels in samples representative of LSLs. Water distribution infrastructure was considered typical of older North American municipalities. The system was characterized by several risk factors for elevated lead release, including (1) a significant number of unlined cast iron distribution mains,[26] (2) distributed water with low alkalinity (20 mg L^{-1} as $CaCO_3$) and pH (7.3),[29] (3) a low orthophosphate residual (0.5 mg L^{-1} as PO_4^{3-}),[29] and (4) a chloride-to sulfate mass ratio above the critical threshold (0.5− 0.77) identified in previous work as a driver of galvanic corrosion.[30,31] This study contributes to the literature by helping to address limitations identified in the EPA advisory board report: small sample sizes and limited follow-up sampling.[27] This paper also expands on previous work,[26] with analysis of a much greater volume of data: 74 and 61 full and partial LSL replacements—including paired before-

and-after comparisons of 18 partial replacements—and 13 additional sites with LSLs.

2.3 Materials and Methods

2.3.1 Study Area

The study area comprised single-unit residences in Halifax, NS, Canada, that underwent LSLR between 2011 and 2015. In the event of partial LSLR, electrical continuity between lead and copper was expected but not verified. Following open-trench replacement, lead and copper were typically joined via a brass union as described in Clark *et al*.[32] Participating residences were predominantly older homes; in areas of widespread pre-1950 construction, thousands of LSLs are still in use.[26]

Table 1 Typical values for treated water quality parameters, pre-distribution.

Parameter	Typical value
Zinc ortho/polyphosphate (*as* PO_4^{3-})	0.5 mg L^{-1}
Alkalinity (*as* $CaCO_3$)	20.0 mg L^{-1}
Free chlorine	1.2 mg L^{-1}
Hardness (*as* $CaCO_3$)	12.0 mg L^{-1}
Total organic carbon	1.5 mg L^{-1}
pH	7.3
Chloride	9 mg L^{-1}
Sulfate	8.5 mg L^{-1}
Turbidity	0.06 NTU
Iron	<0.05 mg L^{-1}
Lead	<0.5 µg L^{-1}

Sample sites received distributed water from a treatment facility employing free chlorine disinfection; this facility is described in detail elsewhere.[33] Table 1 lists typical values in 2013−14 for key treated water quality parameters. No relevant changes in treatment were made over the study period.[34] Beginning in 2002, a blended zinc ortho/polyphosphate corrosion inhibitor (75% orthophosphate, 25% polyphosphate) was added at a treated water residual of 0.5 mg L^{-1} (as PO_4^{3-}).

2.3.2 Sample Collection

With direction from utility staff, residents collected profiles of four sequential 1 L standing samples from kitchen cold-water taps, beginning with the first draw following a minimum 6 h standing period. The 4 × 1-L sample profile (L1− L4) was followed by a 5

min flush of the outlet and subsequent collection of a fifth 1 L sample (L5). Profile sampling was carried out before and at four follow-up rounds (3 days, 1 month, 3 months, and 6 months) after LSLR. Residents were instructed to record exact stagnation times (median, 7 h, 40 min; minimum, 6 h; maximum, 23 h) and to sample at a constant flow rate. They were not instructed to remove faucet aerators prior to sample collection. Sampling instructions given to residents are provided in Appendix A, and data were excluded from analysis when these instructions were not followed.

A complete series of pre- and post-replacement sample profiles was not available for every residential site owing to incomplete resident participation. For this reason, sample sizes for before-and-after comparisons differ by follow-up round. However, lead levels at a given follow-up round were not significantly different at sites where residents participated at the next round compared to sites where they did not (two-tailed rank-sum tests, $\alpha = 0.05$). That is, reporting lead levels to residents did not appear to influence subsequent participation.

To assess the effect of water temperature on lead release, 13 × 1-L sample profiles were collected from kitchen cold-water taps at two other sites with LSLs (denoted sites A and B). These profiles were collected following a 5 min flush of the outlet and subsequent 30 min stagnation. The final liter of the 13 × 1-L profile was a free-flowing sample collected after a second 5 min flush of the outlet. Sample collection by the authors at these two sites, as opposed to residents, necessitated use of an alternate sampling protocol; however, differences in collection methods limit the comparisons that can be made between these two sites and the rest of the data. Samples were collected weekly over a period of 7 or 8 weeks (sites A and B, respectively). Water temperature was measured, using a glass thermometer, in the first and last liter of each profile from the second week on.

2.3.3 Analytical Methods

Total lead, copper, iron, and aluminum were measured by ICP-MS (Thermofisher X Series II) according to Standard Methods 3125 and 3030.[35] Reporting limits for Pb, Cu, Fe, and Al were 0.4, 0.7, 6.0, and 4.0 μg L^{-1}, respectively. Lead was also quantified in 0.45 μm filtrate for a subset of 386 sample profiles. Filtration via cellulose nitrate

membrane filters was generally performed within 2 days of sample collection (but prior to acid preservation), so results should be interpreted with care, as changes in speciation between collection and filtration cannot be ruled out. Loss of lead to sample bottles was 1.2% (SD 17.3%). This estimate was made by comparing total lead in 10 mL aliquots drawn from well-mixed 1 L samples before and 24 h after acid preservation of the entire sample (N = 82 sample profiles of 5 × 1-L).[36] Losses due to filtration were estimated at 21.1% (SD 0.4%) by comparing lead in 10 mL aliquots filtered once with lead in 10 mL aliquots filtered twice, using a new filter each time.[36] Polyethylene (HDPE) bottles and caps were immersed in ~2 M reagent grade HNO_3 for a minimum of 24 h and rinsed three times with ultrapure water prior to use. Method blanks were prepared by holding ultrapure water preserved with trace-metal grade HNO_3 in acid-washed bottles for 24 h at 4 °C.

2.3.4 Data Analysis

Lead levels at each of the four follow-up rounds after LSLR were compared with pre-replacement lead levels. Sample profiles collected after full LSLR were compared, using two-tailed rank-sum tests,[37] with an independent set of 45 profiles collected at sites with full LSLs. Differences between groups were multiplicative (i.e., best described as ratios), but a natural log transformation yielded additive differences (i.e., best described as constants). Changes in lead level were quantified using a Hodges−Lehmann estimator, c, where $c = \text{median}(y_i / x_j)$ for all $i = 1, ..., n$ and j = 1, ..., m. Variables x and y denote lead levels observed at m and n sites with full and fully replaced LSLs, respectively. The quantity c estimates the ratio of lead levels between the two groups, where $y = cx$.[38]

Sample profiles collected before and after partial LSLR were paired by address and compared using two-tailed signed rank tests by profile liter and follow-up round.[37] Natural log transformations were applied to the paired data to promote symmetry in the distribution of differences. Multiplicative differences in before-and-after replacement lead levels were also quantified using a Hodges−Lehmann estimator; details, though similar to those provided above, may be found elsewhere.[38] No control of the familywise error rate for multiple comparisons was employed.

2.4 Results And Discussion

2.4.1 Pre-Replacement Lead Levels

Lead and copper levels representing 5 × 1-L sample profiles collected at 45 sites with full LSLs are provided in Figure 2. Peak copper levels occurred in L1 (90th percentile: 151 µg L^{-1}) and peak lead levels in L4 (90th percentile: 44 µg L^{-1}). For single-unit residences, peak lead levels are often observed by L4 of the sample profile.[39] The higher median (11 µg L^{-1}) and increased variability in L3 lead levels (90th percentile: 29 µg L^{-1}) suggest that L3 stagnated at least partially within the LSL at some of the 45 sites. This is consistent with previous work, where Cartier *et al.*[40] estimated median (mean) premises plumbing volumes in 88 pre-1970 homes at 2.0 L (2.3 L). At sites with full LSLs, L1 significantly underestimated peak lead levels; in systems where lead(II) compounds form preferentially, lead in water that contacted the LSL during stagnation may be considerably higher than lead in the first-draw sample.[26,28,41]

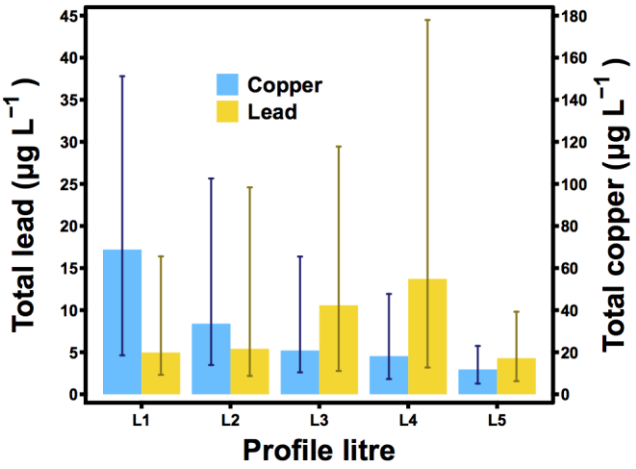

Figure 2 Median lead and copper levels in 5 × 1-L sample profiles collected at 45 sites with full LSLs. L5 is a 5 min flushed sample, and error bars represent the 10th and 90th percentiles.

Longer sample profiles (13 × 1-L) collected at two residential sites with LSLs (sites A and B, Figure 3) provide insight into the ability of the 5 × 1-L profile to estimate lead exposure. Plumbing configuration can be inferred by comparing lead and copper levels over each profile, although mixing among profile liters and the 5 min flush prior to stagnation (sites A and B only) may have influenced apparent plumbing volumes. Site A is a typical example of the single-unit residences that underwent LSLR (the large

apparent premises plumbing volume of 8− 9 L at site B is explained by sample collection from a second-level kitchen). The apparent volume of premises plumbing at site A was 2− 3 L.

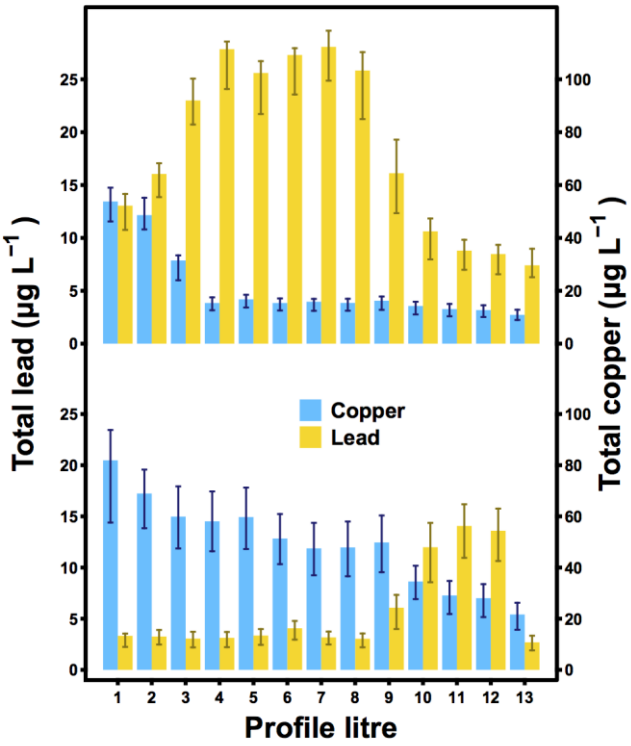

Figure 3 Median lead and copper in 13 × 1-L sample profiles collected at two sites. Site A (*top*) is a typical site with a full LSL, while the large apparent premises plumbing volume (8−9 L) at site B (*bottom*) is explained by sample collection from a second-level kitchen. Liter 13 is a 5 min flushed sample, and error bars represent the 10th and 90th percentiles.

Copper declined sharply after the first 2 liters and quickly approached the level of the flushed sample (L13, 10 µg L^{-1}). Peak lead levels were observed by L4, although L3− L9, or parts thereof, appear to have stagnated within the LSL. In light of LSL lead release observed at sites A and B following 30 min of stagnation (maximum 28 and 14 µg L^{-1}, respectively), the apparent LSL lead release at the 45 sites represented in Figure 2 was lower than expected (minimum 6 h stagnation, 90th percentile of 44 µg L^{-1} in L4). This implies that L4 may sometimes have fallen short of the LSL. Furthermore, while L4 does appear to have reached the LSL in at least some cases, it may not have reached the lead−copper junction at sites with partial LSLs, as sample profiles reported in previous

work have shown.[42] In some cases, 4 × 1-L standing sample profiles may only provide an indirect assessment of the effect of galvanic corrosion following partial LSLR.

2.4.2 Influence of Water Temperature

Pre-replacement profiles were collected in summer, and collection dates of the initial round had a July median. This introduces water temperature as a potential confounding variable. One-month follow-up collection dates had a September median, and on this interval the variation in water temperature is likely to have been low: the typical 5 min flushed sample temperature was 17.9 °C in July (this study) and 17.8 °C in October.[43] Comparisons between full and partial LSLR for the same follow-up round are also unlikely to have been strongly influenced by temperature. However, partial LSL profile collection dates for the 3- and 6-month follow-up rounds had December and April medians, respectively. Pre- and post-replacement comparisons on these intervals are subject to decreases in water temperature of approximately 10 °C: the typical 5 min flushed sample temperature in February was 7.2 °C.[43]

The effect of water temperature on lead release is complex: the positive effect of temperature on the rate of electrochemical reactions may be counterbalanced by the reduced solubility of lead minerals at higher temperatures, depending on the composition of corrosion scale.[44] Temperature effects also depend on whether the source of lead is premises plumbing, where seasonal variation is expected to be minimal, or LSLs, where variation is greater.[17] Previous work has shown that lead release can be temperature dependent,[40,45] and data from the 13 × 1-L profiles collected at sites A and B show that lead release was moderately-to-highly correlated with water temperature (R^2 = 0.46−0.98, average of 0.79, Table 10). Between 13 and 19 °C, a 1 °C increase in 5 min flushed sample temperature accompanied an average 1.1 μg L^{-1} increase in lead release from LSLs (Figure 36, Appendix A). Other seasonally varying water quality parameters, such as free chlorine residual, may also have influenced observed lead levels.

Water temperature was correlated with lead release from premises plumbing at sites A and B as well; this was likely a consequence of the short (30 min) stagnation time. More generally, lead release from premises plumbing does not often exhibit strong temperature dependence, provided that stagnation time is sufficient for standing water to

reach building temperatures (e.g., 6 h).[17] In a survey of 365 U.S. drinking water utilities, 90th percentile first draw lead levels—collected following a minimum 6 h stagnation—were not a function of season.[46] Within the present study area, first-draw lead levels (minimum 6 h stagnation, 34 residential sites) were no higher in October than in February.[43]

Owing to the effect of water temperature on lead release from LSLs, long-term (3 and 6 month) pre- and post-replacement comparisons were only interpreted for the portion of the sample profile least likely to have been influenced by temperature, L1 and L2. It is possible that, for sites with very small premises plumbing volumes, L2 lead levels were affected by temperature variation, but no significant drop in L2 lead levels from summer to winter was observed following partial LSLR (Table 2). For L3 and L4, however, decreasing water temperature likely contributed to—and may have been entirely responsible for—observed reductions in lead release.

2.4.3 Effect of Full LSL Replacement

For each profile liter and follow-up round, the fraction of pre-replacement lead remaining after LSLR was estimated (Table 2). Full LSLR reduced lead levels in every liter of the sample profile within 1 month. Before and after differences were multiplicative—not additive—meaning that sites with high lead levels pre-replacement tended to see greater reductions in lead post-replacement. For a given profile liter, a ratio of less than 1 signifies a reduction in lead over pre-replacement levels, and a ratio greater than 1 denotes an increase.

At sites that underwent full LSLR, public and private LSL sections were not often replaced on the same day, and a delay of several months was not uncommon. In many cases, the pre-replacement profile represented the partial LSL configuration. In order to properly evaluate the effect of full LSLR, lead levels after full replacement were compared, without pairing, against 45 sites with full LSLs; 41 of these 45 underwent partial LSLR only. Unpaired comparisons have the advantage of larger sample sizes, but they are expected to be less accurate when other sources of lead are present (e.g., in L1 and L2). A key benefit of pairwise comparisons is that they tend to account for variation due to uncontrolled factors (e.g., other sources of lead, variations in flow rate).[47]

Table 2 Estimated fraction of pre-replacement lead levels remaining after full and partial LSLR.

	Follow-up round	Litre 1	Litre 2	Litre 3	Litre 4	Flushed	No. of sites
Partial LSLR (paired)	3 d.	**2.89**[a]**	**2.45****	1.55	1.04	0.65	15
	1 mo.	**1.65****	1.26	1.15	1.22	0.61**	18
	3 mo.	1.24	0.86	0.54[b]	0.28[b]	0.24[b]	16
	6 mo.	1.04	0.57	0.31[b]	0.25[b]	0.17[b]	16
Full LSLR (unpaired)[c]	3 d.	1.04	0.85	0.38***	0.29***	0.22***	48
	1 mo.	0.65*	0.43***	0.20***	0.13***	0.13***	56
	3 mo.	0.62*	0.41***	0.16[b]	0.08[b]	0.09[b]	45
	6 mo.	0.60*	0.33***	0.10[b]	0.06[b]	0.07[b]	45

[a]*Statistical significance: * $p < 0.05$, ** $p < 0.01$, *** $p < 0.001$*
[b]Statistically significant, but likely to have been influenced by variation in water temperature
[c]Compared against an independent set of 45 sites with full LSLs

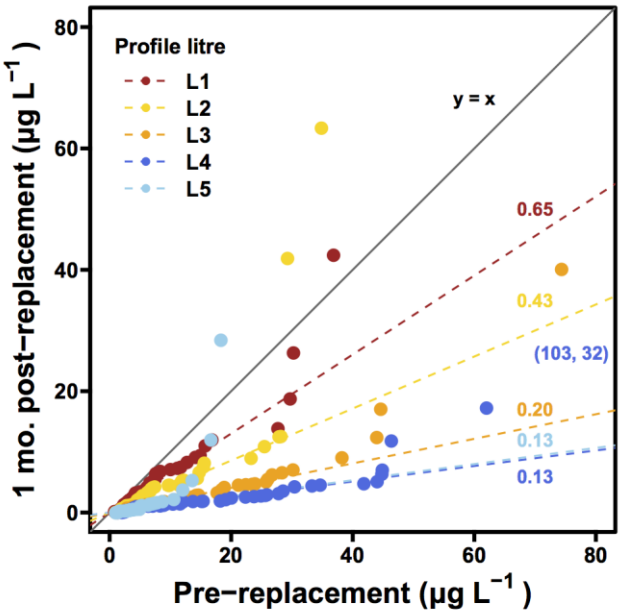

Figure 4 Lead levels (as distribution quantiles) before (45 sites) and 1 month after full LSLR (56 sites). Dashed lines (representing $y = cx$) are labeled by the corresponding c, where c is the estimated fraction of pre-replacement lead levels remaining at the 1-month follow-up. Points beyond the plot limits are represented as (x,y) coordinates.

Reductions in lead following full LSLR were almost immediate: lead levels in L3− L5 were less than half that of their pre-replacement counterparts at the 3-day follow-up (Table 2). One month after full replacement, lead release from premises plumbing (L1, L2) had dropped significantly as well. Distribution quantiles, representing before and after full LSLR comparisons at the 1-month follow-up, are provided in Figure 4.

Quantiles adhered well to the ratio estimates listed in Table 2, except in the upper extremes, where outliers occasionally deviated. One month post-replacement, 90th percentile lead levels ranged from 2 to 12 μg L^{-1} (L5 and L1, respectively), while pre-replacement 90th percentiles ranged from 10 to 44 μg L^{-1} (L5 and L4, respectively). Reductions in lead release from premises plumbing (L1, L2) may be attributed to gradual flushing of lead that had accumulated pre-replacement, as previous work has suggested.[3] Since premises plumbing upgrades were not performed in conjunction with LSLR, leaded solder and brass were not expected to have contributed to changes in lead release postreplacement. Accumulation of lead in premises plumbing may have been driven in part by adsorption to iron deposits or surfaces: as described elsewhere, colloidal lead (<0.45 μm) was strongly associated with colloidal iron at residential sites within the same water system.[36] Previous work has accounted for a correlation between iron and lead at the point of use with reference to the strong tendency for lead to adsorb to iron oxide deposits or galvanized iron plumbing.[42,48,49] Manganese deposits in premises plumbing have also been implicated as a sink for—and subsequent source of—lead in drinking water.[50]

2.4.4 Effect of Partial LSL Replacement

Partial LSLR more than doubled premises plumbing (L1, L2) lead levels at the 3-day follow-up (Table 2). One month post-replacement, L1 was still elevated by more than 60%, while subsequent standing sample lead levels (L2−L4) had not changed significantly relative to their pre-replacement counterparts. Even 6 months after partial LSLR, no significant reductions in L1 or L2 lead levels were observed. Reductions in L3 and L4 lead release at the 3- and 6-month follow-up rounds were expected to have been enhanced by—and could have been entirely due to—decreasing water temperature. (Increases, relative to pre-replacement, in LSL lead release at 3 and 6 months were sometimes observed despite temperature differences; see Figure 37, Appendix A) Applying a 1.1 μg L^{-1} °C^{-1} correction (described in Appendix A)—based on expected water temperature differences—eliminated statistically significant reductions in L3 and L4 lead release that would otherwise have been attributed to partial LSLR.

In contrast to standing samples, L5 lead levels were not significantly different

from their pre-replacement counterparts at the 3-day follow-up (90th percentile of 14 µg L^{-1}) and were significantly lower at the 1-month follow-up (90th percentile of 6 µg L^{-1}). However, data from this study do not support 5 min of flushing as a strategy for protecting against the short-term effects of partial LSLR: 9% of L5 samples were greater than 15 µ g L^{-1} at the 3-day follow-up compared with just 4% pre-replacement. Moreover, an L5 sample collected 3 days post-replacement measured 230 µg L^{-1}.

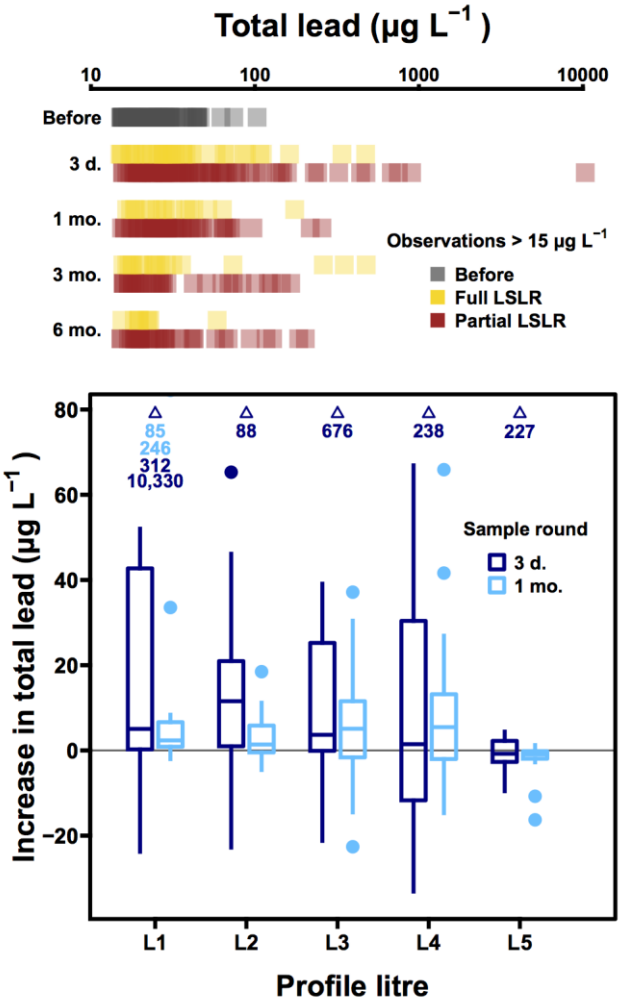

Figure 5 (*Top*) Lead levels greater than 15 µg L^{-1} over the 5 × 1-L sample profile, pre-LSLR, and at four follow-up rounds after full and partial LSLR. (*Bottom*) Box-and-whisker plots of the increase in total lead (pairwise differences) at the 3-day and 1-month follow-up rounds after partial LSLR, relative to pre-replacement. Boxes enclose the interquartile range (IQR), medians divide the boxes, and whiskers extend from the upper and lower quartile to the most extreme value within 1.5 times the IQR. Increases in lead beyond the plot limits are annotated.

Changes in lead release due to partial LSLR are illustrated in Figure 5 (*bottom*),

which displays the distribution of pairwise differences in lead release (after - before), grouped by profile liter for the first two follow-up rounds (3 days and 1 month). Positive differences correspond to an increase in lead release post-replacement, and negative differences correspond to a decrease (sample sizes are provided in Table 2). Increased lead release following partial LSLR is evident, especially at the 3-day follow-up. On this interval, more than a quarter of sites saw increases of 20 μg L^{-1} in at least one standing sample (L1− L4). At the 1-month interval, L3 and/or L4 lead increased by 10 μg L^{-1} at more than a quarter of sites.

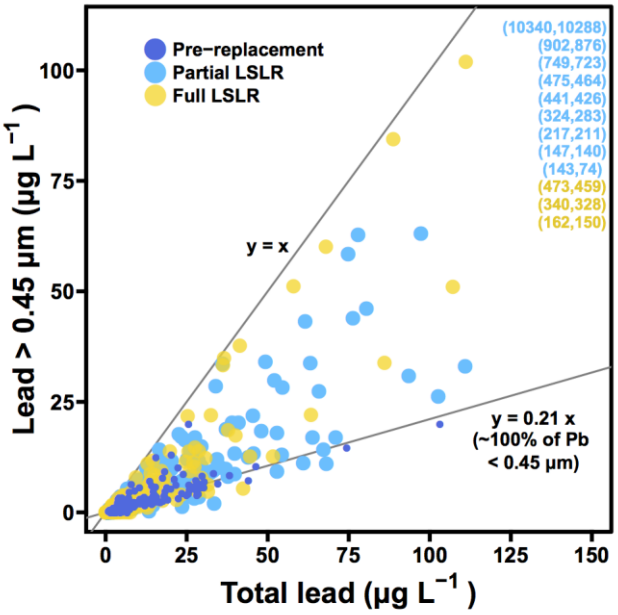

Figure 6 Particulate (>0.45 μm) lead release as a function of total lead, pre-replacement and at the first two follow-up rounds (72 h and 1 mo post-replacement). Points beyond the plot limits are represented as (*x*,*y*) coordinates and the line *y* = 0.21*x* represents the estimated loss due to 0.45 μm filtration (~100% of lead <0.45 μm).

Increased lead release to L1 and L2 can likely be attributed to accumulation of particulate lead in premises plumbing following replacement-induced destabilization of LSL corrosion scale.[3] Galvanic corrosion at the lead−copper junction has been linked with elevated particulate lead release as well.[18−21] Indeed, occurrence of particulate lead (>0.45 μm) was more frequent following partial (relative to full) LSLR (Figure 6). At the 3-day follow-up, 11 and 26% of samples collected following full and partial LSLR, respectively, had more than 10 μg L^{-1} of particulate lead (compared to 3% pre-

replacement). Elevated lead release in general was dominated by particles, and at higher total lead levels, the particulate fraction was larger, approaching unity at lead levels higher than approximately 100 μg L^{-1} (Figure 6). Available data suggest that lead in 0.45 μm filtrate was dominated by colloidal particles (0.05− 0.45 μm).[36]

2.4.5 Post-Replacement Lead Exposure

Serious spikes in lead sometimes followed LSLR but were much more frequent following partial LSLR. Elevated lead levels after partial replacement have been reported previously as well.[3,24,25,51] In this work, trends in post-replacement lead release diverged immediately according to replacement type. At sites with full LSLs (pre-replacement), 29% of standing sample (L1− L4) lead levels were greater than 15 μg L^{-1} (45 sites). Three days after partial LSLR, 45% of L1−L4 lead levels were greater than 15 μg L^{-1} (34 sites), while 3 days after full LSLR, just 14% were greater (48 sites). Lead levels exceeding 15 μg L^{-1}, by follow-up round and LSL configuration, are displayed in Figure 5 (*top*). This threshold represents a concentration above which the Centers for Disease Control and Prevention considers drinking water unsuitable for consumption by children and pregnant women.[52] At the 3-day follow-up, three observations also exceeded the U.S. Consumer Product Safety Commission's acute exposure level for children (700 μg L^{-1}, based on a 250 mL intake)[53]—all at sites with partial LSLs. These extreme lead levels, including a sample with 10,340 μg L^{-1}, were associated with premises plumbing (L1 or L2). High-velocity, multiple outlet flushing post-replacement is a possible strategy for protecting against these short-term spikes in lead.[51]

Unusually high lead levels were also observed at several sites following full LSLR (Figure 5, *top*). The highest observations at 1 and 6 months were both first-draw samples, and the highest four observations at 3 months represent standing samples (L1−L4) collected at a single site. Lead in these four samples was more than 90% particulate (>0.45 μm). These samples were also unusually rich in particulate iron, copper, and aluminum, suggesting that the source was corrosion scale within premises plumbing that had accumulated multiple contaminants over time. In the case of full LSLR, public and private LSL replacements were not often performed simultaneously, and disturbances associated with two replacements—as well as possible galvanic

corrosion in the interim—may have contributed to elevated lead release and accumulation of particulate lead within premises plumbing. While full LSLR was associated with substantial reductions in lead levels, staggered replacements may have caused the true benefit of full replacement to be underestimated.

In the long term, elevated lead was observed more often at sites with partial LSLs than at sites with either full LSLs or with full copper service lines (post-LSLR). At the 6-month follow-up after partial LSLR, 22% of premises plumbing (L1, L2) lead levels—and 30% of service line lead levels (L3, L4)—were greater than 15 μg L^{-1} (30 sites). At sites with copper service lines, 7% of L1 and L2 samples—and none of the L3 or L4 samples—were greater than 15 μg L^{-1} (45 sites). The frequency of high (>15 μg L^{-1}) L1, L2 lead levels was substantially greater—even 6 months post-replacement—at sites with partial LSLs relative to sites with full LSLs (22 vs. 16% respectively). Moreover, the fraction of first-draw samples greater than 15 μg L^{-1} at 6 months was double the pre-replacement fraction (27 vs. 13%). Despite the possibility that the sample profile did not reach the lead−copper junction—and that the flow regime did not represent a worst-case scenario—these data captured the greater tendency, identified in previous work,[19,20] for elevated lead at sites with partial LSLs compared to sites with full LSLs.

2.4.6 Implications for Controlling Lead In Drinking Water

This study used a standardized profile sampling protocol to assess the effect of full and partial LSLR on lead release to drinking water. The strength of this work was the comparatively large volume of data collected pre- and post-replacement, and the principal limitations were the inevitable uncertainties associated with sample collection by residents and the lack of information on plumbing volumes and configurations that limits a mechanistic understanding of the results.

Full LSLR reduced service line (L3, L4) and 5 min flushed sample (L5) lead levels within 3 days. At 1 month, full replacement had caused lead level reductions in every liter of the sample profile. Partial LSLR, on the other hand, caused substantial short-term increases in premises plumbing (L1, L2) lead levels and did not significantly reduce L1 and L2 lead levels within 6 months. Furthermore, first-draw lead levels were greater than 15 μg L^{-1} at a considerably higher frequency than at sites with full LSLs,

even 6 months post-replacement. This finding could have important implications in jurisdictions where drinking water lead is regulated based on the first-draw sample.

This study generated a considerable volume of data corroborating previous work that showed (1) full LSLR—in addition to removing the primary source of lead—is effective for reducing lead release from premises plumbing, (2) partial LSLR dramatically increases lead at the point of use in the short term, (3) partial LSLR may be worse than leaving the LSL intact due to the potential for elevated lead release in the long term, (4) in Pb(II)-dominated water systems, first-draw lead levels are likely to underestimate lead exposure at residences with LSLs, and (5) lead release from LSLs is sometimes strongly influenced by water temperature.

The short-term elevated lead levels that sometimes followed partial LSLR are a serious concern: some were high enough to pose acute health risks. High-velocity flushing of outlets,[51] use of pipe-cutting methods that minimize disturbances to LSLs,[3] and point-of-use lead removal[54] are potential strategies that could be implemented to reduce health risks associated with this mode of exposure. In assessing the effects of full and partial LSLR, the potential for dramatically elevated lead levels post-replacement is an important consideration. While the rapid reductions in lead that typically follow full LSLR outweigh the risk of short term disturbance-induced spikes, the modest long term benefits from partial LSLR described in some previous work[24,25] may be overshadowed by the greater risk of elevated lead in both the short- and long-term.

2.5 References

(1) Triantafyllidou, S.; Edwards, M. Lead (Pb) in tap water and in blood: implications for lead exposure in the United States. *Crit. Rev. Environ. Sci. Technol.* **2012**, *42* (13), 1297−1352.
(2) *Guidance on Controlling Corrosion in Drinking Water Distribution Systems*; Catalogue H128-1/09-595E; Health Canada: Ottawa, Canada, 2009; http://www.hcsc.gc.ca/ewh-semt/alt_formats/hecs-sesc/pdf/pubs/water-eau/corrosion/corrosion-eng.pdf.
(3) Sandvig, A.; Kwan, P.; Kirmeyer, G.; Maynard, B.; Mast, D.; Trussell, R.; Trussell, S.; Cantor, A. F.; Prescott, A. *Contribution of Service Line and Plumbing Fixtures to Lead and Copper Rule Compliance Issues, 91229*; American Water Works Association Research Foundation and U.S. Environmental Protection Agency: Denver, CO, 2008.
(4) Watt, G. C.; Britton, A.; Gilmour, W. H.; Moore, M. R.; Murray, G. D.; Robertson, S. J.; Womersley, J. Is lead in tap water still a public health problem? An observational study in Glasgow. *Br. Med. J.* **1996**, *313* (7063), 979−981.
(5) Watt, G. C. M.; Britton, A.; Gilmour, H. G.; Moore, M. R.; Murray, G. D.; Robertson, S. J. Public health implications of new guidelines for lead in drinking water: a case study in an area with historically high water lead levels. *Food Chem. Toxicol.* **2000**, *38*, S73−S79.
(6) Fertmann, R.; Hentschel, S.; Dengler, D.; Janßen, U.; Lommel, A. Lead exposure by drinking water: an epidemiologial study in Hamburg, Germany. *Int. J. Hyg. Environ. Health* **2004**, *207* (3), 235−244.

(7) Edwards, M.; Triantafyllidou, S.; Best, D. Elevated blood lead in young children due to lead-contaminated drinking water: Washington, DC, 2001− 2004. *Environ. Sci. Technol.* **2009**, *43* (5), 1618−1623.
(8) Lanphear, B. P.; Dietrich, K.; Auinger, P.; Cox, C. Cognitive deficits associated with blood lead concentrations <10 microg/dL in US children and adolescents. *Public Health Rep.* **2000**, *115* (6), 521−529.
(9) Canfield, R. L.; Henderson, C. R.; Cory-Slechta, D. A.; Cox, C.; Jusko, T. A.; Lanphear, B. P. Intellectual Impairment in Children with Blood Lead Concentrations below 10 μg per Deciliter. *N. Engl. J. Med.* **2003**, *348* (16), 1517−26.
(10) Miranda, M. L.; Kim, D.; Galeano, M. A. O.; Paul, C. J.; Hull, A. P.; Morgan, S. P. The relationship between early childhood blood lead levels and performance on end-of grade tests. *Environ. Health Perspect.* **2007**, *115* (8), 1242−1247.
(11) Loghman-Adham, M. Renal effects of environmental and occupational lead exposure. *Environ. Health Perspect.* **1997**, *105* (9), 928−938.
(12) Navas-Acien, A.; Guallar, E.; Silbergeld, E. K.; Rothenberg, S. J. Lead exposure and cardiovascular disease–A systematic review. *Environ. Health Perspect.* **2007**, *115* (3), 472−482.
(13) Edwards, M. Fetal death and reduced birth rates associated with exposure to lead contaminated drinking water. *Environ. Sci. Technol.* **2014**, *48* (1), 739−746.
(14) Maximum contaminant level goals and national primary drinking water regulations for lead and copper. Final rule *Fed. Regist.*, **1991**, *56*, 26460
(15) *A Guide to Assist Nova Scotia Municipal Water Works Prepare Annual Sampling Plans*; Nova Scotia Environment: Halifax, Canada, 2010; https://www.novascotia.ca/nse/water/docs/GuideToAnnualSamplingPlans.pdf.
(16) *Guidelines for Canadian Drinking Water Quality—Summary Table*; Health Canada, Water, Air and Climate Change Bureau, Healthy Environments and Consumer Safety Branch: Ottawa, Canada, 2012; http://www.hc-sc.gc.ca/ewh-semt/pubs/water-eau/sum_guideres_recom/index-eng.php.
(17) Britton, A.; Richards, W. N. Factors Influencing Plumbosolvency in Scotland. *J. Inst. Water Eng. Sci.* **1981**, *35* (5), 349−364.
(18) Triantafyllidou, S.; Edwards, M. Galvanic corrosion after simulated small-scale partial lead service line replacements. *J. Am. Water Works Assoc.* **2011**, *103* (9), 85−99.
(19) Cartier, C.; Arnold, R. B.; Triantafyllidou, S.; Prevost, M.; Edwards, M. Effect of flow rate and lead/copper pipe sequence on lead release from service lines. *Water Res.* **2012**, *46* (13), 4142−4152.
(20) Cartier, C.; Doré, E.; Laroche, L.; Nour, S.; Edwards, M.; Prévost, M. Impact of treatment on Pb release from full and partially replaced harvested lead service lines (LSLs). *Water Res.* **2013**, *47* (2), 661−671.
(21) Wang, Y.; Jing, H.; Mehta, V.; Welter, G. J.; Giammar, D. E. Impact of galvanic corrosion on lead release from aged lead service lines. *Water Res.* **2012**, *46*, 5049−5060.
(22) DeSantis, M. K.; Welch, M.; Shock, M. Mineralogical evidence of galvanic corrosion in domestic drinking water pipes. In *Proceedings of the 2009 AWWA Water Quality Technology Conference*; AWWA, 2009.
(23) Brown, M. J.; Raymond, J.; Homa, D.; Kennedy, C.; Sinks, T. Association between children's blood lead levels, lead service lines, and water disinfection, Washington, DC, 1998−2006. *Environ. Res.* **2011**, *111* (1), 67−74.
(24) Swertfeger, J.; Hartman, D. J.; Shrive, C.; Metz, D. H.; DeMarco, J. Water quality effects of partial lead line replacement. In *Proceedings of the 2006 AWWA Annual Conference*; AWWA, 2006.
(25) Muylwyk, Q.; Gilks, J.; Suffoletta, V.; Olesiuk, J. Lead occurrence and the impact of LSL replacement in a well buffered groundwater. In *Proceedings of the 2009 AWWA Water Quality Technology Conference*; AWWA, 2009.
(26) Camara, E.; Montreuil, K. R.; Knowles, A. K.; Gagnon, G. A. Role of the water main in lead service line replacement: A utility case study. *J. Am. Water Works Assoc.* **2013**, *105* (8), E423−E431.
(27) *Science Advisory Board Evaluation of the Effectiveness of Partial Lead Service Line Replacements*; EPA-SAB-11e015; US Environmental Protection Agency (US EPA): Washington, DC, 2011; https://www.epa.gov/sites/production/files/2015-09/documents/sab_evaluation_partial_lead_service_lines_epa-sab-11-015.pdf.
(28) Triantafyllidou, S.; Schock, M. R.; DeSantis, M. K.; White, C. Low contribution of PbO_2-coated lead service lines to water lead contamination at the tap. *Environ. Sci. Technol.* **2015**, *49* (6), 3746−3754.
(29) Dodrill, D. M.; Edwards, M. Corrosion control on the basis of utility experience. *J. Am. Water Works*

Assoc. **1995**, *87* (7), 74−85.
(30) Edwards, M.; Triantafyllidou, S. Chloride-to-sulfate mass ratio and lead leaching to water. *J. Am. Water Works Assoc.* **2007**, *99* (7), 96−109.
(31) Nguyen, C. K.; Clark, B. N.; Stone, K. R.; Edwards, M. A. Role of chloride, sulfate, and alkalinity on galvanic lead corrosion. *Corrosion* **2011**, *67* (6), 065005-1−065005-9.
(32) Clark, B.; Cartier, C.; St. Clair, J.; Triantafyllidou, S.; Prévost, M.; Edwards, M. Effect of connection type on galvanic corrosion between lead and copper pipes. *J. Am. Water Works Assoc.* **2013**, *105* (10), E576−E586.
(33) Stoddart, A. K.; Gagnon, G. A. Full-scale prechlorine removal: impact on filter performance and water quality. *J. Am. Water Works Assoc.* **2015**, *107* (12), E638−E647.
(34) *2013/2014 Annual Report*; Halifax Regional Water Comission: Halifax, Canada, 2014; http://www.halifax.ca/hrwc/documents/AnnualReportFinal-2014.pdf.
(35) American Public Health Association, American Waterworks Association, Water Pollution Control Federation. *Standard Methods For the Examination of Water and Wastewater*, 22nd ed.; American Public Heath Association: Washington, DC, 2012.
(36) Trueman, B. F.; Gagnon, G. A. A new analytical approach to understanding nanoscale lead-iron interactions in drinking water distribution systems. *J. Hazard. Mater.* **2016**, *311*, 151−157.
(37) *R: A language and environment for statistical computing*; R Foundation for Statistical Computing: Vienna, Austria, 2014; https://www.r-project.org.
(38) Helsel, D. R.; Hirsch, R. M. *Statistical Methods in Water Resources*; Elsevier: Amsterdam, 1992.
(39) Desmarais, M.; Trueman, B.; Wilson, P.; Huggins, D.; Swertfeger, J.; Deshommes, E.; Prévost, M. Impact of partial lead service line replacements on water quality: Lead profiling sampling results in 6 North American utilities. In *Proceedings of the 2015 AWWA Water Quality Technology Conference*; AWWA, 2015.
(40) Cartier, C.; Laroche, L.; Deshommes, E.; Nour, S.; Richard, G.; Edwards, M.; Prévost, M. Investigating dissolved lead at the tap using various sampling protocols. *J. Am. Water Works Assoc.* **2011**, *103* (3), 55−67.
(41) Del Toral, M. A.; Porter, A.; Schock, M. R. Detection and evaluation of elevated lead release from service lines: a field study. *Environ. Sci. Technol.* **2013**, *47* (16), 9300−9307.
(42) McFadden, M.; Giani, R.; Kwan, P.; Reiber, S. H. Contributions to drinking water lead from galvanized iron corrosion scales. *J. Am. Water Works Assoc.* **2011**, *103* (4), 76−89.
(43) McIlwain, B. Investigating sources of elevated lead in drinking water. M.A.Sc. Dissertation, Dalhousie University, Halifax, Canada, 2013.
(44) Schock, M. R. Causes of temporal variability of lead in domestic plumbing systems. *Environ. Monit. Assess.* **1990**, *15* (1), 59−82.
(45) Masters, S.; Welter, G. J.; Edwards, M. A. Seasonal variations in lead release to potable water. *Environ. Sci. Technol.* **2016**, *50*, 5269−5277.
(46) Dodrill, D. M.; Edwards, M. Corrosion control on the basis of utility experience. *J. Am. Water Works Assoc.* **1995**, *87* (7), 74−85.
(47) Berthouex, P. M., Brown, L. C. *Statistics for Environmental Engineers*; CRC Press: Boca Raton, FL, 2002.
(48) Masters, S.; Edwards, M. Increased lead in water associated with iron corrosion. *Environ. Eng. Sci.* **2015**, *32* (5), 361−369.
(49) Deshommes, E.; Laroche, L.; Nour, S.; Cartier, C.; Prévost, M. Source and occurrence of particulate lead in tap water. *Water Res.* **2010**, *44* (12), 3734−3744.
(50) Schock, M. R.; Cantor, A. F.; Triantafyllidou, S.; Desantis, M. K.; Scheckel, K. G. Importance of pipe deposits to Lead and Copper Rule compliance. *J. Am. Water Works Assoc.* **2014**, *106* (7), E336−E349.
(51) Brown, R. A.; Cornwell, D. A. High-velocity household and service line flushing following LSL replacement. *J. Am. Water Works Assoc.* **2015**, *107* (3), E140−E151.
(52) *Lead tips: Sources of lead in water*; Centers for Disease Control and Prevention: Atlanta, GA, 2010; http://www.cdc.gov/nceh/lead/tips/water.htm.
(53) Triantafyllidou, S.; Edwards, M. Lead (Pb) in tap water and in blood: Implications for lead exposure in the United States. *Crit. Rev. Environ. Sci. Technol.* **2012**, *42* (13), 1297−1352.
(54) Deshommes, E.; Zhang, Y.; Gendron, K.; Sauvé, S.; Edwards, M.; Nour, S.; Prévost, M. Lead removal from tap water using POU devices. *J. Am. Water Works Assoc.* **2010**, *102* (10), 91−105.

Chapter 3 A New Analytical Approach To Understanding Nanoscale Lead-Iron Interactions In Drinking Water Distribution Systems

This chapter is reprinted with permission from the following:

Trueman, B. F.; Gagnon, G. A. A new analytical approach to understanding nanoscale lead-iron interactions in drinking water distribution systems. *J. Hazard. Mater.* **2016**, *311*, 151-157. https://doi.org/10.1016/j.jhazmat.2016.03.001

B.F.T. developed the method, collected and analyzed the data, wrote the paper, and prepared the figures.

3.1 Abstract

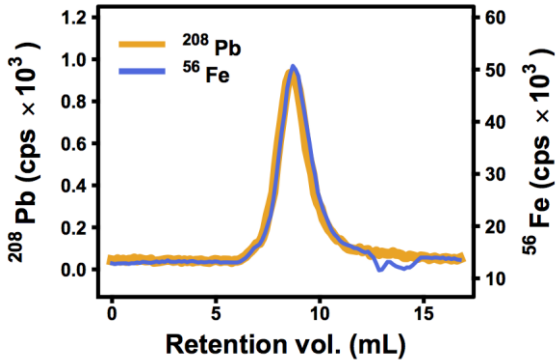

Figure 7 ^{56}Fe and ^{208}Pb elution profiles were highly correlated in point-of-use drinking water separations.

High levels of iron in distributed drinking water often accompany elevated lead release from lead service lines and other plumbing. Lead-iron interactions in drinking water distribution systems are hypothesized to be the result of adsorption and transport of lead by iron oxide particles. This mechanism was explored using point-of-use drinking water samples characterized by size exclusion chromatography with UV and multi-element (ICP-MS) detection. In separations on two different stationary phases, high apparent molecular weight (>669 kDa) elution profiles for ^{56}Fe and ^{208}Pb were strongly correlated (average $R^2 = 0.96$, N = 73 samples representing 23 single-unit residences). Moreover, ^{56}Fe and ^{208}Pb peak areas exhibited an apparent linear dependence ($R^2 = 0.82$), consistent with mobilization of lead via adsorption to colloidal particles rich in iron. A UV_{254} absorbance peak, coincident with high molecular weight ^{56}Fe and ^{208}Pb, implied

that natural organic matter was interacting with the hypothesized colloidal species. High molecular weight UV_{254} peak areas were correlated with both ^{56}Fe and ^{208}Pb peak areas (R^2 = 0.87 and 0.58, respectively). On average, 45% (SD 10%) of total lead occurred in the size range 0.05–0.45 μm. (Graphical abstract provided as Figure 7.)

3.2 Introduction

Lead in distributed drinking water originates primarily from lead service lines (pipes linking distribution mains with residences).[1] Brass fittings and leaded solder also represent important sources.[2,3] While full or partial lead service line replacement can reduce lead at the point of use,[4] disturbances associated with replacement may increase lead levels in drinking water.[1]

High iron in distributed water often accompanies elevated lead at the point of use.[4-8] This phenomenon has been attributed primarily to adsorption of lead onto iron corrosion scale or iron-rich deposits within lead service lines and premise plumbing; these sites may subsequently serve as sources for the release of lead and iron. Lead-manganese and arsenic-iron correlations at the point of use have been explained via similar mechanisms.[9,10] In soil matrices, mobilization of lead into streams and rivers has been attributed to adsorption and transport by iron-rich colloidal particles.[11-13] This may point to a related mechanism governing lead-iron interactions in drinking water: mobilization of lead from sources to points of use by suspended colloidal iron.

As an explanation for observed correlations between lead and iron in distributed drinking water, adsorption mechanisms are supported by a significant body of literature demonstrating these phenomena using synthesized iron oxides with and without organic ligands.[14-19] The established propensity of lead to adsorb onto iron mineral surfaces is linked to its high solid-water partition coefficient.[20] Given this property, it is expected that lead would be found predominantly in the particulate phase in aqueous environments.[11,21,22]

However, direct observation of adsorbed lead on iron particles is challenging, especially in the colloidal size range. The low concentrations of lead typically present in the environment and the mixed mineral structures of natural colloidal particles limit the applicability of X-ray spectroscopic techniques and analytical electron microscopy.[11] One

approach to bridge the gap between observed correlation and laboratory synthesis is the use of physical separation techniques to characterize the size distributions of lead and iron in environmental samples. Pokrovsky *et al*.[23] used ultrafiltration and multi-element detection to determine that colloidal iron in remote Siberian rivers was strongly associated with trace metals. However, the ability to resolve size fractions via filtration is limited by available filter pore sizes.

This shortcoming can be overcome by physical separation on a continuous spectrum using techniques such as field-flow fractionation and size exclusion chromatography (SEC). In soil and river systems, transport of lead by iron-rich colloidal particles has been demonstrated using field-flow fractionation with detection by inductively coupled plasma – mass spectrometry (ICP-MS).[11] Separation of natural water colloids by SEC with ICP-MS and UV detection has also been established,[24-27] mainly for the characterization of heavy metal interactions with natural organic matter.

Given the role of colloidal iron particles as transport vectors for lead in natural water systems, understanding their behavior in engineered distribution systems is valuable in the interest of limiting exposure to lead via drinking water. The goal of this study was to characterize the size distributions, below 450 nm, of lead, iron, and natural organic matter in drinking water samples collected from single-unit residences with lead service lines or where lead service lines had recently been replaced. This work represents a novel approach to understanding nanoscale lead-iron interactions in distributed drinking water and provides evidence that lead is mobilized via adsorption to colloidal particles rich in natural organic matter and iron.

3.3 Experimental

3.3.1 Study Area

The study area comprised single-unit residences in the Canadian city of Halifax. Subject to resident participation, two types of sites were sampled: (1) residences with intact lead service lines scheduled to be fully or partially replaced and (2) residences where full or partial replacement had occurred in the nine months prior to sample collection. Full replacement signifies removal of the lead service line from the distribution main to the internal plumbing, and partial replacement signifies removal of

only a portion of the lead line. In areas of the city with pre-1940 construction, thousands of lead service lines are still in use.[4] Table 3 displays a typical set of values for key drinking water quality parameters measured in the treated water supplied to all sites where samples were collected.[28]

3.3.2 Sample Collection And Filtration

At each sampling round, participating residents collected a 4 × 1L sequential profile from the kitchen cold-water tap, beginning with the 1st draw following six hours without water use. Subsequently, the tap was flushed for five minutes and a fifth 1L sample was collected. Residents collected sample profiles before full or partial lead service line replacement, 3 days post-replacement, and 1, 3, 6, and 9 months post-replacement. A detailed description of sampling protocol is provided in Camara *et al*.[4] Seventy three samples, representing 23 sites, were analyzed by SEC-ICP-MS as they were retrieved from participating residents between November 2014 and September 2015. Sites known in advance to have drinking water iron concentrations below 6.0 μg L^{-1} were excluded. The last 13 of the 73 samples, representing 8 sites, were also analyzed by SEC with UV detection. Size fractionation was performed on a separate set of 10 samples, representing 2 randomly selected sites from the original 23.

Table 3 Typical values for treated water quality parameters, prior to distribution.

Parameter	Typical value
Orthophosphate (as PO_4^{3-})	0.5 mg L^{-1}
Alkalinity (as $CaCO_3$)	20.0 mg L^{-1}
Hardness (as $CaCO_3$)	12.0 mg L^{-1}
Chloride	9.0 mg L^{-1}
Sulfate	8.5 mg L^{-1}
Total organic carbon	1.5 mg L^{-1}
Turbidity	0.06 NTU
pH	7.3
Iron	<0.050 mg L^{-1}
Lead	<0.5 μg L^{-1}

Prior to collection, 1L HDPE bottles were immersed in 10% reagent-grade HNO_3 for a minimum of 24 hours and rinsed 3 times with ultrapure water. For size fractionation, separate 10 mL aliquots from well-mixed 1L samples were filtered 0 – 2 days after sample collection using 0.45 μm cellulose nitrate and 0.05 μm polycarbonate membrane

filters via syringe filter cartridges. Adsorption losses due to filtration were estimated by comparing lead in triplicate 10 mL aliquots filtered once with lead in triplicate aliquots filtered twice, using a new membrane each time.[29] Average losses due to 0.45 and 0.05 μm filtration were 21.1% (SD 0.4%) and 20.8% (SD 11.4%), respectively. For SEC-ICP-MS analysis, a 10 mL aliquot from each sample was filtered at 0.45 μm and divided in two. Approximately 2 mL were stored in a glass chromatography vial, and the remaining 8 mL were reserved for direct quantification by ICP-MS. Sample filtrate for SEC was stored at 4°C and analyzed within 1 week without further pre-treatment. Sample filtrate for direct quantification was preserved immediately (pH < 2, concentrated trace metal grade HNO_3).

After drawing aliquots for filtration, 1L samples were preserved with HNO_3 and held for a minimum of 24 hours at 4˚C prior to direct quantification. Total lead was measured in 10 mL aliquots drawn from the 1L samples following mixing. Adsorption losses to HDPE sample bottles between sample collection and HNO_3 preservation were estimated by comparing lead in 10 mL aliquots drawn before and 24 hours after preservation. Average loss of lead was 1.2% (SD 17.3%, N = 82).

3.3.3 Reagents

Buffers, standards, and other solutions were prepared using ultrapure water (18.2 MΩ cm, 5 ppb or less total organic carbon) and analytical or trace metal grade chemicals. Tris buffer (tris (hydroxymethyl) aminomethane), trace metal grade HCl and HNO_3, and disodium EDTA were purchased from Fisher Scientific. Thyroglobulin was purchased from GE Healthcare and ICP-MS standards from SCP Science.

3.3.4 Apparatus

The high-performance liquid chromatography (HPLC) system used for SEC-ICP-MS analysis comprised a vacuum membrane degasser (SCM1000, Thermo Fisher), gradient pump (P4000, Thermo Fisher) and autosampler (AS3000, Thermo Fisher) with a 1 mL sample loop (Rheodyne). All tubing and wetted parts were made from polyether ether ketone or other inert materials. The HPLC system for SEC with UV detection comprised a vacuum degasser, pump, autosampler with a 200 μL sample loop, and UV-Vis detector

(Series 200, Perkin Elmer).

Separation was performed on two different SEC columns with stationary phases composed of polymethacrylate (TSKGel Bioassist G6PW, 7.8 × 300 mm, 17 µm particle size, Tosoh bioscience) and a composite of cross-linked agarose and dextran (Superdex 200, 10 × 300 mm, 13 µm particle size, GE Healthcare). A 2.0 µm pre-column filter was used for all separations.

For multi-element detection, the effluent of the HPLC system was delivered directly to the nebulizer of an ICP-MS instrument (X series II, Thermo Fisher). ^{208}Pb and ^{56}Fe were monitored using a collision cell with 7% H_2 in He for the removal of the $^{40}Ar^{16}O$ interference on ^{56}Fe. Direct quantification of 0.45 µm sample filtrate was performed without a collision cell, according to Standard Method 3125.[30] Reporting limits for lead and iron were 0.4 and 6.0 µg L^{-1}, respectively, and ^{45}Sc, ^{115}In, and ^{159}Tb were used as internal standards.

The ICP-MS instrument was tuned in standard mode using a 10 µg L^{-1} multielement solution prepared in 50 mM tris-HCl with 2% concentrated trace metal grade HNO_3. Transmission was maximized at ^{238}U, ^{115}In, ^{59}Co, and ^{7}Li while minimizing the formation of oxides and doubly charged ions. The instrument was then tuned using the H_2/He collision cell in order to maximize transmission of ^{208}Pb while minimizing the $^{40}Ar^{40}Ar^{+}$ interference on $^{80}Se^{+}$.

3.3.5 Analysis

Separation on agarose/dextran and polymethacrylate stationary phases was performed at flow rates of 0.5 and 1.0 mL min^{-1}, with sample injection volumes of 212 and 180 µL for multi-element and UV detection, respectively. A mobile phase of 50 mM tris-HCl (pH 7.3) was used for all separations. Ammonium acetate, ammonium chloride, and sodium chloride were found to be unsuitable as mobile phase additives, resulting in no detectable analyte recovery. This may have been due to the effects of these salts on the stability of colloidal lead and iron. Mobile phase blanks were used routinely to guard against sample carryover and to ensure a stable baseline prior to sample analysis. All illustrations of SEC data were composed in R.[31]

Typically, SEC allows estimation of the molecular weight of proteins and other

analytes according to their retention times on a stationary phase, given a suitable set of standards. Since the macromolecular structure of colloidal lead and iron in distributed water samples was not known, no standards for molecular weight determination were available. The retention volume of thyroglobulin (molecular weight 669 kDa, Stoke's radius 8.5 nm, monitored as ^{127}I and via absorbance at 254 nm) on agarose/dextran and polymethacrylate is indicated on SEC chromatograms as a qualitative point of reference. Retention volumes were measured using 100 µL injections of thyroglobulin dissolved in 50 mM tris-HCl and passed through a 0.2 µm polycarbonate filter.

Total losses of ^{208}Pb and ^{56}Fe on the two stationary phases were estimated by comparing peak areas for samples injected with and without the analytical columns. Separation on polymethacrylate reduced peak area significantly (by 96.0 and 92.5% for ^{208}Pb and ^{56}Fe, respectively), likely due to negatively charged groups on the surface of the stationary phase. Separation on agarose/dextran also reduced peak areas (by 79.6 and 74.8% for ^{208}Pb and ^{56}Fe, respectively). Adsorption of ionic or labile lead (and nickel) on size-exclusion columns has been reported previously[24,26,32,33] and is supported in this case by the occurrence of large peaks for both elements following injection of a chelating agent (1 mM disodium EDTA dissolved in the mobile phase, as described by Rottmann and Heumann)[24] or 0.1 M HCl.

Soluble lead and iron, injected as standards at neutral pH, were entirely retained on the stationary phases (see Section 5.4.2 and 6.4.1). An important consequence is that high apparent molecular weight peaks in SEC-ICP-MS chromatograms represent only the colloidal fraction of lead and iron—soluble lead and iron did not elute at high apparent molecular weight under separation conditions.

3.4 Results And Discussion

3.4.1 Separation On Agarose/Dextran

On agarose/dextran, ^{56}Fe and ^{208}Pb co-eluted at retention volumes of 7.9 to 8.8 mL at 0.5 mL min^{-1}—approximately one third of the 24 mL column volume. Co-elution 1 – 2 mL before thyroglobulin (669 kDa, Stoke's radius 8.5 nm) indicated that the two metals were present in a high apparent molecular weight fraction. High molecular weight (> 669 kDa) elution profiles for ^{56}Fe and ^{208}Pb were strongly correlated ($R^2 = 0.96$) in all

samples separated on agarose/dextran.

Figure 8 displays typical ^{208}Pb and ^{56}Fe chromatograms for a full 5 × 1L sample profile (samples A1 – 5, Table 2). Negative peaks were due to the sample matrix and were not present in mobile phase blanks. Association of ^{208}Pb with a colloidal ^{56}Fe fraction was a common feature of the entire sample profile, including the free-flowing sample. Since this sample represents distributed water that did not stagnate in contact with a source of lead, the association may be explained by fast reaction kinetics—rapid adsorption of lead onto iron mineral surfaces has been demonstrated previously.[34,35] It is also possible that colloidal ^{208}Pb and ^{56}Fe in the free-flowing sample represent release from established iron deposits within the service line or premise plumbing that had accumulated lead over time.

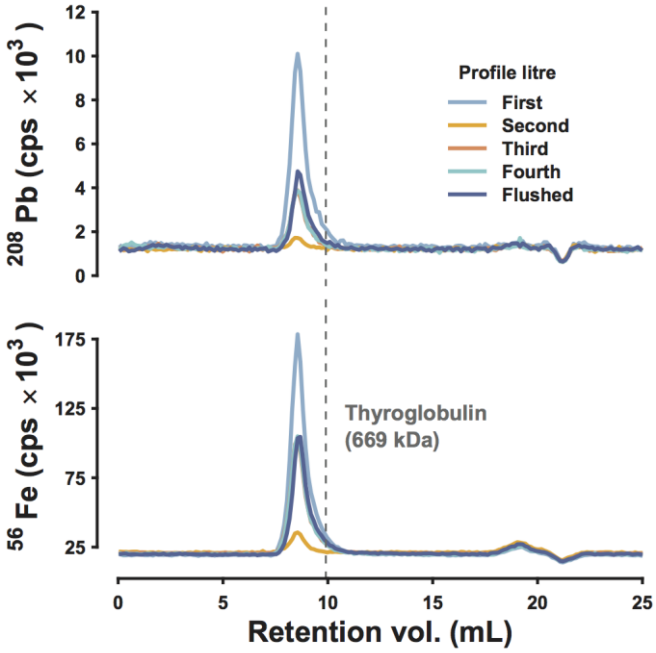

Figure 8 ^{208}Pb and ^{56}Fe chromatograms (cps denotes counts s^{-1}) for a 5 × 1L point-of-use sample profile (A1 – 5, 0.45 µm filtrate) separated on agarose/dextran.

^{208}Pb and ^{56}Fe chromatograms representing separations on agarose/dextran were occasionally bimodal at high apparent molecular weight. Figure 9 (sample B, Table 4) represents the separation of a 1st draw sample collected at a site supplied by a full lead service line. Filtration at 0.1 µm removed the early-eluting peak, indicating that two colloidal size fractions were present—one below 0.1 µm and another between 0.1 and 0.45 µm. ^{56}Fe also eluted in a low apparent molecular weight fraction with a retention

volume of approximately 18.7 mL, but ^{208}Pb was only weakly associated with this fraction.

Co-elution of ^{27}Al along with ^{56}Fe and ^{208}Pb in the two high molecular weight fractions is also evident in Figure 9. Detection of ^{27}Al along with ^{56}Fe and ^{208}Pb was a common—but not universal—feature of separations on agarose/dextran. Aluminum in 0.45 µm filtrate, quantified directly, had a median (interquartile range) of 32.4 µg L^{-1} (21.4 – 55.3 µg L^{-1}) and can in general be attributed to the use of alum in water treatment.[36] Occasionally, ^{55}Mn, ^{65}Cu, and ^{66}Zn were detected in the same elution volume as high molecular weight ^{56}Fe and ^{208}Pb, while ^{24}Mg eluted in a broad band and exhibited no association with ^{56}Fe.

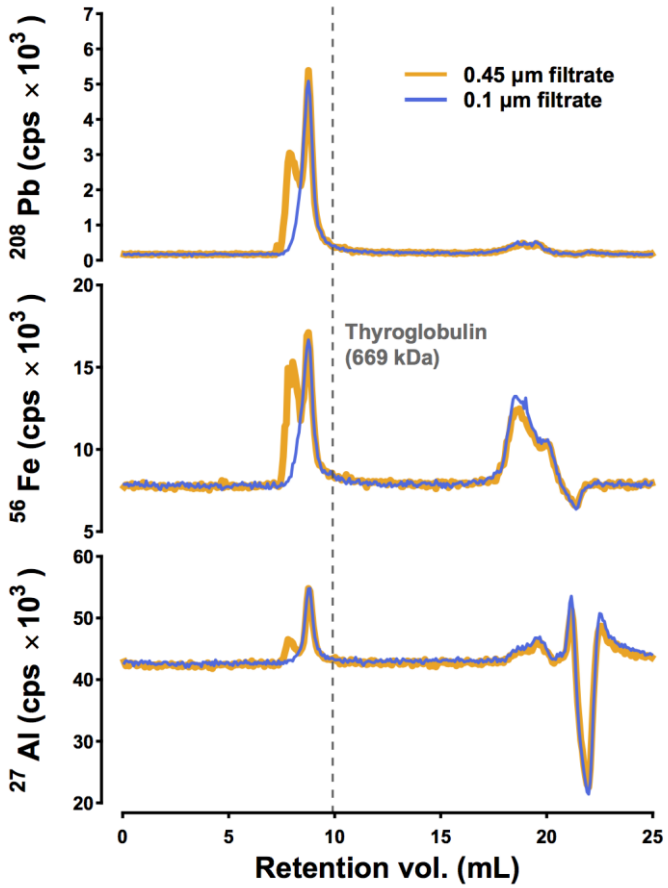

Figure 9 ^{208}Pb, ^{56}Fe, and ^{27}Al chromatograms for a point-of-use sample from site B (0.45 and 0.1 µm filtrate) separated on agarose/dextran.

Signal-to-noise ratio (SNR) was quantified as peak height divided by baseline range. For high molecular weight ^{56}Fe and ^{208}Pb peaks on agarose/dextran, the SNR was always greater than 3, even for 0.45 µm filtered samples with iron and lead concentrations below

the direct quantification reporting limits (0.4 and 6.0 μg L^{-1}, respectively). Use of a collision gas and a neutral pH, low ionic strength mobile phase reduced the ^{56}Fe and ^{208}Pb baseline noise levels for SEC analysis relative to direct quantification.

Table 4 Site, sample round, service line configuration, and iron and lead concentration ranges (0.45 μm filtrate) for SEC chromatograms.

Site	Round	Service line configuration	Iron (μg L^{-1})	Lead (μg L^{-1})
A (1 – 5)	9 mo. post-replacement	CSL[a]	26.7 – 58.8	ND[c] – 1.9
B	Pre-replacement	Full LSL[b]	6.4	17.9
C (1 – 5)	9 mo. post-replacement	Partial LSL	30.7 – 72.0	1.6 – 4.1

[a]copper service line, post-replacement
[b]lead service line
[c]below direct quantification reporting limit of 0.4 μg L^{-1}

3.4.2 Separation On Polymethacrylate

On polymethacrylate, ^{56}Fe and ^{208}Pb co-eluted at retention volumes of 8.4 –9.1 mL at 1.0 mL min^{-1}, or 56 – 61% of the 15 mL column volume. ^{208}Pb and ^{56}Fe chromatograms for a full 5 × 1L sample profile, collected from a residence with a partial lead service line, are provided in Figure 10 (C1 – 5, Table 4). Co-elution of the two analytes 1 – 2 mL before thyroglobulin provided a robust confirmation of the correlation between high molecular weight ^{208}Pb and ^{56}Fe elution profiles observed in separations on agarose/dextran. Given that agarose/dextran had a positive surface charge at neutral pH[27] and polymethacrylate had a negative charge,[37] similar elution on the two stationary phases also confirmed that the analytes represented colloidal and not ionic species. High apparent molecular weight (> 669 kDa) elution profiles for ^{56}Fe and ^{208}Pb were strongly correlated in all samples with quantifiable concentrations of both metals ($R^2 = 0.96$).

The SNR for high molecular weight ^{208}Pb and ^{56}Fe peaks on polymethacrylate was always below 3 for 0.45 μm sample filtrate with less than 6.0 μg Fe L^{-1}. For samples with higher iron concentrations, the SNR for high molecular weight ^{208}Pb was greater than 3 even when samples contained less than 0.4 μg Pb L^{-1} (Figure 38, Appendix B).

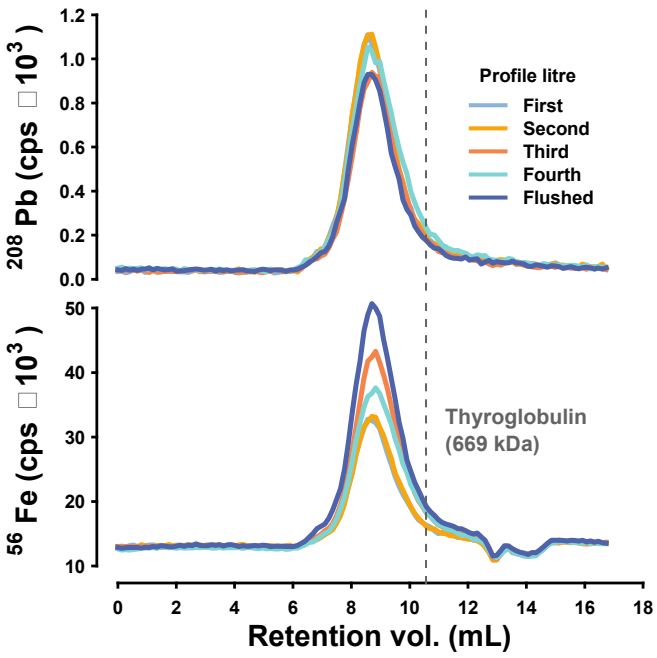

Figure 10 ^{208}Pb and ^{56}Fe chromatograms for a 5 × 1L point-of-use sample profile (C1 – 5, 0.45 µm filtrate) separated on polymethacrylate.

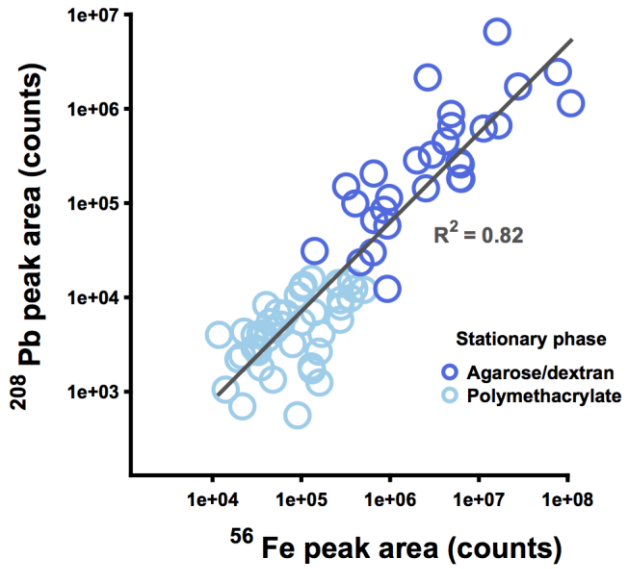

Figure 11 Apparent linear dependence of ^{208}Pb peak area on ^{56}Fe (*log-log* scale, *N* = 73 samples representing 23 sites).

On both stationary phases, the mass of colloidal lead in point-of-use samples exhibited an apparent dependence on the mass of colloidal iron, both estimated qualitatively by high molecular weight peak area counts. Figure 11 displays the linear correlation (R^2 = 0.82, *log-log* scale) between ^{208}Pb and ^{56}Fe peak areas. This association

supports the interpretation that co-eluting iron and lead represented a single colloidal species, and it is consistent with adsorption of lead to colloidal iron oxides or iron-rich organic colloidal particles. Contrary to results obtained using agarose/dextran, the ^{27}Al signal did not correspond with ^{56}Fe or ^{208}Pb in separations on polymethacrylate. The negative surface charge of the latter stationary phase may have retained labile aluminum that had been weakly associated with a colloidal particle.

3.4.3 Absorbance At 254 nm

A subset of 13 samples, representing 8 sites, was characterized by absorbance at 254 nm (UV_{254}) on a separate HPLC system. Retention volumes for thyroglobulin differed by approximately 1.3 mL between the two systems. Typical chromatograms for a 5 × 1L sample profile (A1 – 5) are provided in Figure 12. The high apparent molecular weight UV_{254} signal had the same retention, relative to thyroglobulin, as corresponding peaks for ^{56}Fe and ^{208}Pb (Figure 8). The predominant UV_{254} signal eluted in the same volume, also with respect to thyroglobulin, as the low molecular weight ^{56}Fe peak that was often observed (Figure 9). This association may have been due to complexation of iron by natural organic matter.[38]

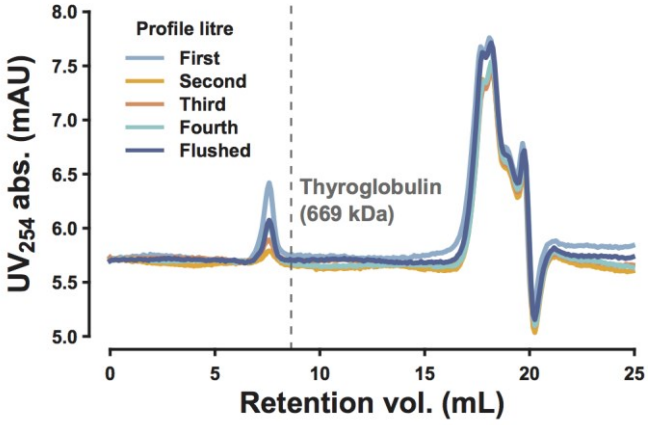

Figure 12 Typical UV_{254} chromatograms for a 5 × 1L point-of-use sample profile (A1 – 5, 0.45 µm filtrate).

High molecular weight UV_{254} and ^{56}Fe peak areas were strongly correlated (Figure 13, $R^2 = 0.87$), supporting the interpretation that signals for the two analytes represented a single colloidal species. UV_{254} and ^{208}Pb peak areas were also correlated ($R^2 = 0.58$). A possible explanation for the apparent dependence of UV_{254} on ^{56}Fe and ^{208}Pb is the

adsorption of natural organic matter, as well as lead, on a colloidal iron oxide surface; this phenomenon has been demonstrated previously.[39,40] Similar—but distinct—UV_{254} and iron retention profiles have also been noted previously for natural water samples.[11,24,41]

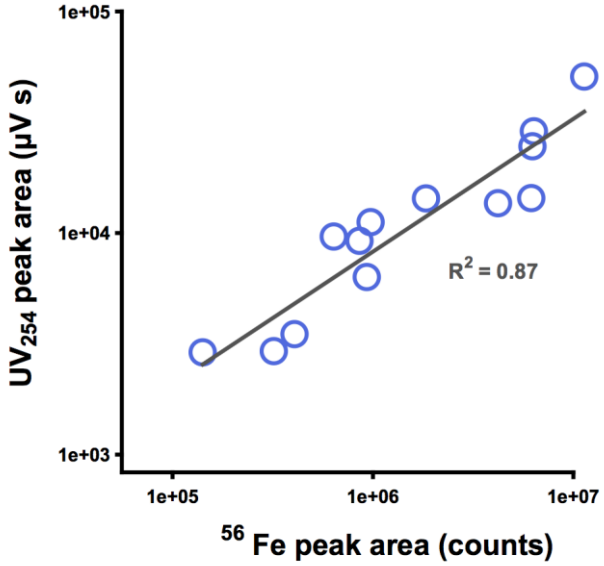

Figure 13 Apparent linear dependence of UV_{254} absorbance peak area on ^{56}Fe peak area (*log-log* scale, *N* = 13 samples representing 8 sites).

3.4.4 Size Fractionation

A considerable fraction (0.45, SD 0.10) of total lead in point-of-use samples occurred in the 0.05 – 0.45 µm size range (Figure 14). This fraction was estimated as the difference between lead in 0.45 and 0.05 µm filtrates (*N* = 10 samples representing 2 sites). Particulate lead (> 0.45 µm) was estimated as the difference between total and 0.45 µm-filtered lead. While changes in the size distribution of lead between sample collection and filtration are possible, the presence of a substantial fraction of total lead in the colloidal size range is consistent with the findings of Hullsmann,[42] Harrison and Laxen,[43] Bisogni *et al.*,[44] and de Mora *et al*.[45] Colloidal lead and iron appeared to be relatively stable and were detectable by SEC-ICP-MS even six weeks after sample collection.

A considerable fraction of total iron also occurred in the 0.05 – 0.45 µm size range. Particulate iron (> 0.45 µm) as a proportion of total iron was 0.40 (SD 0.06), and iron in 0.05 µm filtrate was consistently below the reporting limit, 6.0 µg L^{-1}. Lead and iron in the smallest size fraction (< 0.05 µm) should not necessarily be interpreted as ionic

species: colloidal ^{56}Fe and ^{208}Pb were detected in 0.05 µm filtrate by SEC-ICP-MS (Figure 39, Appendix B).

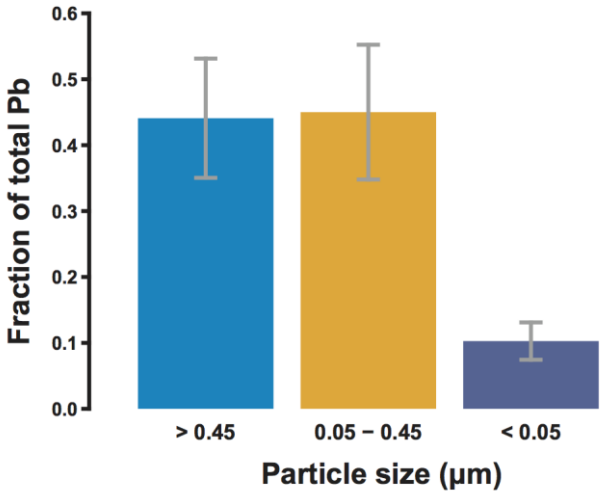

Figure 14 Mean fraction of total lead in each size range; error bars represent one standard deviation about the mean.

3.5 Conclusion

This study used SEC with UV and multi-element detection, as well as size fractionation via filtration, to explore the hypothesis that lead occurs in distributed drinking water adsorbed to colloidal particles rich in iron and natural organic matter. At all residential sites where samples were collected, strong correlations among high molecular weight elution profiles for ^{208}Pb, ^{56}Fe, and UV_{254} were observed. Correlations among peak areas supported the interpretation that the three analytes represented a single colloidal species, and size fractionation confirmed that colloidal lead and iron comprised a substantial fraction of total concentrations. These findings provide evidence that lead is mobilized via adsorption to iron-rich colloidal particles. High iron levels often accompany elevated lead, and, in the interest of limiting lead exposure via drinking water, this work contributes to an understanding of the relationship between the two metals.

3.6 References

(1) Sandvig, A.; Kwan, P.; Kirmeyer, G.; Maynard, B.; Mast, D.; Trussell, R.; Trussell, S.; Cantor, A. F.; Prescott, A. *Contribution of Service Line and Plumbing Fixtures to Lead and Copper Rule Compliance Issues, 91229*; American Water Works Association Research Foundation and U.S. Environmental Protection Agency: Denver, CO, 2008.

(2) Kimbrough, D. E. Brass corrosion as a source of lead and copper in traditional and all-plastic distribution systems. *J. Am. Water Works Assoc.* **2007***, 99* (8), 70-76.
(3) Nguyen, C. K.; Stone, K. R.; Edwards, M. A. Chloride-to-sulfate mass ratio: practical studies in galvanic corrosion of lead solder. *J. Am. Water Works Assoc.* **2011**, *103* (1), 81-92.
(4) Camara, E.; Montreuil, K. R.; Knowles, A. K.; Gagnon, G. A. Role of the water main in lead service line replacement: A utility case study. *J. Am. Water Works Assoc.* **2013**, *105* (8), E423-E431.
(5) Deshommes, E.; Laroche, L.; Nour, S.; Cartier, C.; Prevost, M. Source and occurrence of particulate lead in tap water. *Water Res.* **2010**, *44* (12), 3734-3744.
(6) McFadden, M.; Giani, R.; Kwan, P.; Reiber, S. H. Contributions to drinking water lead from galvanized iron corrosion scales. *J. Am. Water Works Assoc.* **2011**, *103* (4), 76-89.
(7) Masters, S.; Edwards, M. A. Increased lead in water associated with iron corrosion. *Environ. Eng. Sci.* **2015**, 32 (5), 361-369.
(8) Knowles, A. D.; Nguyen, C. K.; Edwards, M. A.; Stoddart, A.; McIlwain, B.; Gagnon, G. A. Role of iron and aluminum coagulant metal residuals in lead release from service lines. *J. Environ. Sci. Heal. A* **2015**, *50* (4), 414-423.
(9) Lytle, D. A.; Sorg, T. J.; Muhlen, C.; Wang, L. Particulate arsenic release in a drinking water distribution system. *J. Am. Water Works Assoc.* **2010**, *102* (3), 87-98.
(10) Schock, M. R.; Cantor, A. F.; Triantafyllidou, S.; Desantis, M. K.; Scheckel, K. G. Importance of pipe deposits to Lead and Copper Rule Compliance. *J. Am. Water Works Assoc.* **2014**, *106* (7), 336-349.
(11) Hassellöv, M.; von der Kammer, F. Iron oxides as geochemical nanovectors for metal transport in soil-river systems. *Elements* **2008**, *4* (6), 401-406.
(12) Erel, Y.; Morgan, J. J. The relationships between rock-derived lead and iron in natural waters. *Geochim. Cosmochim. Acta* **1992**, *56* (12), 4157-4167.
(13) Kaste, J. M.; Bostick, B. C.; Friedland, A. J.; Schroth, A. W.; Siccama, T. G. Fate and speciation of gasoline-derived lead in organic horizons of the northeastern USA. *Soil Sci. Soc. Am. J.* **2006**, *70* (5), 1688-1698.
(14) Xu, Y.; Thipnakarin, B.; Lisa, A.; Sungmin, M.; Trevor, T. Surface complexation of Pb (II) on amorphous iron oxide and manganese oxide: spectroscopic and time studies. *J. Colloid Interf. Sci.* **2006**, *299*, 28-40.
(15) Benjamin, M. M.; Leckie, J. O. Multiple-site adsorption of Cd, Cu, Zn, and Pb on amorphous iron oxyhydroxide. *J. Colloid Interf. Sci.* **1981**, *79* (1), 209-221.
(16) Hua, M.; Shujuan, Z.; Bingcai, P.; Weiming, Z.; Lu, L.; Quanxing, Z. Heavy metal removal from water/wastewater by nanosized metal oxides: a review. *J. Hazard. Mater.* **2012**, *211-212*, 317-331.
(17) Nelson, Y. M.; Lion, L. W.; Shuler, M. L.; Ghiorse, W. C. Effect of oxide formation mechanisms on lead adsorption by biogenic manganese (hydr)oxides, iron (hydr)oxides, and their mixtures. *Environ. Sci. Technol.* **2002**, *36* (3), 421-425.
(18) Vu, H. P.; Shaw, S.; Brinza, L.; Benning, L. G. Partitioning of Pb (II) during goethite and hematite crystallization: Implications for Pb transport in natural systems. *Appl. Geochem.* **2013**, *39*, 119-128.
(19) Violante, A.; Ricciardella, M.; Pigna, M. Adsorption of heavy metals on mixed Fe-Al oxides in the absence or presence of organic ligands. *Water Air Soil Poll.* **2003**, *145*, 289-306.
(20) Allison, J. D.; Allison, T. L. *Partition coefficients for metals in surface water, soil, and waste*; EPA/600/R-05/0742005; U.S. Environmental Protection Agency, Office of Research and Development: Washington DC, 2005.
(21) Karathanasis, A. D. Colloid-mediated transport of Pb through soil porous media. *Int. J. Environ. Stud.* **2000**, *57* (5), 579-596.
(22) Veselý, J.; Majer, V.; Kučera, J.; Havránek, V. Solid–water partitioning of elements in Czech freshwaters. *Appl. Geochem.* **2001**, *16* (4), 437-450.
(23) Pokrovsky, O. S.; Schott, J.; Dupré, B. Trace element fractionation and transport in boreal rivers and soil porewaters of permafrost-dominated basaltic terrain in Central Siberia. *Geochim. Cosmochim. Acta* **2006**, *70* (13), 3239-3260.
(24) Rottmann, L.; Heumann, K. G. Determination of heavy metal interactions with dissolved organic materials in natural aquatic systems by coupling a high-performance liquid chromatography system with an inductively coupled plasma mass spectrometer. *Anal. Chem.* **1994**, *66* (21), 3709-3715.
(25) Vogl, J.; Heumann, K. G. Determination of heavy metal complexes with humic substances by HPLC/ICP-MS coupling using on-line isotope dilution technique. *Fresenius. J. Anal. Chem.* **1997**, *359* (4-5), 438-441.

(26) Schmitt, D.; Müller, M. B.; Frimmel, F. H. Metal distribution in different size fractions of natural organic matter. *Acta Hydroch. Hydrob.* **2001**, *28* (7), 400-410.
(27) Kozai, N.; Ohnuki, T.; Iwatsuki, T. Characterization of saline groundwater at Horonobe, Hokkaido, Japan by SEC-UV-ICP-MS: Speciation of uranium and iodine. *Water Res.* **2013**, *47* (4), 1570-1584.
(28) *2013/2014 Annual Report*; Halifax Regional Water Comission: Halifax, Canada, 2014; http://www.halifax.ca/hrwc/documents/AnnualReportFinal-2014.pdf.
(29) de Mora, S. J.; Harrison, R. M. The use of physical separation techniques in trace metal speciation studies. *Water Res.* **1983**, *17* (7), 723-733.
(30) American Public Health Association, American Waterworks Association, Water Pollution Control Federation. *Standard Methods For the Examination of Water and Wastewater*, 22nd ed.; American Public Heath Association: Washington, DC, 2012.
(31) *R: A language and environment for statistical computing*; R Foundation for Statistical Computing: Vienna, Austria, 2014; https://www.r-project.org.
(32) Schaumlöffel, D.; Ouerdane, L.; Bouyssiere, B.; Łobiński, R. Speciation analysis of nickel in the latex of a hyperaccumulating tree *Sebertia acuminata* by HPLC and CZE with ICP MS and electrospray MS-MS detection. *J. Anal. At. Spectrom.* **2003**, *18* (2), 120-127.
(33) Jackson, B. P.; Ranville, J. F.; Bertsch, P. M.; Sowder, A. G. Characterization of colloidal and humic-bound Ni and U in the "dissolved" fraction of contaminated sediment extracts. *Environ. Sci. Technol.* **2005**, *39* (8), 2478-2485.
(34) Eick, M. J.; Peak, J. D.; Brady, P. V.; Pesek, J. D. Kinetics of lead adsorption/desorption on goethite: residence time effect. *Soil Sci.* **1999**, 164 (1), 28-39.
(35) Liu, C.; Huang, P. M. Pressure-jump relaxation studies on kinetics of lead sorption by iron oxides formed under the influence of citric acid. *Geoderma.* **2001**, *102* (1), 1-25.
(36) Knowles, A. D.; MacKay, J.; Gagnon, G. A. Pairing a pilot plant to a direct filtration water treatment plant. *Can. J. Civ. Eng.* **2012**, *39* (6), 689-700.
(37) Kato, Y.; O'Donnell, J. K.; Fisher, J. Size exclusion chromatography using TSK-Gel columns and Toyopearl resins. In *Column Handbook for Size Exclusion Chromatography*; Wu, C.S., Ed.; Academic Press: San Diego 1999; pp. 93-158.
(38) Fujii, M.; Imaoka, A.; Yoshimura, C.; Waite, T. D. Effects of molecular composition of natural organic matter on ferric iron complexation at circumneutral pH. *Environ. Sci. Technol.* **2014**, *48* (8), 4414-4424.
(39) Rahman, M. S.; Whalen, M.; Gagnon, G. A. Adsorption of dissolved organic matter (DOM) onto the synthetic iron pipe corrosion scales (goethite and magnetite): Effect of pH. *Chem. Eng. J.* **2013**, *234*, 149-157.
(40) Gu, B.; Schmitt, J.; Chen, Z.; Liang, L.; McCarthy, J. F. Adsorption and desorption of different organic matter fractions on iron oxide. *Geochim. Cosmochim. Acta* **1995**, *59* (2), 219-229.
(41) Lyvén, B.; Hassellöv, M.; Turner, D. R.; Haraldsson, C.; Andersson, K. Competition between iron-and carbon-based colloidal carriers for trace metals in a freshwater assessed using flow field-flow fractionation coupled to ICPMS. *Geochim. Cosmochim. Acta* **2003**, *67* (20), 3791-3802.
(42) Huslmann, A. D. Particulate lead in water supplies. *Water Environ. J.* **1990**, *4* (1), 19-25.
(43) Harrison, R. M.; Laxen, D. P. H. Physicochemical speciation of lead in drinking water. *Nature* **1980**, *286*, 791-793.
(44) Bisogni, J. J.; Nassar, I. S.; Menegaux, A. M. Effect of calcium on lead in soft-water distribution systems. *J. Environ. Eng.* **2000**, *126* (5), 475-478.
(45) de Mora, S. J.; Harrison, R. M.; Wilson, S. J. The effect of water treatment on the speciation and concentration of lead in domestic tap water derived from a soft upland source. *Water Res.* **1987**, *21* (1), 83-94.

Chapter 4 Understanding The Role Of Iron Particles In Lead Release To Drinking Water

This chapter is reprinted with permission from the following:

Trueman, B. F.; Gagnon, G. A. Understanding the role of iron particles in lead release to drinking water. *Environ. Sci. Technol.* **2016**, *50*, 9053−9060. http://pubs.acs.org/doi/abs/10.1021/acs.est.6b01153

B.F.T. collected and analyzed the experimental data, wrote the paper, and prepared the figures.

4.1 Abstract

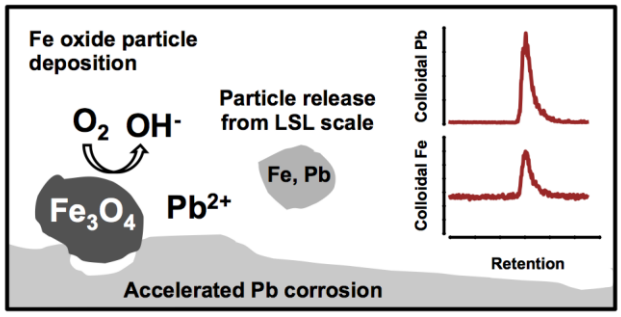

Figure 15 Conceptual diagram summarizing proposed mechanisms of lead release under the influence of particulate/colloidal iron (oxyhydr)oxides.

Lead service lines (LSLs) are a major source of lead in drinking water, and high iron levels are frequently observed along with elevated lead release. A model distribution system, dosed with orthophosphate, was used to evaluate the effect of corroded iron distribution mains on lead release from recovered LSLs. Lead release was higher by 96 μg L^{-1}, on average, from LSLs supplied by corroded iron compared to the inert reference material (PVC). This effect may be explained by deposition of semiconducting iron oxide particles within LSLs. When galvanic cells with lead and magnetite (Fe_3O_4) electrodes were short-circuited, lead release increased 8-fold and a current averaging 26 μA was observed. In effluent from LSLs with an upstream iron main, colloidal lead and iron occurred in the same size fraction—possibly due to release of colloidal particles from LSL corrosion scale enriched with iron. Under these circumstances, high molecular weight (>669 kDa) ^{208}Pb and ^{56}Fe elution profiles, observed via size-exclusion

chromatography, were highly correlated (average $R^2 = 0.97$). Increasing orthophosphate from 0.5 to 1.0 mg L^{-1} (as PO_4^{3-}) accompanied an average reduction in lead release of 6 μg L^{-1} $month^{-1}$ but did not significantly reduce the effect of an upstream iron main. (Graphical abstract provided as Figure 15.)

4.2 Introduction

Elevated blood lead levels are associated with learning deficits and neurobehavioral disorders in children,[1] and drinking water lead levels have been shown to correlate with blood lead.[2,3] At lower levels of exposure, increases in blood lead accompany steeper declines in children's cognitive performance.[4,5]

High levels of iron in distributed drinking water have been observed in previous work along with elevated lead measured at the point of use.[6-8] Unlined cast iron distribution mains—especially disturbed iron mains—have been linked with greater lead release from lead service lines (LSLs).[8] Accumulation of iron within LSL corrosion scale is a widespread phenomenon,[9-11] and iron deposits within LSLs could function both as sites for adsorption of lead and as sources from which lead and iron are subsequently released.[6,11-13] Elevated arsenic in drinking water systems has been attributed to adsorption and transport by particulate iron,[14] and iron-rich particles may also play a role in mobilizing lead from sources to the point of use via adsorption.[15-17]

Magnetite (Fe_3O_4), hematite (α-Fe_2O_3), maghemite (γ -Fe_2O_3), goethite (α-FeOOH), lepidocrocite (γ-FeOOH), siderite ($FeCO_3$), ferrous hydroxide ($Fe(OH)_2$), ferric hydroxide ($Fe(OH)_3$), ferrihydrite ($5Fe_2O_3$ $9H_2O$), and green rusts have all been identified in previous work as constituents of iron main corrosion scale.[18-22] Magnetite in particular has sufficiently high electrical conductivity (approximately 2×10^4 Ω^{-1} m^{-1}) to support cathodic reduction of oxygen,[23-24] although oxygen reduction on hematite and lepidocrocite has also been demonstrated.[25,26] As an electrode, magnetite is known to promote galvanic attack on iron,[23,27,28] and deposition of magnetite particles can induce galvanic corrosion of aluminum surfaces as well.[29] Magnetite is predicted to be cathodic to lead in neutral waters,[30,31] and previous work has identified magnetite in drinking water sampled at the point of use downstream from a corroded iron distribution main.[32]

Efforts to control lead in drinking water often include addition to distributed water of an orthophosphate-based corrosion inhibitor.[34,35] Lead phosphate minerals are relatively insoluble in the neutral pH range and can act as a passivating film, separating lead from the aqueous environment.[36] The ability of orthophosphate to reduce lead release has been well documented, especially at doses greater than 3 mg L^{-1} (as PO_4^{3-}).[37-41]

Given the prevalence of unlined and corroding iron distribution mains, the use of iron-based coagulants in water treatment, and the high levels of iron sometimes present in source waters, there is value in an improved understanding of lead–iron interactions in drinking water systems. This work investigated the link between iron distribution mains and elevated lead release observed via residential sampling in previous work.[7,8] A model distribution system was used—along with a new analytical tool, size-exclusion chromatography with ICP-MS detection—to evaluate the effect of an upstream source of iron on lead release from LSLs at two commonly applied orthophosphate doses.[34] A follow-up study explored galvanic corrosion of lead by semiconducting iron oxide particles as a possible mechanism for the effect of an upstream iron main on lead release. This work highlights the importance of distribution main condition for controlling lead in drinking water and has relevance for the implementation of lead corrosion control schemes, especially for low-alkalinity distributed waters.

4.3 Experimental

4.3.1 Model Distribution System

The model distribution system comprised four pipe loops (2 unlined cast iron, 2 PVC) and four pairs of LSL sections configured such that each pipe loop supplied a full and partial LSL section in parallel (Figure 16). Each of the four combinations of distribution main material and LSL configuration was represented by two LSL sections. The pipe loop apparatus, excluding the simulated LSLs, is described in detail elsewhere.[42,43] Iron distribution main sections, recovered from the same water system as the LSL sections, were 150 mm in diameter and moderately to-heavily tuberculated. PVC sections were 100 mm in diameter.

The simulated partial and full LSLs comprised 30 and 60 cm sections, respectively, of lead pipe (1 in. ID, 1.5 in. o.d.), recovered from a single-unit residence supplied by

distributed water with an orthophosphate residual of approximately 0.5 mg L^{-1} (as PO_4^{3-}). Recovered lead pipe had been in use for at least 40 years. Following recovery, lead pipe sections were stored in the same distributed water (with 0.5 mg L^{-1} of orthophosphate) for a period of 4 weeks prior to installation in the model system. Partial LSL sections included 30 cm of new copper pipe ($^3/_4$ in. type 'K') coupled to the reclaimed lead with a brass fitting. Electrical continuity between lead and copper was confirmed using a digital multimeter (Extech Instruments). Based on distribution system water quality and the relatively low orthophosphate residual, lead(II) carbonates and phosphates were expected as the primary and secondary crystalline phases, respectively. Owing to the prevalence of unlined iron distribution mains in the water system,[8] iron deposits within LSL corrosion scale were probable. Despite the use of free chlorine as a secondary disinfectant, lead(IV) oxides were not expected due to the demonstrated inhibition of lead(IV) oxide formation by orthophosphate.[44] Furthermore, the long stagnation regime applied over the duration of the experiment was expected to have inhibited formation of lead(IV) compounds by depleting the free chlorine residual.[45]

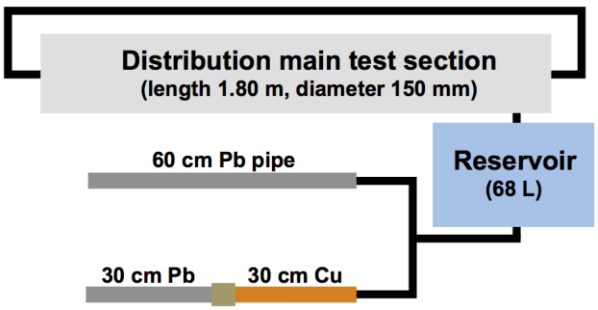

Figure 16 Simplified diagram of a cast iron pipe loop (1 of 2) and set of LSL test sections (30 and 60 cm sections, both configurations had lead-brass junctions). Reference (PVC) distribution mains had a diameter of 100 mm.

Water from the clearwell of a full-scale water treatment facility[46] was collected prior to chlorination and corrosion inhibitor addition for use as the feedwater to the model system. Typical feedwater pH, alkalinity, and total organic carbon were 5.5, 5.0 mg L^{-1} (as $CaCO_3$), and 1.5 mg L^{-1}, respectively. Lead and iron were below their respective reporting limits. The feedwater was modified with sodium hypochlorite (1.0 mg L^{-1} free chlorine), sodium hydroxide (pH 7.4), and the blended zinc ortho/polyphosphate corrosion inhibitor added to distributed water at the treatment facility (0.5 and 1.0 mg L^{-}

^{1} as PO_4^{3-}). Effluent from each pipe loop was discharged into a separate 68 L reservoir and pumped into the LSL sections for alternating 23 h 55 min standing and 5 min flow periods. Flow through the LSLs was approximately 2.0 L min^{-1}, and each held an approximate volume of 250 mL. Water entered and exited LSL sections via plastic tubing connected to lead or copper with a brass fitting. That is, both full and partial LSL configurations had the potential for galvanic corrosion via lead-brass couples. LSL effluent water temperature varied seasonally within the range 9.9–23 °C, with summer maxima in the last week of August.

Following installation of the LSL sections, orthophosphate was applied at a nominal dose of 0.5 mg L^{-1} (as PO_4^{3-}) for a 23-week conditioning phase and an 18-week baseline phase. The applied orthophosphate dose was chosen to match the distributed water residual in the system from which the lead pipes were recovered. Following 41 weeks—the combined conditioning and baseline phases—the nominal dose was increased to 1.0 mg L^{-1} (as PO_4^{3-}) and the system was operated for an additional 74 weeks (the test phase). Table 11 summarizes LSL influent water quality over the baseline and test phases. The duration of the conditioning period (23 weeks) fell between the duration of conditioning for reclaimed lead pipes adopted by Wang *et al.*[47,48] and Cartier *et al.*[37] (13 weeks and 8 months, respectively). Conditioning in the present study was aided by the fact that water circulated in the model system closely approximated the distributed water that lead pipes had been exposed to prior to recovery.

4.3.2 Standards And Reagents

Stock solutions of NaOH, NaOCl (Fisher Scientific), and blended zinc ortho/polyphosphate (ZOP-123, Shannon Chemical) were made each week and diluted with feedwater for addition to the pipe loops. Sample preservation and hot acid digestion were performed with trace metal grade HNO_3 (Fisher Scientific). For size exclusion chromatography, tris buffer (tris (hydroxymethyl) aminomethane) and trace metal grade HCl (Fisher Scientific) were used. Thyroglobulin was purchased from GE Healthcare. Mobile phases, blanks, sample dilutions, and electrolyte were prepared using ultrapure water (18.2 MΩ cm^{-1}, 5 ppb or less total organic carbon).

4.3.3 Analytical Methods

LSL effluent was collected in 250 mL polyethylene (HDPE) bottles following a 23 h 55 min stagnation within LSL sections. Total lead in LSL effluent was quantified following HNO_3 digestion according to Standard Method 3030.[49] Lead contamination as a result of the digestion procedure was estimated, using method blanks (n = 70), at 0.4 μg L^{-1} (95% CI: 0.3–0.5). Metals were quantified by inductively coupled plasma-mass spectrometry (ICP-MS, X Series II, Thermo Scientific) according to Standard Method 3125,[49] with reporting limits of 0.4 and 6.0 μg L^{-1} for lead and iron, respectively. Sample bottles, tubes, flasks, and caps were immersed in 2 M HNO_3 for 24 h and rinsed three times with ultrapure water prior to use. Orthophosphate and free chlorine were measured using a colorimeter (Standard Methods 4500-P E and 4500-Cl G, respectively).[49] A combination pH/conductivity/dissolved oxygen meter was used to measure pH (Accumet XL-50).

Lead was also quantified after filtration—within 20 min of LSL effluent collection—through 0.45 μm cellulose nitrate membrane filters with a syringe filter cartridge. Mean recovery was estimated, using a solution of 35 mg L^{-1} $NaHCO_3$ (pH 7.0) spiked with $Pb(NO_3)_2$ (35–500 μg L^{-1} as Pb), at 84.9% (95% CI: 82.7–87.1). Lead contamination due to filtration and acid preservation was estimated using method blanks (n = 119) at 0.6 μg L^{-1} (95% CI: 0.6–0.7). During the test phase, lead in 0.45 μm filtrate was quantified for 23 weeks longer than total lead.

4.3.4 Size-Exclusion Chromatography With ICP-MS Detection

The size-exclusion chromatography (SEC) method applied for the separation of LSL effluent is described in detail elsewhere.[15] The stationary phase used for all separations was a composite of cross-linked agarose and dextran (Superdex 200, 10 × 300 mm, 13 μm particle size, GE Healthcare). Separations were performed using a 50 mM tris-HCl (pH 7.3) mobile phase at a flow rate of 0.5 mL min^{-1}. The retention volume of thyroglobulin (669 kDa, Stoke's radius 8.5 nm), indicated in chromatograms as a qualitative point of reference, was monitored as ^{127}I.

4.3.5 Galvanic Cells

Commercial magnetite powder (Fisher Scientific) was densified into solid electrodes using a spark plasma sintering (SPS) instrument (model 10–3, Thermal Technology LLC). SPS allows consolidation of powders under applied mechanical pressure at relatively low temperatures; heating is provided by an electric current.[50] Densification of the magnetite powder was performed in a graphite die, using graphite foil to isolate the powder from the die, at 50 MPa with a pulsed DC current (25 ms on, 5 ms off). Prepressurized samples were heated under a vacuum at 100 °C min^{-1} to 800 °C, held isothermally for 10 min, and rapidly cooled. Postdensification, samples were polished with 320-grit aluminum oxide paper and rinsed thoroughly with ultrapure water. Electrodes were 0.4 cm thick and had flat faces with apparent surface areas of approximately 1 cm^2. The X-ray diffraction pattern of the magnetite powder is provided as Figure 40 (Appendix C) (Bruker D8 Advance XRD system, Co Kα radiation, λ = 1.79 Å). Consistent with previous work at comparable or higher sintering temperatures,[51,52] densification of magnetite by SPS did not result in any significant changes in diffraction peaks, other than the appearance of some small reflections attributable to hematite.

Lead coupons (3.8 cm × 1.3 cm × 0.2 cm) were immersed in 2 M HNO_3 for 2 h in order to remove surface deposits. Coupons were subsequently conditioned for 2 weeks by immersion in daily changes of 35 mg L^{-1} $NaHCO_3$. Electrodes were suspended, via insulated copper wires fastened to copper alligator clips, in 250 mL Erlenmeyer flasks sealed with rubber stoppers (Figure 41, Appendix C). Magnetite and lead electrodes were suspended such that approximately $^1/_3$ and $^1/_2$, respectively, of the total surface areas were submerged in the electrolyte; the submerged portions were approximately 1.5 cm apart. Copper wires passed through the rubber stoppers and were connected above the flasks via a second set of clips; circuits were interrupted at this point in order to measure galvanic current. Current was measured immediately after changing the electrolyte by connecting the multimeter (Extech Instruments) inline for 10 s. The 35 mg L^{-1} $NaHCO_3$ electrolyte (pH 7.5, 20–23 °C) was changed daily over the duration of the experiment, allowing for a stagnation time of 24 h. Daily electrolyte changes were accomplished by transferring the electrode assembly to a new flask and preserving the contents of the previous flask by

adding HNO_3 to a final concentration of 0.5%. Preserved 200 mL samples were held for 24 h prior to direct quantification.

4.3.6 Data Analysis

Where applicable, medians and interquartile ranges were used, instead of means and standard deviations, to describe distributions that were skewed due to outliers or were approximately log-normal. Linear regression models with autoregressive errors[53] were used to estimate the effects of distribution main material (categorical variable), LSL configuration (categorical variable), and orthophosphate (as a time-trend) on total and 0.45 μm-filtered lead release. To reduce serial correlation, lead release data from the model system were aggregated into 4-week averages prior to model fitting.[54] Trends in lead release with time were estimated separately for each orthophosphate dose (baseline and test phases). Model residuals were examined graphically for approximate normality and constant variance. Final fitted models were additive: no significant interaction between LSL configuration and distribution main material was observed. For the time series illustrations of lead in LSL effluent, a local linear smooth with a kernel window spanning 40% of the data was used.[54,55] This smoothing algorithm performs function estimation by computing a separate weighted least-squares linear regression estimate at each point in time, with weights supplied by a tricube kernel of user-specified width.

4.4 Results And Discussion

4.4.1 Effect Of An Iron Distribution Main

Relative to the reference condition (inert PVC pipe), corroded iron distribution mains accompanied increases in total and 0.45 μm-filtered lead release of 96 and 34 μg L^{-1}, respectively (Table 5). These increases were nearly as great as the effect of doubling the length of lead pipe from 30 to 60 cm. Total lead release from 60 cm LSLs—relative to 30 cm partial LSLs—was higher by 108 μg L^{-1} on average. Since brass fittings were used throughout to connect plastic tubing to LSL sections at the influent and effluent ends, galvanic corrosion of lead was likely in both full and partial LSL configurations. Brass and copper are both expected to be cathodic to lead under these

circumstances.[56] For this reason, the area of the lead–water interface (i.e., length of lead pipe) was likely the most important difference between the two configurations.

Table 5 Linear model coefficient estimates and confidence intervals.

	Total lead		0.45 µm filtrate	
Variable	**Estimate**	**95% CI**	**Estimate**	**95% CI**
LSL length (30 / 60 cm)	108.4[c]	67.2, 149.6	49.9	34.3, 65.5
Iron distribution main	96.3[c]	66.8, 125.7	34.3	20.8, 47.7
Time, baseline phase[a]	9.0	-6.1, 24.1	8.2	0.6, 15.7
Time, test phase[b]	-6.1	-9.5, -2.7	-3.1	-4.2, -1.9

[a]Orthophosphate dosed at 0.5 mg L^{-1} (as PO_4^{3-}), coefficients represent change in lead (in µg L^{-1}) over 4 weeks
[b]Orthophosphate dosed at 1.0 mg L^{-1}, coefficients have same significance
[c]Units of µg L^{-1}

Lead release over both experimental phases was higher than is typically observed in residential point-of-use monitoring.[6-8,12] Elevated lead was attributed to galvanic corrosion at lead-brass or lead–copper couples; low-alkalinity, pH, and orthophosphate; and the long stagnation period (23 h 55 m vs. 30 min or a minimum of 6 h in typical residential sampling). Previous work has shown that stagnation time is an important predictor of lead release, and that solubility equilibrium with lead corrosion scale may take longer than 24 h.[57-59] For this reason, a net release of lead to standing water was expected over the full stagnation period, with the majority occurring in the first 6 h.[57,59]

4.4.2 Effect Of Orthophosphate

After 41 weeks at 0.5 mg L^{-1} (as PO_4^{3-}, conditioning and baseline phases), the nominal orthophosphate dose in the model system was increased to 1.0 mg L^{-1}. Figure 17 compares the distribution of total lead grouped according to LSL configuration, distribution main material, and orthophosphate dose. The baseline phase (0.5 mg L^{-1} orthophosphate) is compared with an equivalent period (February to June) during the test phase (1.0 mg L^{-1} orthophosphate). In this illustration, medians and interquartile ranges were used to better represent the skewed distributions of lead release (confidence intervals for the linear model are provided in Table 5).

The effect of an iron distribution main was approximately consistent at the two orthophosphate doses evaluated (Figure 18 and Figure 42, Appendix C); allowing for a change in the effect of iron according to experimental phase did not improve the linear model fit significantly. While increasing orthophosphate did accompany reductions in

total and 0.45 µm-filtered lead release (Table 5, approximately 6 and 3 µg L^{-1} $month^{-1}$ respectively), lead in LSL effluent was stratified by distribution main material over both experimental phases. LSLs with an upstream source of iron released significantly more lead over the full experiment duration.

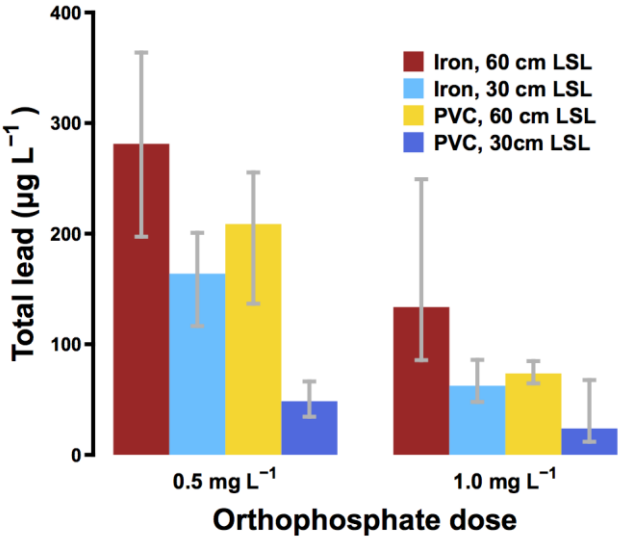

Figure 17 Median lead in LSL effluent grouped by LSL configuration, distribution main material, and orthophosphate dose (equivalent periods at each dose). Error bars span the interquartile range.

The increase in orthophosphate at the beginning of the test phase was immediately followed by a reversal of the trend in lead (0.45 µm filtrate) observed over the duration of the baseline phase (approximately 8 µg L^{-1} $month^{-1}$, Table 5 and Figure 42, Appendix C). The initial positive trend could have various explanations, including the increase in water temperature over the baseline phase (from 9.9–17.5 °C) or other seasonal factors. A strong dependence of lead release on temperature at low orthophosphate doses has been reported previously.[60] However, the trend reversal immediately following the orthophosphate dose increase is poorly explained by seasonality: the series maxima preceded the summer water temperature peak by approximately 10 weeks.

4.4.3 Colloidal Particles In LSL Effluent

Lead and iron concentrations were poorly correlated in both filtered and unfiltered LSL effluent. However, high apparent molecular weight (>669 kDa) ^{56}Fe and ^{208}Pb SEC elution profiles were highly correlated in separations representing filtrate from LSLs with

upstream iron (average $R^2 = 0.97$, Figure 19). (Pronounced tailing of high molecular weight ^{56}Fe and ^{208}Pb peaks is consistent with a common secondary interaction with the stationary phase.) Traces of ^{208}Pb, along with a significant ^{56}Fe signal (Figure 19), were also detected in a low molecular weight fraction at a comparable retention volume to the principal UV_{254} peak for the same source water.[15] This may have been due to complexation with natural organic matter.[61,62] In filtrate from LSLs with upstream PVC, a high molecular weight ^{208}Pb peak was detected without a corresponding ^{56}Fe peak.

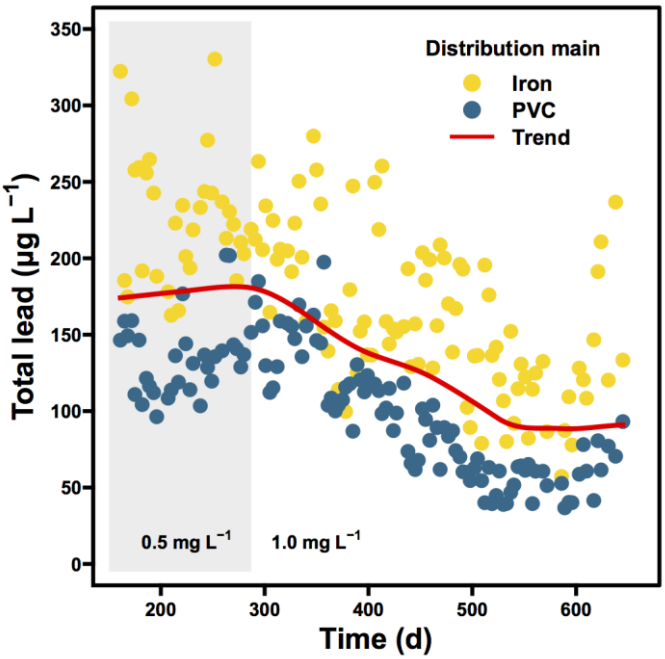

Figure 18 Mean lead in LSL effluent (N = 122 per LSL section), aggregated at each point in time by distribution main material. Orthophosphate doses (0.5 and 1.0 mg L^{-1}) are separated by background shading and a local linear smooth is superimposed to represent the overall trend.

Previous work has shown that high molecular weight peaks represented colloidal lead and iron: SEC separation effectively isolated colloidal particles by retaining the soluble fraction on the agarose/dextran stationary phase.[15] At environmentally relevant concentrations soluble lead and iron standards were completely adsorbed, and at higher concentrations they eluted at peak retention volumes greater than 20 mL.[15] Consistent with the presence of colloidal particles, filtration at 0.1 or 0.05 µm altered high molecular weight ^{56}Fe and ^{208}Pb peaks significantly and in identical fashion.[15] In SEC separations of residential samples collected within the water system from which LSL sections were

recovered, high molecular weight elution profiles for ^{56}Fe and ^{208}Pb were also correlated (average $R^2 = 0.96$).[15] Under these circumstances, coeluting lead and iron were taken to represent a single colloidal species. This interpretation was corroborated by a correlation ($R^2 = 0.82$) in the masses of colloidal lead and iron (estimated qualitatively via peak area) and by comparable elution profiles for the two metals on stationary phases with opposite surface charges (agarose/dextran and polymethacrylate) and different separation ranges (up to 8×10^6 Da on polymethacrylate).[15]

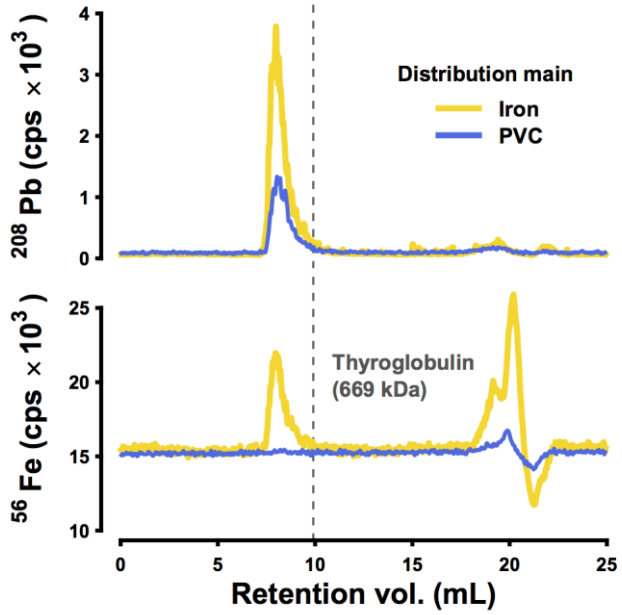

Figure 19 Typical ^{208}Pb and ^{56}Fe chromatograms representing separation of 0.45 µm-filtered effluent from LSL sections supplied by iron and PVC distribution mains (cps denotes counts s^{-1}). As a qualitative point of reference, the retention volume of thyroglobulin (669 kDa, Stoke's radius 8.5 nm) is indicated.

In the context of the present study, coelution of ^{56}Fe and ^{208}Pb is consistent with several possible phenomena. First, high molecular weight peaks may represent colloidal particles released from LSL corrosion scale; this was the expected source of colloidal lead in effluent from PVC systems. In cast iron systems, iron enrichment of LSL scale was probable,[9-11] and release from LSLs of particles rich in iron and lead would explain ^{56}Fe and ^{208}Pb coelution. The high degree of similarity in ^{208}Pb elution profiles representing cast iron and PVC systems is noteworthy, and could be explained by the controlled water quality and flow regime. Previous work has identified water quality parameters (e.g., dissolved organic matter, phosphate, free chlorine, pH) as important

determinants of (iron) particle size,[63-65] and flow characteristics may also be influential in this regard. The apparent size distribution of colloidal lead—as determined on two stationary phases with different separation characteristics—was also remarkably consistent in residential sampling within the same water system, as described elsewhere.[15] In separations representing 23 residential sites, coefficients of variation for peak retention volumes on polymethacrylate and agarose/dextran were 1.7% and 3.3%, respectively.[15]

Alternatively, ^{56}Fe and ^{208}Pb coelution could be explained by adsorption of soluble lead to suspended colloidal iron particles released from iron corrosion scale upstream: extensive research has shown that soluble lead adsorbs readily to particulate iron oxides.[66-70] Despite the expectation that soluble lead would adsorb to any colloidal iron oxides present, the occurrence of independent, noninteracting colloidal lead and iron cannot be completely ruled out either, especially in light of diminished size resolution at low retention volumes.

4.4.4 Galvanic Corrosion Of Lead By Magnetite

Deposition of semiconducting iron mineral particles within LSLs may explain elevated lead release in the presence of an upstream source of iron. Depending on particle size, a relatively small particle mass deposited within LSLs could provide a large surface area for cathodic reactions such as oxygen reduction. The potential for deposition corrosion of lead by iron oxides was explored using triplicate galvanic cells with lead anodes and magnetite (Fe_3O_4) cathodes. Magnetite was selected as a model electrically conductive iron oxide.

Prior to the introduction of magnetite, lead release to the electrolyte was 20–41 μg L^{-1} (Figure 20, *gray shaded region*). When lead was made anode by coupling to a densified magnetite cathode (day 17), lead release increased by 140–251 μg L^{-1} and a galvanic current of 22–29 μA was observed. Following this initial spike, both lead release and galvanic current declined, rapidly at first and then gradually. On day 33, current was 3.6–8.4 μA and lead release was 50–67 μg L^{-1}. When the surface layer of magnetite cathodes was removed by polishing on day 34, galvanic current increased to 17–19 μA (data not shown). Galvanic current and lead release were moderately correlated (R^2 = 0.53): a strong correlation between current and lead release was neither observed nor

expected due to the formation of corrosion scale on lead coupons.[45,71] Adsorption of lead to magnetite was expected,[70] and may have influenced both cathodic reactions at the magnetite surface and lead release to the electrolyte. Iron concentrations in the electrolyte were consistently below the reporting limit, however this does not rule out release of particles: magnetite was poorly soluble in 0.5% HNO_3.

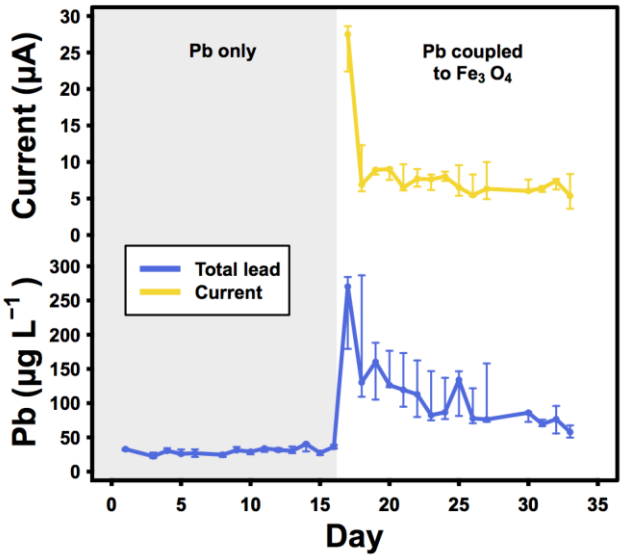

Figure 20 Lead release and galvanic current from triplicate galvanic cells with magnetite (Fe_3O_4) cathodes and lead anodes. Points represent medians, error bars span the range, and background shading indicates the introduction of magnetite.

4.4.5 Iron Retention Within LSL Sections

While iron corrosion scale was not analyzed to identify crystalline phases, previous work has shown that magnetite is often a primary scale constituent, in the presence of free chlorine and otherwise.[18-22] Furthermore, magnetite has been identified in point-of-use drinking water samples collected downstream from a corroded iron main and in deposits mobilized by hydrant flushing.[20,32,33] Iron in LSL influent was apparently dominated by particles: as a linear predictor, variation in iron explained 82% of the variation in turbidity at an orthophosphate dose of 0.5 mg L^{-1} (consistent with previous work).[22] At the 1.0 mg L^{-1} dose, iron levels explained 51% of the variation in turbidity.

Iron released from iron corrosion scale was largely retained within LSL sections. While median iron in LSL effluent differed according to distribution main material by less than 3 μg L^{-1}, influent iron concentrations from cast iron and PVC pipes differed more substantially. Figure 21 illustrates iron retention via pairwise differences in LSL

influent and effluent iron concentrations. Median iron in LSL influent from iron distribution mains was 24.0 μg L^{-1} (interquartile range 9.0–47.3 μg L^{-1}), and 75% of pairwise differences were positive, indicating a net retention of iron within LSL sections (18.2 μg L^{-1} day^{-1} on average). The distribution of iron released from iron mains was positively skewed with frequent high outliers. Conversely, median iron in LSL influent from PVC mains was below the reporting limit (4.6 μg L^{-1}, interquartile range 3.6–12.1 μg L^{-1}), and 73% of pairwise differences were negative, indicating a small net release of iron (1.1 μg L^{-1} day^{-1} on average). This release was attributed primarily to iron deposits that had accumulated within LSL sections prior to recovery.

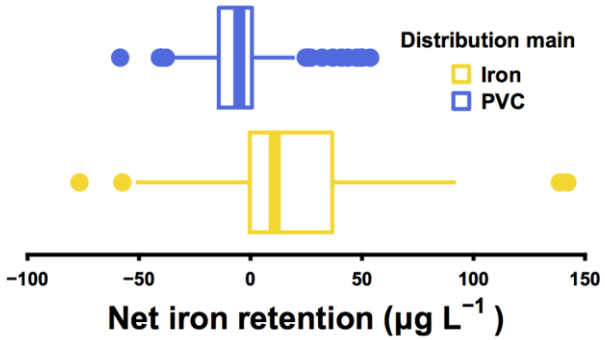

Figure 21 Iron retention within LSL sections, shown via box-and whisker plots of pairwise differences between influent and effluent iron concentrations (*N* = 100 paired measurements for each distribution main material). Boxes enclose the interquartile range (IQR), medians divide the boxes, and whiskers extend from the upper and lower quartiles to the most extreme value within 1.5 times the IQR.

Iron retention within LSL sections is consistent with widespread observations of iron deposits in LSL corrosion scale.[9-11] Schock *et al.*[9] recovered lead pipes from multiple water systems that were coated in scales rich in iron oxyhydroxides at the water-scale interface. In the present study, iron deposits within LSL sections likely served as sites for adsorption and release of lead and may have induced galvanic corrosion of lead. The role of drinking water parameters such as orthophosphate, free chlorine, and natural organic matter in the hypothesized galvanic reaction remains a subject for future work.

A potential consequence of iron accumulation is that lowering LSL influent iron levels may not immediately reduce lead release. Following a reduction in influent iron levels, accumulated iron could release lead—by facilitating cathodic reactions or via desorption and hydraulic mechanisms—until deposits were depleted. In a recent study,[7] a

decrease in distributed water pH (from 10.3 to 9.7) accompanied elevated levels of iron and lead in residential drinking water samples. Following an increase back to pH 10.3, iron levels decreased substantially, but at some sites, lead levels remained high. These observations were explained with reference to the higher adsorption density of lead on iron oxides at higher pH and to the likely accumulation over time of iron deposits within LSLs—a significant potential reservoir of lead and iron. The present study contributes to an understanding of the role of iron particles in lead release to drinking water, highlighting the importance of distribution main condition for lead corrosion control. The composition of iron corrosion scale may be particularly important if the particulate release of semiconducting oxide phases, such as magnetite, induces elevated lead release via deposition corrosion. Given the prevalence of unlined iron distribution mains in many drinking water systems and the significant public health risks posed by low-level lead exposure, an improved understanding of the mechanisms governing lead–iron interactions in this context is important.

4.5 References

(1) Evens, A.; Hryhorczuk, D.; Lanphear, B. P.; Rankin, K. M.; Lewis, D.A.; Forst, L.; Rosenberg, D. The impact of low-level lead toxicity on school performance among children in the Chicago Public Schools: a population- based retrospective cohort study. *Environ. Health* **2015**, *14* (21), 1-9.
(2) Fertmann, R.; Hentschel, S.; Dengler, D.; Janßen, U.; Lommel, A. Lead exposure by drinking water: an epidemiologial study in Hamburg, Germany. *Int. J. Hyg. Envir. Heal.* **2004**, *207* (3), 235-244.
(3) Edwards, M.; Triantafyllidou, S.; Best, D. Elevated blood lead in young children due to lead-contaminated drinking water: Washington, DC, 2001− 2004. *Environ. Sci. Technol.* **2009**, *43* (5), 1618-1623.
(4) Canfield, R.L.; Henderson, C.R.; Cory-Slechta, D.A.; Cox, C.; Jusko, T.A.; Lanphear, B.P. Intellectual impairment in children with blood lead concentrations below 10 μg per deciliter. *New Engl. J. Med.* **2003**, *348* (16), 1517-1526.
(5) Lanphear, B. P.; Hornung, R.; Yolton, K.; Baghurst, P.; Bellinger, DC.; Canfield, R. L.; et al. Low-level environmental lead exposure and children's intellectual function: an international pooled analysis. *Environ. Health Persp.* **2005**, *113* (7), 894-899.
(6) Deshommes, E.; Laroche, L.; Nour, S.; Cartier, C.; Prévost, M. Source and occurrence of particulate lead in tap water. *Water Res.* **2010**, *44*, 3734- 3744.
(7) Masters, S.; Edwards, M. Increased lead in water associated with iron corrosion. *Environ. Eng. Sci.* **2015**, *32* (5), 361-369.
(8) Camara, E.; Montreuil, K.R.; Knowles, A.K.; Gagnon, G.A. Role of the water main in lead service line replacement: A utility case study. *J. Am. Water Works Assoc.* **2013**, *105* (8) E423-E431.
(9) Schock, M. R.; Hyland, R. N.; Welch, M. M. Occurrence of contaminant accumulation in lead pipe scales from domestic drinking-water distribution systems. *Environ. Sci. Technol.* **2008**, *42* (12), 4285-4291.
(10) Friedman, M.; Hill, A.; Reiber, S.; Valentine, R.L.; Larsen, G.; Young, A.; Korshin, G.V.; Peng, C.Y. *Assessment of inorganics accumulation in drinking water system scales and sediments*; Water Research Foundation: Denver, CO, 2010.
(11) Schock, M. R.; Cantor, A. F.; Triantafyllidou, S.; Desantis, M. K.; Scheckel, K. G. Importance of pipe deposits to Lead and Copper Rule compliance. *J. Am. Water Works Assoc*. **2014**, *106* (7), E336-E349.

(12) McFadden M.; Giani, R.; Kwan, P.; Reiber, S.H. Contributions to drinking water lead from galvanized iron corrosion scales. *J. Am. Water Works Assoc.* **2011***, 103* (4), 76-89.
(13) Knowles, A.K.; Nguyen, C.K.; Edwards, M.; Stoddart, A.; McIlwain, B.; Gagnon, G.A. Role of iron and aluminum coagulant metal residuals in lead release from service lines. *J Environ. Sci. Heal. A.* **2015**, *50* (4), 414- 423.
(14) Lytle, D.A.; Sorg, T.J.; Muhlen, C.; Wang, L. Particulate arsenic release in a drinking water distribution system. *J. Am. Water Works Assoc.* **2010**, *102* (3), 87-98.
(15) Trueman, B.F.; Gagnon, G.A. A new analytical approach to understanding nanoscale lead-iron interactions in drinking water distribution systems. *J. Hazard. Mater.* **2016**, *311*, 151-157.
(16) Huslmann, A.D. Particulate lead in water supplies, *Water Environ. J.* **1990**, *4* (1), 19-25.
(17) Harrison, R.M.; Laxen, D.P.H. Physicochemical speciation of lead in drinking water. *Nature.* **1980**, *286*, 791-793.
(18) Sarin, P.; Snoeyink, V. L.; Bebee, J.; Jim, K. K.; Beckett, M. A.; Kriven, W. M.; Clement, J. A. Iron release from corroded iron pipes in drinking water distribution systems: effect of dissolved oxygen. *Water Res.* **2004**, *38* (5), 1259-1269.
(19) Sarin, P.; Snoeyink, V. L.; Bebee, J.; Kriven, W. M.; Clement, J. A. Physico-chemical characteristics of corrosion scales in old iron pipes. *Water Res.* **2001**, *35* (12), 2961-2969.
(20) Peng, C. Y., Korshin, G. V., Valentine, R. L., Hill, A. S., Friedman, M. J., Reiber, S. H. Characterization of elemental and structural composition of corrosion scales and deposits formed in drinking water distribution systems. *Water Res.* **2010**, *44* (15), 4570-4580.
(21) Gerke, T.L.; Maynard, J.B.; Schock, M.R.; Lytle, D.L. Physiochemical characterization of five iron tubercles from a single drinking water distribution system: Possible new insights on their formation and growth. *Corros. Sci.* **2008**, *50*, 2030-2039.
(22) Sarin, P.; Clement, J. A.; Snoeyink, V. L.; Kriven, W. M. Iron release from corroded, unlined cast-iron pipe. *J. Am. Water Works Assoc.* **2003**, *95* (11), 85-96.
(23) Stansbury, E.E.; Buchanan, R.A. *Fundamentals of electrochemical corrosion*; ASM International: Ohio, 2000.
(24) Vago, E. R.; Calvo, E. J. Electrocatalysis of oxygen reduction at Fe_3O_4 oxide electrodes in alkaline solutions. *J. Electroanal. Chem.* **1992***, 339*, 41- 67.
(25) Wilhelm, S.M. Galvanic corrosion caused by corrosion products. In *Galvanic Corrosion.* ASTM STP 978. Hack, H.P., Ed.; American Society for Testing and Materials: Philadelphia, 1988.
(26) Vago, E. R.; Calvo, E. J.; Stratmann, M. Electrocatalysis of oxygen reduction at well-defined iron oxide electrodes. *Electrochim. Acta* **1994**, *39* (11), 1655-1659.
(27) Francis, R. *Bimetallic corrosion*; National Physical Laboratory: Teddington, U.K., 2000.
(28) Fushimi, K.; Yamamuro, T.; Seo, M. Hydrogen generation from a single crystal magnetite coupled galvanically with a carbon steel in sulfate solution. *Corros. Sci.* **2002**, *44* (3), 611-623.
(29) Davis, J.R., Ed. *Corrosion of Aluminum and Aluminum Alloys*; ASM International: Ohio, 1999.
(30) Peabody, A.W., Bianchetti, R.L., Eds. *Peabody's control of pipeline corrosion*, 2nd ed.; NACE International: Houston, 2001.
(31) Roberge, P.R. *Corrosion inspection and monitoring*; John Wiley & Sons: Hoboken, New Jersey, 2007.
(32) Barkatt, A.; Pulvirenti, A. L.; Adel-Hadadi, M. A.; Viragh, C.; Senftle, F. E.; Thorpe, A. N.; Grant, J. R. Composition and particle size of superparamagnetic corrosion products in tap water. *Water Res.* **2009**, *43* (13), 3319-3325.
(33) Senftle, F. E.; Thorpe, A. N.; Grant, J. R.; Barkatt, A. Superparamagnetic nanoparticles in tap water. *Water Res.* **2007**, *41* (13), 3005-3011.
(34) McNeill, L. S.; Edwards, M. Phosphate inhibitor use at US utilities. *J. Am. Water Works Assoc*. **2002**, *94* (7), 57-63.
(35) Dodrill, D. M.; Edwards, M. Corrosion control on the basis of utility experience. *J. Am. Water Works Assoc.* **1995**, *87* (7), 74-85.
(36) Schock, M. R. Understanding corrosion control strategies for lead. *J. Am. Water Works Assoc.* **1989**, *81* (7), 88-100.
(37) Cartier, C.; Doré, E.; Laroche, L.; Nour, S.; Edwards, M.; Prévost, M. Impact of treatment on Pb release from full and partially replaced harvested lead service lines (LSLs). *Water Res.* **2013**, *47*, 661-671.
(38) Xie, Y.; Giammar, D. E. Effects of flow and water chemistry on lead release rates from pipe scales. *Water Res.* **2011**, *45*, 6525-6534.
(39) McNeill, L. S.; Edwards, M. Importance of Pb and Cu particulate species for corrosion control. *J.*

Environ. Eng.-ASCE. **2004**, *130* (2), 136- 144.
(40) Edwards, M.; McNeill, L. S. Effect of phosphate inhibitors on lead release from pipes. *J. Am. Water Works Assoc*. **2002**, *94* (1), 79-90.
(41) Colling, J. H.; Whincup, P. A. E.; Hayes, C. R. The measurement of plumbosolvency propensity to guide the control of lead in tapwaters. *Water Environ. J.* **1987**, *1* (3), 263-269.
(42) Gagnon, G.A.; Doubrough, J. D. Lead release from premise plumbing: a profile of sample collection and pilot studies from a small system. *Can. J. Civil Eng.* **2011**, *38* (7), 741-750.
(43) Woszczynski, M.; Bergese, J.; Gagnon, G. A. Comparison of chlorine and chloramines on lead release from copper pipe rigs. *J. Environ. Eng- ASCE*. **2013**, *139* (8), 1099-1107.
(44) Lytle, D. A.; Schock, M. R.; Scheckel, K. The inhibition of Pb(IV) oxide formation in chlorinated water by orthophosphate. *Environ. Sci. Technol.* **2009**, *43* (17), 6624-6631.
(45) Arnold Jr, R. B.; Edwards, M. Potential reversal and the effects of flow pattern on galvanic corrosion of lead. *Environ. Sci. Technol.* **2012**, *46* (20), 10941-10947.
(46) Stoddart, A.K.; Gagnon, G.A. Full-scale pre-chlorine removal: impact on filter performance and water quality. *J. Am. Water Works Assoc.* **2015**, *107* (12), E638-E647.
(47) Wang, Y.; Jing, H.; Mehta, V.; Welter, G.J.; Giammar, D.E. Impact of galvanic corrosion on lead release from aged lead service lines. *Water Res.* **2012**, *46*, 5049-5060.
(48) Wang, Y.; Mehta, V.; Welter, G.J.; Giammar, D.E. Effect of connection methods on lead release from galvanic corrosion. *J. Am. Water Works Assoc.* **2013**, *105* (7), E337-E351.
(49) American Public Health Association; American Waterworks Association; Water Pollution Control Federation. *Standard Methods For the Examination of Water and Wastewater*, 22nd ed.; American Public Heath Association: Washington, DC, 2012.
(50) Garay, J. E. Current-activated, pressure-assisted densification of materials. *Annu. Rev. Mater. Res.* **2010**, *40*, 445-468.
(51) Gaudisson, T.; Vázquez-Victorio, G.; Bañobre-López, M.; Nowak, S.; Rivas, J.; Ammar, S.; Mazaleyrat, F.; Valenzuela, R. The Verwey transition in nanostructured magnetite produced by a combination of chimie douce and spark plasma sintering. *J. Appl. Phys.* **2014**, *115*, 17E117.
(52) Bajpai, I.; Balani, K.; Basu, B. Spark plasma sintered HA-Fe_3O_4-based multifunctional magnetic biocomposites. *J. Am. Ceram. Soc.* **2013**, *96* (7), 2100-2108.
(53) Johnson, R.A.; Wichern, D.W. *Applied multivariate statistical analysis,* 6thed; Peason Education: New Jersey, 2007.
(54) Helsel, D.R.; Hirsch, R.M. *Statistical methods in water resources;* Elsevier: Amsterdam, 1992.
(55) *R: A language and environment for statistical computing;* R Foundation for Statistical Computing: Vienna, Austria, 2014; https://www.r-project.org/.
(56) Clark, B.; Cartier, C.; St. Clair, J.; Triantafyllidou, S.; Prévost, M.; Edwards, M. Effect of connection type on galvanic corrosion between lead and copper pipes. *J. Am. Water Works Assoc.* **2013**, *105* (10), E576-E586.
(57) Kuch, A.; Wagner, I. A mass transfer model to describe lead concentrations in drinking water. *Water Res.* **1983**, *17* (10), 1303-1307.
(58) Schock, M. R. Causes of temporal variability of lead in domestic plumbing systems. *Environ. Monit. Assess.* **1990**, *15* (1), 59-82.
(59) Clement, M., Seux, R., Rabarot, S. A practical model for estimating total lead intake from drinking water. *Water Res.* **2000**, *34* (5), 1533-1542.
(60) Colling, J. H.; Croll, B. T.; Whincup, P. A. E.; Harward, C. Plumbosolvency effects and control in hard waters. *Water Environ. J.* **1992**, *6* (4), 259-268.
(61) Fujii, M.; Imaoka, A.; Yoshimura, C.; Waite, T.D. Effects of molecular composition of natural organic matter on ferric iron complexation at circumneutral pH. *Environ. Sci. Technol.* **2014**, *48* (8), 4414-4424.
(62) Weng, L.; Temminghoff, E. J.; Lofts, S.; Tipping, E.; Van Riemsdijk, W. H. Complexation with dissolved organic matter and solubility control of heavy metals in a sandy soil. *Environ. Sci. Technol.* **2002**, *36* (22), 4804-4810.
(63) Rahman, M. S.; Gagnon, G. A. Bench-scale evaluation of drinking water treatment parameters on iron particles and water quality. *Water Res.* **2014**, *48*, 137-147.
(64) Baalousha, M.; Manciulea, A.; Cumberland, S.; Kendall, K.; Lead, J. R. Aggregation and surface properties of iron oxide nanoparticles: influence of pH and natural organic matter. *Environ. Toxicol. Chem.* **2008**, *27* (9), 1875-1882.
(65) Magnuson, M. L.; Lytle, D. A.; Frietch, C. M.; Kelty, C. A. Characterization of submicrometer

aqueous iron (III) colloids formed in the presence of phosphate by sedimentation field flow fractionation with multiangle laser light scattering detection. *Anal. Chem.* **2001**, *73* (20), 4815-4820.
(66) Benjamin, M.M.; Leckie, J.O. Multiple-site adsorption of Cd, Cu, Zn, and Pb on amorphous iron oxyhydroxide, *J. Colloid Interf. Sci.* **1981**, *79* (1), 209-221.
(67) McKenzie, R. M. The adsorption of lead and other heavy metals on oxides of manganese and iron. *Soil Res.* **1980**, *18* (1), 61-73.
(68) Nelson, Y. M.; Lion, L. W.; Shuler, M. L.; Ghiorse, W. C. Effect of oxide formation mechanisms on lead adsorption by biogenic manganese (hydr) oxides, iron (hydr) oxides, and their mixtures. *Environ. Sci. Technol.* **2002**, *36* (3), 421-425.
(69) Rodda, D. P.; Johnson, B. B.; Wells, J. D. The effect of temperature and pH on the adsorption of copper (II), lead (II), and zinc (II) onto goethite. *J. Colloid Interf. Sci* **1993**, *161* (1), 57-62.
(70) Liu, J. F.; Zhao, Z. S.; Jiang, G. B. Coating Fe_3O_4 magnetic nanoparticles with humic acid for high efficient removal of heavy metals in water. *Environ. Sci. Technol.* **2008**, *42* (18), 6949-6954.
(71) Nguyen, C. K.; Stone, K. R.; Dudi, A.; Edwards, M. A. Corrosive microenvironments at lead solder surfaces arising from galvanic corrosion with copper pipe. *Environ. Sci. Technol.* **2010,** *44,* 7076–7081.

Chapter 5 Galvanic Corrosion Of Lead By Iron (Oxyhydr)Oxides: Potential Impacts On Drinking Water Quality

This chapter is reprinted with permission from the following:

Trueman, B. F.; Sweet, G. A.; Harding, M. D.; Estabrook, H.; Bishop, D. P.; Gagnon, G. A. Galvanic corrosion of lead by iron (oxyhydr)oxides: potential impacts on drinking water quality. *Environ. Sci. Technol*. **2017**, *51* (12), 6812–6820. http://pubs.acs.org/doi/abs/10.1021/acs.est.7b01671

B.F.T. collected and analyzed the experimental data, wrote the paper, and prepared the figures.

5.1 Abstract

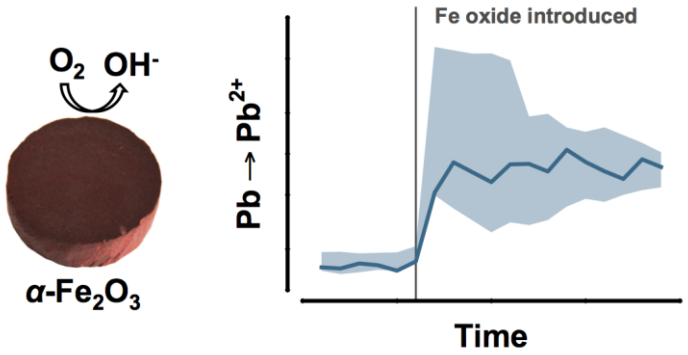

Figure 22 Iron (oxyhydr)oxides acted as efficient cathodes for oxygen reduction, dramatically elevating lead release under some conditions.

Lead exposure via drinking water remains a significant public health risk; this study explored the potential effects of upstream iron corrosion on lead mobility in water distribution systems. Specifically, galvanic corrosion of lead by iron (oxyhydr)oxides was investigated. Coupling an iron mineral cathode with metallic lead in a galvanic cell increased lead release by 531 μg L^{-1} on average—a 9-fold increase over uniform corrosion in the absence of iron. Cathodes were composed of spark plasma sintered Fe_3O_4 or α-Fe_2O_3 or field-extracted Fe_3O_4 and α-FeOOH. Orthophosphate immobilized oxidized lead as insoluble hydroxypyromorphite, while humic acid enhanced lead mobility. Addition of a humic isolate increased lead release due to uniform corrosion by 81 μg L^{-1} and—upon coupling lead to a mineral cathode—release due to galvanic corrosion by 990 μg L^{-1}. Elevated lead in the presence of humic acid appeared to be

driven by complexation, with ^{208}Pb and UV_{254} size-exclusion chromatograms exhibiting strong correlation under these conditions ($R^2_{average}$ = 0.87). A significant iron corrosion effect was consistent with field data: lead levels after lead service line replacement were greater by factors of 2.3–4.7 at sites supplied by unlined cast iron distribution mains compared with the alternative, lined ductile iron. (Graphical abstract provided as Figure 22.)

5.2 Introduction

Exposure to lead—even at low levels—is strongly linked with cognitive deficits in children.[1] Lead in drinking water is correlated with lead in blood,[2,3] and many jurisdictions regulate lead as a drinking water contaminant due to human health risks.[4,5] The principal sources of lead in water systems are plumbing components: lead-soldered joints, brass fittings, and lead service lines.

Appreciable levels of iron are often present in distributed drinking water, and iron is frequently correlated with lead.[6-8] The presence of corroded iron distribution mains has been linked specifically with elevated lead release from lead service lines.[9] While the mechanisms governing lead–iron interactions in drinking water systems are not well understood, both adsorption[6-8] and electrochemical phenomena may be important.[10]

Lead adsorbs readily to the iron oxides and oxyhydroxides commonly found in iron corrosion scale.[11-12] These may include magnetite (Fe_3O_4), goethite (α-FeOOH), hematite (α-Fe_2O_3), maghemite (λ-Fe_2O_3), and lepidocrocite (λ-FeOOH).[13-16] Iron scales are known to release nanosize (<100 nm) iron (oxyhydr)oxide particles to distributed drinking water.[17,18] Given their high specific surface areas, the presence of nanoparticulate iron phases could be a particularly important determinant of lead mobility. Indeed, a strong correlation between colloidal/nanosize iron and lead in drinking water has been identified in previous work via ultrafiltration[19] and size-exclusion chromatography with multielement detection.[20]

Iron (oxyhydr)oxides may also promote lead release via deposition corrosion within lead service lines,[10] although this phenomenon has not been verified in the field. While previous work has identified numerous instances of lead service line corrosion scale rich in iron (oxyhydr)oxides at the water-scale interface,[21] the catalytic activity of

these mineral deposits has not been established. Nevertheless, deposition corrosion of lead by iron (oxyhydr)oxides is analogous to the role of the magnetite-rich envelope layer typically present in well-developed iron corrosion scale as cathode (i.e., oxygen electrode) in an electrochemical cell where metallic iron is anode.[22] Semiconducting zinc oxide may also function as an oxygen electrode, reversing the potential of zinc with respect to iron when the two metals are coupled (i.e., zinc becomes cathode when a zinc oxide layer forms on its surface).[22] A number of iron corrosion products—including magnetite, hematite, and lepidocrocite—are also known to support oxygen reduction.[23,24] Magnetite in particular has been shown to corrode metallic lead galvanically.[10] However, the influence of other drinking water constituents on these galvanic interactions has not been investigated. This study explored the phenomena that may be involved in lead–iron interactions within drinking water systems. The goals were two-fold: (1) to investigate galvanic corrosion of lead by iron oxides in the presence of chemical species that influence lead mobility and (2) to estimate the effect of upstream iron corrosion on lead release using residential field data.

5.3 Materials And Methods

5.3.1 Experimental Design And Data Analysis

Three factors influencing lead release—humic acid (1.8 mg L^{-1} as total organic carbon), orthophosphate (2.0 mg L^{-1} as P), and iron (oxyhydr)oxide—were investigated using a two-level full factorial design.[25] Three iron-based cathode materials were examined: spark plasma sintered magnetite (Fe_3O_4), spark plasma sintered hematite (α-Fe_2O_3), and field-extracted iron corrosion scale composed of magnetite and goethite (α-FeOOH). Magnetite and goethite represent the two most common phases present in iron distribution main corrosion scale.[13-16] Maghemite (γ-Fe_2O_3), a polymorph of hematite, has also been identified as a primary scale constituent.[16] However, maghemite undergoes a complete phase transition to hematite at approximately 450 °C,[26] so the latter polymorph was selected for consolidation by sintering. Goethite also undergoes a phase transition to hematite at relatively low temperatures, precluding it as a candidate for consolidation.[27]

Data collection was divided into phases I and II: before and after the introduction of iron mineral cathodes as galvanic couples with lead. For each galvanic cell, lead

release was averaged over phase I and II separately to yield representative values. The full experiment required 12 cells: humic acid (*present/absent*) × orthophosphate (*present/absent*) × 3 cathode materials, treated as replicates for effects calculations. The main effect of each factor was calculated as the difference between the average response across all treatments at one factor setting and the average across all treatments at the other setting. The effects of humic acid and orthophosphate were also estimated over phases I and II separately using a two-factor model. Linear regression, group comparisons, effects calculations, and figure preparation were all performed using R version 3.3.3.[28]

5.3.2 Preparation Of Iron (Oxyhydr)oxide Electrodes

Commercial magnetite and hematite powders were consolidated into solid electrodes using a spark plasma sintering instrument (Model 10–3, Thermal Technology LLC). Spark plasma sintering allows consolidation of powders under applied mechanical pressure at relatively low temperatures; heating is accomplished via an electric current.[29]

Consolidation of the magnetite powder was performed in a graphite die, using graphite foil to isolate the powder from the die, at 60 MPa with a pulsed DC current. Magnetite powder was prepressurized to 10 MPa, and the chamber was evacuated (2.7 Pa or less), backfilled with argon, and evacuated again (2.7 Pa or less). Magnetite was then heated to 525 °C at a rate of 200 °C m^{-1} and held for 5 m to promote removal of volatile surface impurities. Pressure was increased to 60 MPa and samples were held isothermally for 1 h. Samples were cooled in the furnace to 100 °C and then removed for final cooling to room temperature. Hematite powder was prepressurized to 10 MPa, and the chamber was evacuated by the same procedure. Hematite was then heated to 750 °C at a rate of 200 °C m^{-1}. Upon reaching the temperature set point, pressure was increased to 60 MPa and samples were held isothermally for 5 m; hematite samples were cooled in the same manner. After consolidation, electrodes were polished using 320-grit aluminum oxide paper. The relative densities (ratio of measured to nonporous theoretical density) of sintered magnetite and hematite electrodes were estimated at 53.8 and 52.4%, respectively, according to Archimedes' principle.[30] Closed pores within the sintered compacts were assumed to contain argon.

Iron corrosion scale samples were collected from the dense envelope layer of a single iron tubercle removed from a section of unlined cast iron distribution main. The

iron pipe was recovered from a water system characterized by low alkalinity (less than 20 mg L^{-1} as $CaCO_3$), distributed water pH in the circumneutral range, and a history of secondary disinfection by free chlorine.

5.3.3 Galvanic Cells

New lead coupons (11 × 13 × 1.5 mm^3) were preconditioned for 24 h in a 35 mg L^{-1} $NaHCO_3$ solution; this step was repeated 14 times per coupon, with fresh solution each time. The preconditioning procedure was determined in previous work to achieve stable lead release from coupon scale.[10] After preconditioning, lead coupons were suspended via copper wires fastened to copper clips in 200 mL screw-top glass jars containing 100 mL of electrolyte. Approximately two thirds of the coupon surface area was submerged. The electrolyte was a 60 mg L^{-1} $NaHCO_3$ solution representing moderate distributed water alkalinity. Solutions were modified according the experimental design with phosphoric acid and a humic isolate and adjusted to pH 7.5 with 0.1 M NaOH or HCl. At 60 mg L^{-1} $NaHCO_3$, electrolyte conductivity among the treatments varied by less than 5% of the central value, with a mean of 71.8 ± 3.4 μS cm^{-1} (SD).

After adding fresh electrolyte to each cell, coupons were allowed to stand for 48 h before aliquots were withdrawn for analysis. The duration was determined to be sufficient for the system to reach an approximate equilibrium with respect to lead release: at 72 h, lead concentrations in galvanic cells were higher than at 48 h by an average of 12 ± 28 μg L^{-1} (95% CI). Lead release was monitored over a conditioning phase to ensure stability of corrosion scale (Figure 43, Appendix D). After stability had been verified, data were collected over the six 48 h periods comprising phase I.

Following the completion of phase I, iron (oxyhydr)oxide electrodes were coupled with the lead coupons and data were collected for an additional thirteen 48 h periods (phase II). Iron mineral cathodes were suspended such that approximately one half of the total surface area was submerged in the electrolyte; lead and iron-based electrodes were spaced an average of 2.2 ± 0.2 cm apart (SD). Anode and cathode were coupled via copper wires that passed through the cell lids and connected above with a second set of copper clips. Galvanic current was measured at this point, immediately after changing the electrolyte, by connecting a multimeter inline for 10 s.

5.3.4 X-ray Diffraction (XRD)

Identification of the crystalline phases characterizing iron-based cathodes and lead anodes was performed using an X-ray diffractometer (Bruker D8 Advance) equipped with a position sensitive detector (LynxEye) and Co*K*α radiation (λ = 1.79 Å) at 35 kV and 27 mA. Scans were performed with a step size of 0.02° (2θ) and a count time of 0.5 s per step. For scans of iron (oxyhydr)oxide samples, *K*β was filtered from incident radiation in order to reduce iron fluorescence. For scans of lead anode surfaces, *K*β was filtered from scattered radiation. Prior to analysis, sintered magnetite and hematite samples were polished with 600-grit silicon carbide paper. Field-extracted samples were ground with a mortar and pestle and passed through a 200-mesh sieve. Following completion of phase II, lead anodes were air-dried and analyzed by XRD without further processing.

5.3.5 Elemental Analysis

At 48 h, a 10 mL aliquot of electrolyte was decanted from each thoroughly mixed cell for elemental analysis (Pb, Fe, and P) by inductively coupled plasma mass spectrometry (ICP-MS Thermofisher X series II, *Standard method 3125*).[31] A second 10 mL aliquot from each cell was passed through a 0.45 μm cellulose nitrate membrane filter with a syringe filter cartridge, as described elsewhere.[10,20] Reporting limits for Pb, Fe, and P were 0.4, 6.0, and 4.9 μg L^{-1}, respectively. During phase I, aliquots were preserved with concentrated HNO_3 (pH < 2.0) and held for 24 h in polypropylene tubes prior to ICP-MS quantification.

Following the introduction of iron (oxyhydr)oxide cathodes (phase II), a hot HNO_3 digestion (*Standard method 3030 E*)[31] was necessary due to high sample turbidity. Over phase I, acidification with HNO_3 (pH < 2.0) provided near-complete recovery of lead. As a linear predictor, lead concentrations determined following acidification explained 99% (R^2) of the variation in lead levels determined following hot HNO_3 digestion ($\beta_1 = 0.99 \pm 0.12$, 95% CI). Total organic carbon (TOC) was measured at 0 and 48 h using a TOC analyzer (Shimadzu TOC-V_{CPH}, *Standard method 5310 B*).[31] Samples were collected headspace-free in baked glass vials (24 h at 105 °C) and acidified with concentrated H_3PO_4 (pH < 2.0).

5.3.6 Size-Exclusion Chromatography With UV And ICP-MS Detection

The size-exclusion chromatography ICP-MS (SEC-ICP-MS) and SEC-UV methods applied for the separation of experimental samples are described in detail elsewhere.[20] All paired SEC-UV and SEC-ICP-MS separations were performed on an agarose-dextran stationary phase (Superdex 200, 10 × 300 mm^2, 13 μm nominal bead size, GE Healthcare) with a 50 mM tris-HCl mobile phase (pH 7.3) at a flow rate of 0.5 mL min^{-1} and an injection volume of 212 μL. Unpaired SEC-UV separations were performed on a silica stationary phase (TSK G3000SW, 7.5 × 300 mm^2, 10 μm nominal bead size, Tosoh Bioscience) with a 20 mM ammonium acetate mobile phase (pH 6.7) at a flow rate of 0.7 mL min^{-1} and an injection volume of 100 μL. The molecular weight distribution of the humic isolate was estimated on this stationary phase using a calibration curve developed with polystyrene sulfonate standards (1100–17 000 Da) and 4-aminobenzoic acid (137 Da).

5.3.7 Reagents

Ultrapure water (18.2 MΩ cm^{-1}, 5 ppb or less TOC) was used as the starting matrix for all solutions. For electrolyte preparation, orthophosphate was added as phosphoric acid (Fisher Scientific) from a 1.0 M stock solution. Humic acid stock was prepared by dissolving 500 mg sodium humate (Alfa Aesar, 38.4% carbon)[32] in 1 L of ultrapure water; the stock solution was then centrifuged at 3000 rpm for 10 m to remove undissolved particles. For size-exclusion chromatography separations, ammonium acetate was purchased from Sigma-Aldrich and tris (hydroxymethyl) aminomethane from Fisher Scientific. The latter mobile phase was adjusted to pH 7.3 with trace metal-grade concentrated hydrochloric acid (Fisher Scientific). Iron oxide powders consolidated via spark plasma sintering were acquired from commercial sources.

5.3.8 Residential Data

Collection and analysis of residential data within the city of Halifax, NS, Canada, is described in detail elsewhere.[33] Briefly, residents collected 5 × 1L sample profiles at single-unit residences before and after full or partial replacement of lead service lines with copper. Profiles were collected following a minimum 6 h standing period, and the final liter was collected after a 5 m flushing period. Distribution main information was

obtained from water utility records; mains were composed of lined or unlined (corroded) iron. The sum of total lead over the 5 × 1L sample profile was compared according to distribution main composition before and 6 mo. after replacement. Statistical comparisons were made using two-tailed rank sum tests on log-transformed data.[34] Multiplicative group differences were quantified using a Hodges-Lehman estimator, c, where $c = \text{median}(y_i / x_j)$ for all $i = 1, ..., n$ and $j = 1, ..., m$. Variables x and y denote lead levels observed at m and n sites with ductile and cast iron distribution mains, respectively. The constant c estimates the multiplicative difference between the quantiles of the two groups ($y = cx$).

5.4 Results And Discussions

5.4.1 Uniform Corrosion (Phase I)

As a set of linear predictors, electrolyte composition explained 95% of the variation in lead release over phase I (Table 12). Lead release in the presence of dissolved inorganic carbon alone averaged 47 ± 15 μg L^{-1} (SD) (Figure 23). This was lower than expected based on predicted equilibrium solubility at pH 7.5, assuming formation of cerussite ($PbCO_3$) or hydrocerussite ($Pb_3(CO_3)_2(OH)_2$).[35] Lead levels were also lower than expected based on solubility of plumbonacrite ($Pb_5(CO_3)_3O(OH)_2$) at pH 7.5.[36] Hydrocerussite solubility, however, has been measured within the same order of magnitude under similar conditions: pH 7.5 and 10 mg L^{-1}dissolved inorganic carbon.[37] X-ray diffraction patterns characterizing lead anode surfaces were consistent with the presence of all three carbonate phases.

Addition of humic acid increased lead release by 81 ± 20 μg L^{-1} (95% CI): more than four-fold (Table 12). The effect of humic acid was estimated as the average lead release across all treatments with humic acid less the average across all treatments without humic acid. Losses of organic carbon to the system were negligible (mean 0.04 ± 0.07 mg L^{-1}, 95% CI). These were estimated by comparing phase I TOC at 0 and 48 h. Humic substances may comprise as much as 75% of dissolved organic carbon in untreated waters,[38] and their effect on lead release is attributed in part to the formation of lead humates that increase lead solubility.[39-41] Humic acid may also accelerate lead release by ligand-promoted dissolution, wherein crystal lattice bonds are weakened due to

coordination of a surface metal atom by a ligand.[42,43] Lead(IV) oxides dissolve reductively in the presence of natural organic matter.[44,45]

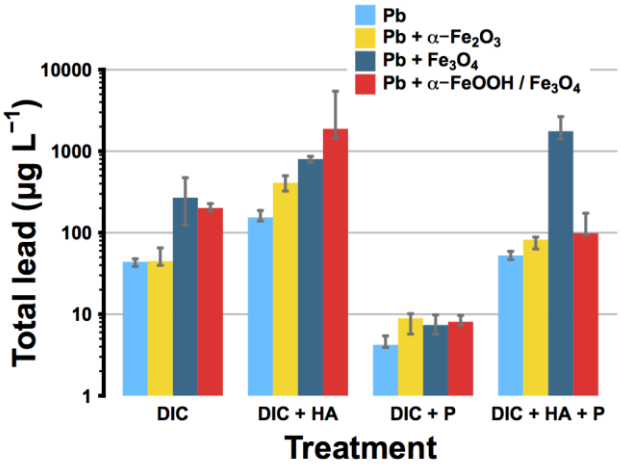

Figure 23 Lead release from anodes was strongly influenced by electrolyte compositionand coupling with iron-based cathodes. Bars represent median lead release at 48 h from anodes grouped according to cathode type (iron mineral) and electrolyte composition (DIC = dissolved inorganic carbon, HA = humic acid, P = orthophosphate). Error bars span the interquartile range.

Lead release across treatments with orthophosphate was lower than release across treatments without orthophosphate by 74 ± 20 µg L^{-1} (95% CI): a three-fold difference (Table 12). Mean phosphorus consumption was 30 ± 11 µg L^{-1} (95% CI). Losses of phosphorus to the system were estimated as the difference between phase I phosphorus at 0 and 48 h. Orthophosphate is commonly applied as a drinking water additive to control lead release,[46] and the dose applied in this study approximates an upper bound on the practical range.[47] The effect of orthophosphate on lead release can in general be attributed to the formation of highly insoluble hydroxypyromorphite ($Pb_5(PO_4)_3OH$), chloropyromorphite ($Pb_5(PO_4)_3Cl$), or tertiary lead phosphate ($Pb_3(PO_4)_2$).[35,48,49] Observed lead concentrations of less than 10 µg L^{-1} in the presence of orthophosphate were in approximate agreement with observations and theoretical predictions under similar conditions.[35,37] However, orthophosphate was less effective in the presence of humic acid: the interaction term for the two factors was 33 ± 20 µg L^{-1} (95% CI). This term represents the decrease in the magnitude of the orthophosphate effect in the presence of humic acid. Previous work has shown that dissolution of lead phosphate compounds at circumneutral pH is enhanced in the presence of humic

substances.[42] Moreover, complexation of lead with humic acid would be expected to reduce the activity of the lead cation in solution and inhibit coprecipitation of lead and phosphate.[50] This is analogous to the role of carbonate, as a complexing ligand, in increasing the equilibrium solubility of hydroxypyromorphite.[37]

5.4.2 Complexation Of Lead With Humic Acid

Interactions between lead and humic acid were investigated via size-exclusion chromatography (SEC) with UV and multielement detection, as demonstrated in previous work.[20,51] Formation of soluble lead humates has been investigated elsewhere using spectroscopic techniques.[39,40] Consistent with this phenomenon, ^{208}Pb and UV_{254} chromatograms were highly correlated in the presence of humic acid ($R^2_{average}$ = 0.87, Figure 24 and Figure 44, Appendix D). Aluminum was present as an impurity and served as a surrogate parameter for the humic isolate: at 0 h, humic-amended electrolyte had 22 μg Al L^{-1} but no detectable lead. At 48 h, the two metals coeluted at a retention volume corresponding to the apparent molecular weight of the isolate, 1537 Da (Figure 24).

Size-exclusion separation appeared to isolate the lead humate complex: in the absence of humic acid, lead was retained on the stationary phase and did not elute under separation conditions. This is consistent with previous work, where soluble lead was completely retained on the same stationary phase at environmentally relevant concentrations.[20] While humic substances may enhance lead release in general via colloidal dispersion of corrosion products,[41] this phenomenon was not observed via SEC over phase I. Nevertheless, in previous SEC characterization of drinking water collected at residential study sites, colloidal/nanosize lead eluted with iron and the UV_{254} signal in a high apparent molecular weight fraction.[20] These observations are consistent with dispersion of iron and lead by natural organic matter.

5.4.3 Identification Of Crystalline Phases

XRD patterns characterizing anodes exposed to dissolved inorganic carbon without orthophosphate were explained primarily by the presence of cerussite (Figure 25*a*). This compound is thermodynamically favored in the Pb–CO_3–H_2O system at pH

7.5.[52] Secondary reflections were attributable to both hydrocerussite and plumbonacrite (Table 6). While bulk water pH remained stable at 7.5 over 48 h, uniform corrosion of lead in the presence of carbonate alkalinity is expected to increase pH within the electrode microenvironment.[53] This may account for the formation of secondary phases, as hydrocerussite and plumbonacrite are favored at higher pH.[52,54] Moreover, the simultaneous presence of multiple carbonate phases is consistent with sequences of formation and conversion of carbonate compounds on lead surfaces that have been proposed elsewhere.[52]

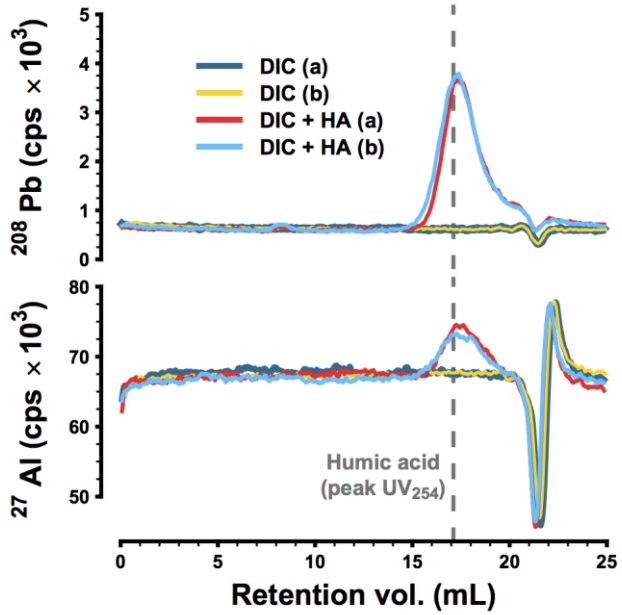

Figure 24 Consistent with formation of lead-humate complexes, ^{208}Pb was strongly correlated with UV$_{254}$ in the presence of humic acid ($R^2_{average}$ = 0.87). The vertical dashed line indicates the peak retention volume of the humic isolate; ^{27}Al was present as an impurity. Elution profiles represent separations of 0.45 µm-filtered electrolyte at 48 h (DIC = dissolved inorganic carbon, HA = humic acid, *a* and *b* are replicates).

Anodes exposed to humic acid yielded diffraction patterns with additional peaks not accounted for by lead carbonate phases; these secondary reflections were attributable to massicot (β-PbO). This compound has been identified as a component of corrosion scale in experimental and field-extracted lead pipes, sometimes below a surface layer of less-soluble hydrocerussite. Lead solubility in these circumstances appears to be controlled by the surface layer.[52]

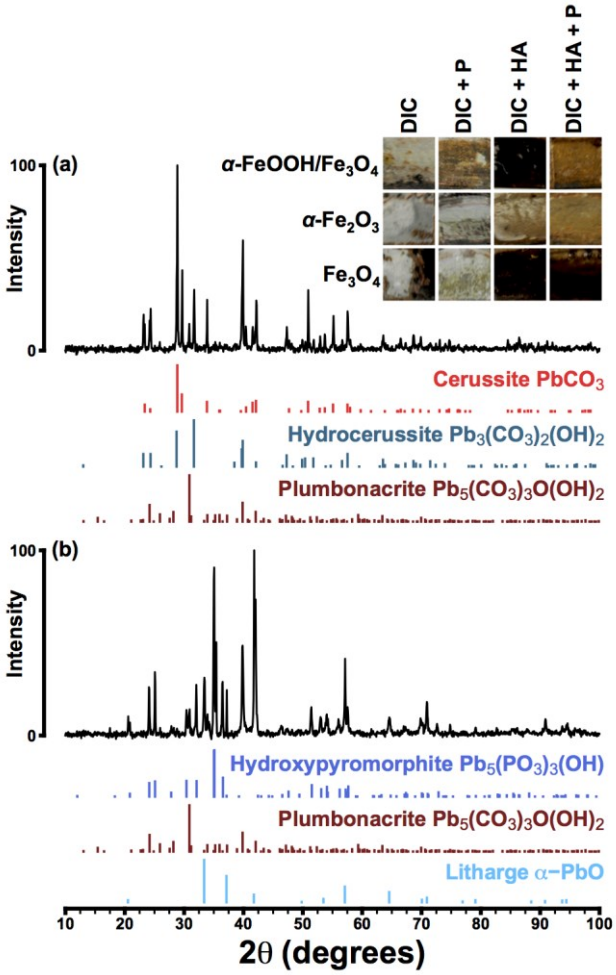

Figure 25 XRD patterns representing lead anodes coupled with field extracted magnetite/goethite in bicarbonate-buffered electrolyte, with (*b*) and without (*a*) orthophosphate. *Inset photographs*: the appearance of lead corrosion scale was influenced by cathode material (rows) and electrolyte composition (columns, DIC = dissolved inorganic carbon, HA = humic acid, P = orthophosphate).

Adsorption of humic substances to anode surfaces was visually apparent: a dark-brown scale formed on anodes exposed to the humic isolate, especially those coupled with magnetite (Figure 25 *inset*). Following the introduction of iron (oxyhydr)oxides, TOC decreased by an average of 0.34 ± 0.20 mg L^{-1} (95% CI) between 0 and 48 h. Accumulation of humic acid within the system was attributed to adsorption at the anode and possibly the mineral cathode;[55] this accumulation is apparent in SEC-UV chromatograms of 0 and 48 h electrolyte (Figure 45, Appendix D).

Anodes exposed to orthophosphate yielded diffraction peaks explained by the presence of insoluble hydroxypyromorphite (Figure 25*b*). This is consistent with the low

concentrations of lead observed under these conditions. Hydroxypyromorphite is assumed to be the thermodynamically stable phase in water–carbonate systems containing orthophosphate ions, and it has been identified in field-extracted corrosion scale from water systems with orthophosphate.[52,56] Secondary peaks were explained by the presence of plumbonacrite and massicot or litharge (α-PbO). Electrolyte modified with both humic acid and orthophosphate appeared to promote the formation of cerussite and hydrocerussite, in addition to plumbonacrite, as secondary phases. A complete set of XRD patterns for anodes, along with ICDD PDF numbers, is available as Figure 46 – 49 (Appendix D).

Table 6 Crystalline phases consistent with XRD patterns representing lead anode surfaces.

Cathode material	Electrolyte composition[b]			
	DIC	DIC + HA	DIC + P	DIC + HA + P
α-FeOOH/Fe_3O_4	CR, HC, PL[a]	CR, HC	HP, LT, PL	HP, HC, PL
α-Fe_2O_3	CR, HC, PL	CR, HC, PL, MS	HP, MS, PL	HP, MS, PL
Fe_3O_4	CR, HC, PL	CR, HC, PL, MS	HP, MS, PL	HP, CR, PL

[a]CR = cerussite, HC = hydrocerussite, PL = plumbonacrite, HP = hydroxypyromorphite, LT = litharge, MS = massicot

[b]DIC = dissolved inorganic carbon, HA = humic acid, P = orthophosphate

The composition of iron mineral cathodes was also verified by XRD: the pattern characterizing sintered hematite (Figure 26) was explained entirely by the hematite standard (ICDD PDF 01-077-9925). Diffraction peaks in the pattern representing sintered magnetite were accounted for primarily by magnetite (PDF 04-015-9120). Secondary reflections indicated that magnetite was partially oxidized to hematite, although this was not visually apparent. Field-extracted samples yielded an XRD pattern that was consistent with the presence of magnetite and goethite (PDF 00-029-0713).

5.4.4 Galvanic Corrosion Of Lead By Iron (Oxyhydr)oxides (Phase II)

Coupling lead anodes with iron mineral cathodes increased lead release by 531 μg L^{-1}, on average, compared with uniform corrosion of lead in the absence of iron (Table 13). Concurrently, a mean galvanic current of 4.5 μA was observed (range: 0.9–19.6 μA). Figure 23 displays lead levels grouped according to cathode material and electrolyte composition; hematite and magnetite cathodes increased lead release by averages of 83 and 721 μg L^{-1}, respectively. Field-extracted magnetite and goethite cathodes increased

lead release by 791 μg L^{-1}. Coupling lead with an iron mineral also substantially increased the variability of lead release, except in the presence of orthophosphate. The standard deviation of lead release to electrolyte dosed with orthophosphate alone increased from 5 to 6 μg L^{-1} between phases I and II, while the standard deviation across all other treatments increased from 61 to 1331 μg L^{-1} (Figure 43).

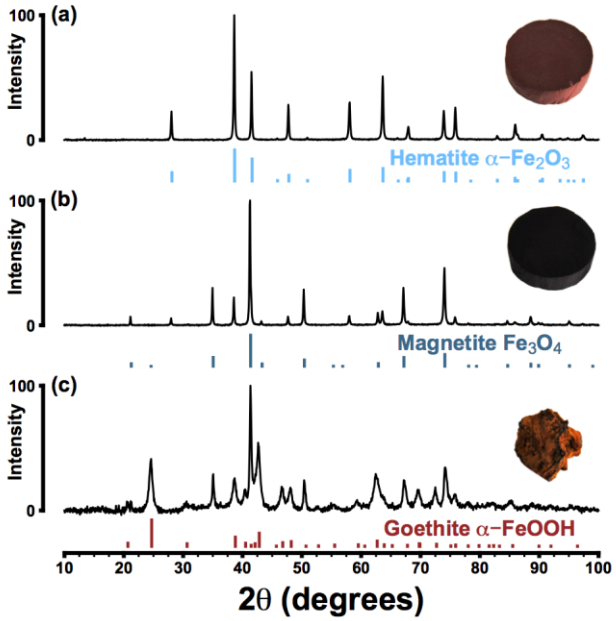

Figure 26 XRD patterns representing spark plasma sintered hematite and magnetite cathodes (*a* and *b*, respectively) and a field-extracted iron corrosion scale sample (*c*). Inset photographs: from top to bottom, sintered hematite, sintered magnetite, and field-extracted magnetite/goethite samples.

The effects of electrolyte modifiers were amplified following galvanic coupling. Humic acid and orthophosphate increased lead release due to uniform corrosion (phase I) by 81 and −74 μg L^{-1}, respectively, whereas these additives increased lead release due to galvanic corrosion (phase II) by 990 and −416 μg L^{-1} (Table 14). Considering phases I and II together allowed simultaneous estimation of the effects of all three experimental factors: humic acid increased lead release by 536 μg L^{-1}, orthophosphate by −245 μg L^{-1}, and iron (oxyhydr)oxide by 531 μg L^{-1}, as noted previously (Table 13). All effects were calculated as average lead release at one factor setting less average release at the other setting. Main effects for the three-factor model were all statistically significant (α = 0.001) following a natural log transformation of the response to improve the highly non-Gaussian and heteroscedastic residuals. Interaction terms were not statistically significant, even after log transformation.

As well as enhancing lead mobility, humic acid increased iron release from (oxyhydr)oxides. Neither orthophosphate nor cathode mineral, however, were statistically significant predictors of iron release. On average, addition of humic acid increased iron concentrations by 85 ± 75 μg L^{-1}(95% CI) (Table 15). Enhanced iron release in the presence of the humic isolate may have been due to complexation or possibly to colloidal dispersion; humic acid has a known stabilizing effect on iron oxide particles.[57,58] Iron in 48 h electrolyte averaged 115 ± 67 μg L^{-1} (SD) across all treatments, and the presence of iron may have promoted additional lead release. Adsorption of lead to suspended iron would be expected to decrease the activity of the lead cation, enhancing dissolution by maintaining undersaturation of the solubility-controlling lead phase.[59] However, the magnitude of galvanic current suggests that galvanic corrosion exerted a dominant influence on observed lead levels.

The pronounced effects of humic acid and orthophosphate on lead mobility can also be understood by comparing expected and observed lead release using current measurements. The differences can be attributed to scale formation. Adsorption at the cathode represents another possible sink, especially in the presence of humic acid, which, as a surface coating, tends to enhance adsorption of lead to iron oxides.[11] Figure 27 displays lead release as a function of oxidized lead, estimated from 0 h galvanic current using Faraday's law. In the presence of orthophosphate, oxidized lead was immobilized: 0.1–0.3% was released to the electrolyte. This may be attributed to accelerated formation of insoluble hydroxypyromorphite; mean 48 h phosphorus consumption increased from 30 μg L^{-1} over phase I to 164 ± 118 μg L^{-1} (95% CI) over phase II. Despite the effect of orthophosphate on lead release in general, coupling lead and magnetite in the presence of both orthophosphate and humic acid generated anomalously high lead levels and galvanic currents: 2071 μg L^{-1} and 13.1 μA, on average, vs 119 μg L^{-1} and 2.6 μA for the other cathode materials under the same conditions (Figure 23). This result may be attributed in part to the uniquely high electrical conductivity (approximately 2×10^4 Ω^{-1} m^{-1})[23] and low bandgap (0.2 eV)[60] of magnetite.

On its own, humic acid caused 11–20% of oxidized lead to be released. This increased mobility appears, based on SEC-ICP-MS analysis, to have been due to the formation of lead-humate complexes that would be expected to increase lead solubility and inhibit precipitation of scale-forming compounds at the anode.[50] This phenomenon is

analogous to the effect of chloride, as a complexing ligand, in promoting release of lead oxidized in galvanic corrosion reactions.[61] However, the effect of humic acid in the presence of an (oxyhydr)oxide cathode cannot be explained entirely by complexation: only 54 ± 28% (SD) of lead released to humic-amended electrolyte was present in 0.45 µm filtrate. In addition to complexing lead in solution, humic acid may have aided in the dispersion of particulate lead or may have inhibited formation of a compact and durable low-solubility scale.

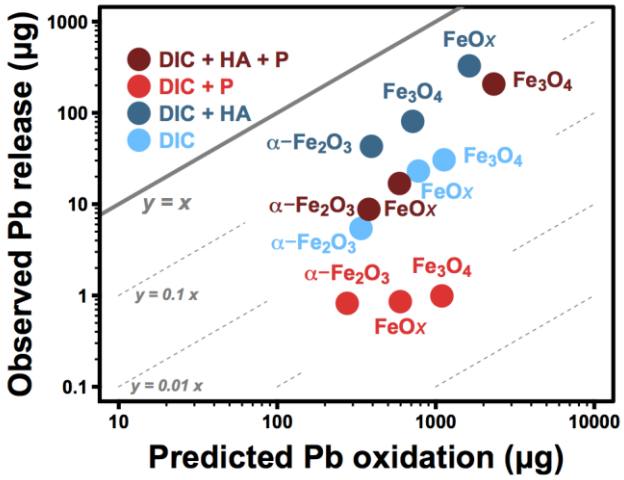

Figure 27 Humic acid enhanced lead mobility, while orthophosphate inhibited it. Points represent mean lead release as a function of mean lead oxidation, grouped by electrolyte composition (DIC = dissolved inorganic carbon, HA = humic acid, P = orthophosphate, and FeO*x* = field-extracted iron corrosion scale composed of magnetite and goethite).

While orthophosphate and humic acid influenced lead release significantly, neither factor was a statistically significant predictor of galvanic current. Electrolyte modifiers appeared to impact lead release to a greater degree than they did the rate of redox reactions as inferred from current measurements. Cathode material, however, did predict galvanic current: sintered magnetite and hematite cathodes yielded mean currents of 7.1 ± 4.1 (SD) and 1.9 ± 0.5 µA, respectively, and field-extracted cathodes yielded a mean current of 4.6 ± 3.7 µA.

5.4.5 Implications For Controlling Lead Release To Drinking Water

Upstream iron corrosion was a significant determinant of lead release from lead service lines. Point-of-use lead levels after lead service line replacement were greater by factors of 1.9 (full LSLR) and 4.8 (partial LSLR) at sites supplied by unlined iron

distribution mains compared with the alternative, lined iron pipe (Figure 28 and Table 7). High levels of iron were also more frequently observed at study sites supplied by unlined iron mains: at the 6 mo. follow-up 40% of samples collected at these sites contained more than 50 μg Fe L^{-1}, compared with just 6% at sites supplied by lined iron. In general, however, iron and lead levels were not highly correlated at the point of use. Partial replacement accompanied considerably greater lead release at all follow-up sampling rounds,[33] but elevated lead levels following full replacement were also observed. These were attributed to corrosion of brass or lead solder or to lead release from particulate deposits within premises plumbing. Potential explanations for higher lead in the presence of upstream iron corrosion include adsorption and transport of lead by iron-rich particles,[8,9,20,62] deposition corrosion of lead by particulate iron (oxyhydr)oxides, and inhibition of protective scale formation by iron.[62] Variation in pH between sites supplied by lined and unlined distribution mains could not explain variation in lead release: pH in flushed samples collected at sites with unlined distribution mains was greater by just 0.06 (95% CI: -0.02 – 0.12, rank-sum test, no transformation). Conversely, turbidity in flushed samples collected at sites with unlined distribution mains was greater by 0.02 NTU (95% CI: 0.01 – 0.04, rank-sum test, no transformation).

Table 7 Lead levels 6 mo. after lead service line replacement were greater by factors of 1.9−4.8 at sites supplied by unlined compared with lined iron distribution mains.

LSL configuration	Unlined iron main		Lined iron main		Multiplicative difference	
	No. of sites	90th percentile Pb (μg L^{-1})	No. of sites	90th percentile Pb (μg L^{-1})	Estimate (c)[a]	95% confidence interval
Pre-LSLR	17	30.2	25	25.7	1.0	0.6 – 1.9
Partial LSLR	15	51.6	15	12.4	4.8**	1.9 – 10.1
Full LSLR	23	9.3	21	4.0	1.9*	1.0 – 4.1

[a]The constant c estimates the ratio y/x, where x and y denote the quantiles of the observations at sites with lined and unlined iron mains, respectively. Multiplying x by c estimates y.
[b]Statistical significance: *$p < 0.05$ and **$p < 0.01$
[c]Percentiles include both standing and flushed samples.

Elevated lead levels due to iron particles could be addressed by replacing corroded iron distribution mains or by implementing rehabilitation regimes that reduce the likelihood of particle release from iron scale.[8,62,63] Orthophosphate has delivered mixed results in reducing iron release from corroded pipes,[64,65] but to the extent that it is effective in this regard, orthophosphate could offer indirect benefits for control of lead

release beyond a reduction in lead solubility (i.e., by also reducing release and deposition of iron particles).

Iron oxide deposition corrosion is analogous to a similar interaction between lead and copper. When copper is installed upstream from lead pipe—typically after partial lead service line replacement—copper deposited on lead downstream may corrode lead galvanically.[66,67] As oxygen electrodes, semiconducting iron (oxyhydr)oxide particles are also expected to be cathodic to copper, and the presence of a corroded iron main upstream from a partial lead service line connection could elevate both lead and copper release via deposition corrosion. Moreover, copper released via interaction with iron might then deposit downstream and promote further corrosion of lead. This could explain particularly high lead release from partial lead service lines supplied by cast iron distribution mains, as described here and elsewhere.[9,33]

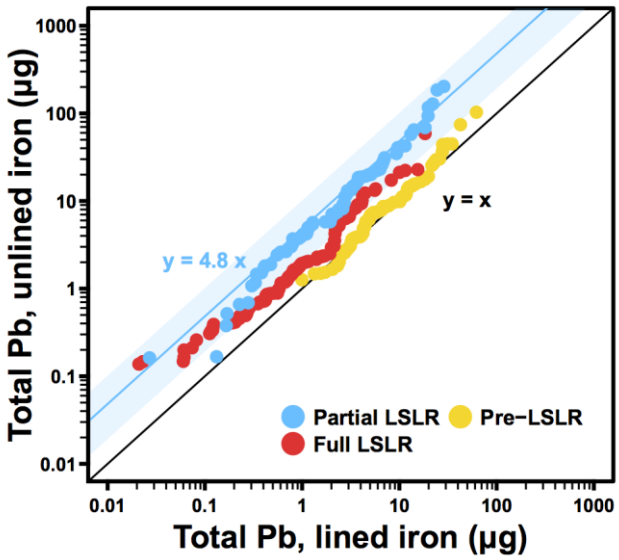

Figure 28 Following lead service line replacement, lead release was significantly greater at sites supplied by unlined compared with lined iron pipe. Points indicate sample quantiles representing the distribution of lead release before and after lead service line replacement. Quantiles were compared by water main composition and service line configuration at the 6 mo. follow-up round post-replacement. The blue line estimates the difference in lead release according to water main type following partial LSL replacement, and the shaded blue region indicates the 95% CI. Owing to unequal group sizes, quantiles representing the smaller group correspond to all n ordered observations, while quantiles representing the larger group correspond to interpolated values dividing the data into n equally spaced parts.

The role of complex-forming organic matter in lead–iron interactions may also be important in water systems that do not have optimized NOM removal. Recent lead

contamination events appear to have been driven by both iron corrosion/release and elevated concentrations of species that form soluble complexes with lead, including chloride and NOM.[68,69] While, in this study, humic acid was found to be highly effective in mobilizing lead oxidized by galvanic corrosion, optimized coagulation, or adsorption processes would be expected to remove the strongest complexing organic fractions, minimizing the effect of NOM on lead mobility.[70,71]

5.5 References

(1) Evens, A.; Hryhorczuk, D.; Lanphear, B. P.; Rankin, K. M.; Lewis, D. A.; Forst, L.; Rosenberg, D. The impact of low-level lead toxicity on school performance among children in the Chicago Public Schools: a population-based retrospective cohort study. *Environ. Health* **2015**, *14* (21), 1−9.
(2) Edwards, M.; Triantafyllidou, S.; Best, D. Elevated blood lead in young children due to lead-contaminated drinking water: Washington, DC, 2001− 2004. *Environ. Sci. Technol.* **2009**, *43* (5), 1618−1623.
(3) Hanna-Attisha, M.; LaChance, J.; Sadler, R. C.; Champney Schnepp, A. Elevated blood lead levels in children associated with the Flint drinking water crisis: a spatial analysis of risk and public health response. *Am. J. Public Health* **2016**, *106* (2), 283-290.
(4) Maximum contaminant level goals and national primary drinking water regulations for lead and copper. Final rule *Fed. Regist.*, **1991**, *56*, 26460
(5) *Guidance on Controlling Corrosion in Drinking Water Distribution Systems*; Catalogue H128-1/09-595E; Health Canada: Ottawa, Canada, 2009; http://www.hc-sc.gc.ca/ewh-semt/alt_formats/hecs-sesc/pdf/pubs/water-eau/corrosion/corrosion-eng.pdf.
(6) Deshommes, E.; Laroche, L.; Nour, S.; Cartier, C.; Prévost, M. Source and occurrence of particulate lead in tap water. *Water Res.* **2010**, *44* (12), 3734−3744.
(7) McFadden, M.; Giani, R.; Kwan, P.; Reiber, S. H. Contributions to drinking water lead from galvanized iron corrosion scales. *J. Am. Water Works Assoc.* **2011**, *103* (4), 76−89.
(8) Masters, S.; Edwards, M. Increased lead in water associated with iron corrosion. *Environ. Eng. Sci.* **2015**, *32* (5), 361−369.
(9) Camara, E.; Montreuil, K. R.; Knowles, A. K.; Gagnon, G. A. Role of the water main in lead service line replacement: A utility case study. *J. Am. Water Works Assoc.* **2013**, *105* (8), E423−E431.
(10) Trueman, B. F.; Gagnon, G. A. Understanding the role of particulate iron in lead release to drinking water. *Environ. Sci. Technol.* **2016**, *50*, 7389−7396.
(11 Liu, J. F.; Zhao, Z. S.; Jiang, G. B. Coating Fe_3O_4 magnetic nanoparticles with humic acid for high efficient removal of heavy metals in water. *Environ. Sci. Technol.* **2008**, *42* (18), 6949−6954.
(12) Rodda, D. P.; Johnson, B. B.; Wells, J. D. The effect of temperature and pH on the adsorption of copper (II), lead (II), and zinc (II) onto goethite. *J. Colloid Interface Sci.* **1993**, *161* (1), 57−62.
(13) Yang, F.; Shi, B.; Gu, J.; Wang, D.; Yang, M. Morphological and physicochemical characteristics of iron corrosion scales formed under different water source histories in a drinking water distribution system. *Water Res.* **2012**, *46*, 5423-5433.
(14) Peng, C. Y.; Korshin, G. V.; Valentine, R. L.; Hill, A. S.; Friedman, M. J.; Reiber, S. H. Characterization of elemental and structural composition of corrosion scales and deposits formed in drinking water distribution systems. *Water Res.* **2010**, *44* (15), 4570−4580.
(15) Gerke, T. L.; Maynard, J. B.; Schock, M. R.; Lytle, D. L. Physiochemical characterization of five iron tubercles from a single drinking water distribution system: Possible new insights on their formation and growth. *Corros. Sci.* **2008**, *50*, 2030−2039.
(16) Sarin, P.; Snoeyink, V. L.; Bebee, J.; Jim, K. K.; Beckett, M. A.; Kriven, W. M.; Clement, J. A. Iron release from corroded iron pipes in drinking water distribution systems: effect of dissolved oxygen. *Water Res.* **2004**, *38* (5), 1259-1269.
(17) Senftle, F. E.; Thorpe, A. N.; Grant, J. R.; Barkatt, A. Superparamagnetic nanoparticles in tap water. *Water Res.* **2007**, *41* (13), 3005−3011.

(18) Barkatt, A.; Pulvirenti, A. L.; Adel-Hadadi, M. A.; Viragh, C.; Senftle, F. E.; Thorpe, A. N.; Grant, J. R. Composition and particle size of superparamagnetic corrosion products in tap water. *Water Res.* **2009**, *43* (13), 3319−3325.
(19) Harrison, R. M.; Laxen, D. P. Physicochemical speciation of lead in drinking water. *Nature* **1980**, *286*, 791-793.
(20) Trueman, B. F.; Gagnon, G. A. A new analytical approach to understanding nanoscale lead-iron interactions in drinking water distribution systems. *J. Hazard. Mater.* **2016**, *311*, 151−157.
(21) Schock, M. R.; Hyland, R. N.; Welch, M. M. Occurrence of contaminant accumulation in lead pipe scales from domestic drinking water distribution systems. *Environ. Sci. Technol.* **2008**, *42* (12), 4285−4291.
(22) Benjamin, M.M.; Sontheimer, H.; Leroy, P. Corrosion of iron and steel. In *Internal corrosion of water distribution systems*; AWWA Research Foundation: Denver, CO, 1996; pp. 29-70.
(23) Vago, E. R.; Calvo, E. J. Electrocatalysis of oxygen reduction at Fe_3O_4 oxide electrodes in alkaline solutions. *J. Electroanal. Chem.* **1992**, *339*, 41−67.
(24) Vago, E. R.; Calvo, E. J.; Stratmann, M. Electrocatalysis of oxygen reduction at well-defined iron oxide electrodes. *Electrochim. Acta* **1994**, *39* (11), 1655−1659.
(25) Berthouex, P. M.; Brown, L. C. *Statistics for environmental engineers*; CRC Press: Boca Raton, Fl., 2002; p. 239.
(26) El Mendili, Y.; Bardeau, J. F.; Randrianantoandro, N.; Grasset, F.; Greneche, J. M. Insights into the mechanism related to the phase transition from γ-Fe_2O_3 to α-Fe_2O_3 nanoparticles induced by thermal treatment and laser irradiation. *J. Phys. Chem. C* **2012**, *116* (44), 23785-23792.
(27) Gialanella, S.; Girardi, F.; Ischia, G.; Lonardelli, I.; Mattarelli, M.; Montagna, M. On the goethite to hematite phase transformation. *J. Therm. Anal. Calorim.* **2010**, *102* (3), 867-873.
(28) R: A language and environment for statistical computing; R Foundation for Statistical Computing: Vienna, Austria, 2014; https://www.r-project.org.
(29) Garay, J. E. Current-activated, pressure-assisted densification of materials. *Annu. Rev. Mater. Res.* **2010**, *40*, 445−468.
(30) MPIF Standard 42. Determination of density of compacted or sintered metal powder products. In *Standard test methods for metal powders and powder metallurgy products*; Metal Powder Industries Federation: Princeton, NJ, 2000.
(31) American Public Health Association, American Waterworks Association, Water Pollution Control Federation. Standard Methods For the Examination of Water and Wastewater, 22nd ed.; American Public Heath Association: Washington, DC, 2012.
(32) Vadasarukkai, Y. S.; Gagnon, G. A. Application of low-mixing energy input for the coagulation process. *Water Res.* **2015**, *84*, 333-341.
(33) Trueman, B. F.; Camara, E.; Gagnon, G. A. Evaluating the effects of full and partial lead service line replacement on lead levels in drinking water. *Environ. Sci. Technol.* **2016**, *50*, 7389-7396.
(34) Helsel, D. R.; Hirsch, R. M. *Statistical Methods in Water Resources*; Elsevier: Amsterdam, 1992.
(35) Schock, M. R. Understanding corrosion control strategies for lead. *J. Am. Water Works Assoc.* **1989**, *81* (7), 88−100.
(36) Masters, S.; Welter, G. J.; Edwards, M. Seasonal variations in lead release to potable water. *Environ. Sci. Technol.* **2016**, *50* (10), 5269-5277.
(37) Noel, J. D.; Wang, Y.; Giammar, D. E. Effect of water chemistry on the dissolution rate of the lead corrosion product hydrocerussite. *Water Res.* **2014**, *54*, 237-246.
(38) Owen, D. M.; Chowdhury, Z. K.; Summers, R. S.; Hooper, S. M.; Solarik, G.; Gray, K. *Removal of DBP precursors by GAC adsorption*; AWWA Research Foundation: USA, 1998.
(39) Xia, K.; Bleam, W.; Helmke, P. A. Studies of the nature of Cu^{2+} and Pb^{2+} binding sites in soil humic substances using X-ray absorption spectroscopy. *Geochim. Cosmochim. Acta* **1997**, *61*(11), 2211-2221.
(40) Manceau, A.; Boisset, M. C.; Sarret, G.; Hazemann, J. L.; Mench, M.; Cambier, P.; Prost, R. Direct determination of lead speciation in contaminated soils by EXAFS spectroscopy. *Environ. Sci. Technol.* **1996**, *30*, 1540-1552.
(41) Korshin, G. V.; Ferguson, J. F.; Lancaster, A. N. Influence of natural organic matter on the morphology of corroding lead surfaces and behavior of lead-containing particles. *Water Res.* **2005**, *39*, 811-818.
(42) Martinez, C. E.; Jacobson, A. R.; McBride, M. B. Lead phosphate minerals: solubility and dissolution by model and natural ligands. *Environ. Sci. Technol.* **2004**, *38*, 5584-5590.
(43) Kuech, T. R.; Hamers, R. J.; Pedersen, J. A. Chemical transformations of metal, metal oxide, and

metal chalcogenide nanoparticles in the environment. In *Engineered nanoparticles and the environment: Biophysicochemical processes and toxicity*; Xing, B., Vecitis, C. D., Senesi, N., Eds.; John Wiley & Sons: Hoboken, NJ 2016; pp 271.
(44) Lin, Y. P.; Valentine, R. L. The release of lead from the reduction of lead oxide (PbO_2) by natural organic matter. *Environ. Sci. Technol.* **2008**, *42*, 760-765.
(45) Dryer, D. J.; Korshin, G. V. Investigation of the reduction of lead dioxide by natural organic matter. *Environ. Sci. Technol.* **2007**, *41* (15), 5510-5514.
(46) McNeill, L. S.; Edwards, M. Phosphate inhibitor use at US utilities. *J. Am. Water Works Assoc.* **2002**, *94* (7), 57−63.
(47) Hayes, C. R.; Incledion, S.; Balch, M. Experience in Wales (UK) of the optimisation of orthophosphate dosing for controlling lead in drinking water. *J. Water Health* **2008**, *6* (2), 177-185.
(48) Xie, L.; Giammar, D. E. Equilibrium solubility and dissolution rate of the lead phosphate chloropyromorphite. *Environ. Sci. Technol.* **2007**, *41*, 8050–8055.
(49) Hopwood, J. D.; Davey, R. J.; Jones, M. O.; Pritchard, R. G.; Cardew, P. T.; Booth, A. Development of chloropyromorphite coatings for lead water pipes. *J. Mater. Chem.* **2002**, *12* (6), 1717-1723.
(50) Debela, F.; Arocena, J. M.; Thring, R. W.; Whitcombe, T. Organic acids inhibit the formation of pyromorphite and Zn-phosphate in phosphorous amended Pb-and Zn-contaminated soil. *J. Environ. Manage.* **2013**, *116*, 156-162.
(51) Kozai, N.; Ohnuki, T.; Iwatsuki, T. Characterization of saline groundwater at Horonobe, Hokkaido, Japan by SEC-UV-ICP-MS: Speciation of uranium and iodine. *Water Res.* **2013**, *47* (4), 1570-1584.
(52) Schock, M. R.; Wagner, I.; Oliphant, R. J. Corrosion and solubility of lead in drinking water. In *Internal corrosion of water distribution systems*; AWWA Research Foundation: Denver, CO, 1996; pp. 131-230.
(53) Hu, J.; Gan, F.; Triantafyllidou, S.; Nguyen, C. K.; Edwards, M. A. Copper-induced metal release from lead pipe into drinking water. *Corrosion* **2012**, *68* (11), 1037-1048.
(54) Wang, Y.; Jing, H.; Mehta, V.; Welter, G. J.; Giammar, D. E. Impact of galvanic corrosion on lead release from aged lead service lines. *Water Res.* **2012**, *46* (16), 5049-5060.
(55) Rahman, M. S.; Whalen, M.; Gagnon, G. A. Adsorption of dissolved organic matter (DOM) onto the synthetic iron pipe corrosion scales (goethite and magnetite): effect of pH. *Chem. Eng. J.* **2013**, *234*, 149–157.
(56) Wang, Y.; Mehta, V.; Welter, G. J.; Giammar, D. E. Effect of connection methods on lead release from galvanic corrosion. *J. Am. Water Works Assoc.* **2013**, *105* (7), E337-E351.
(57) Zhang, Y.; Chen, Y.; Westerhoff, P.; Crittenden, J. Impact of natural organic matter and divalent cations on the stability of aqueous nanoparticles. *Water Res.* **2009**, *43* (17), 4249-4257.
(58) Sander, S.; Mosley, L. M.; Hunter, K. A. Investigation of interparticle forces in natural waters: Effects of adsorbed humic acids on iron oxide and alumina surface properties. *Environ. Sci. Technol.* **2004**, *38* (18), 4791-4796.
(59) Hill, D. M.; Aplin, A. C. Role of colloids and fine particles in the transport of metals in rivers draining carbonate and silicate terrains. *Limnol. Oceanogr.* **2001**, *46* (2), 331-344.
(60) Jordan, K.; Cazacu, A.; Manai, G.; Ceballos, S. F.; Murphy, S.; Shvets, I. V. Scanning tunneling spectroscopy study of the electronic structure of Fe_3O_4 surfaces. *Phys. Rev. B* **2006**, *74*, 085416.
(61) Nguyen, C. K.; Stone, K. R.; Dudi, A.; Edwards, M. A. Corrosive microenvironments at lead solder surfaces arising from galvanic corrosion with copper pipe. *Environ. Sci. Technol.* **2010**, *44* (18), 7076-7081.
(62) Schock, M. R.; Cantor, A. F.; Triantafyllidou, S.; Desantis, M. K.; Scheckel, K. G. Importance of pipe deposits to Lead and Copper Rule compliance. *J. Am. Water Works Assoc.* **2014**, *106* (7), E336-E349.
(63) Cantor, A. F. Optimization of phosphorus-based corrosion control chemicals; *In Proceedings of the 2016 AWWA Water Quality Technology Conference*; AWWA: Indianapolis, IN, 2016.
(64) Lytle, D. A.; Sarin, P.; Snoeyink, V. L. The effect of chloride and orthophosphate on the release of iron from a cast iron pipe section. *J. Water Supply Res. T.* **2005**, *54* (5), 267-281.
(65) McNeill, L. S.; Edwards, M. Phosphate inhibitors and red water in stagnant iron pipes. *J. Environ. Eng.* **2000**, *126* (12), 1096-1102.
(66) Clark, B.; St. Clair, J.; Edwards, M. Copper deposition corrosion elevates lead release to potable water. *J. Am. Water Works. Assoc.* **2015**, *107* (11), E627-E637.
(67) Cartier, C.; Arnold, R. B.; Triantafyllidou, S.; Prévost, M.; Edwards, M. Effect of flow rate and lead/copper pipe sequence on lead release from service lines. *Water Res.* **2012**, *46* (13), 4142-4152.

(68) Pieper, K. J.; Tang, M.; Edwards, M. A. Flint water crisis caused by interrupted corrosion control: investigating “ground zero” home. *Environ. Sci. Technol.* **2017**, *51* (4), 2007-2014.
(69) Winning, L. D.; Gorczyca, B.; Brezinski, K. Effect of total organic carbon and aquatic humic substances on the occurrence of lead at the tap. *Water Qual. Res. J.* **2017**, *52* (1), 2-10.
(70) Colling, J. H.; Croll, B. T.; Whincup, P. A. E.; Harward, C. Plumbosolvency effects and control in hard waters. *Water Environ. J. Can.* **1992**, *6* (4), 259-268.
(71) Korshin, G. V.; Ferguson, J. F.; Lancaster, A. N.; Wu, H. *Corrosion and metal release for lead-containing materials: influence of NOM*; AWWA Research Foundation: USA, 1999.

Chapter 6 Effects Of Ortho- And Polyphosphates On Lead Speciation In Drinking Water

6.1 Abstract

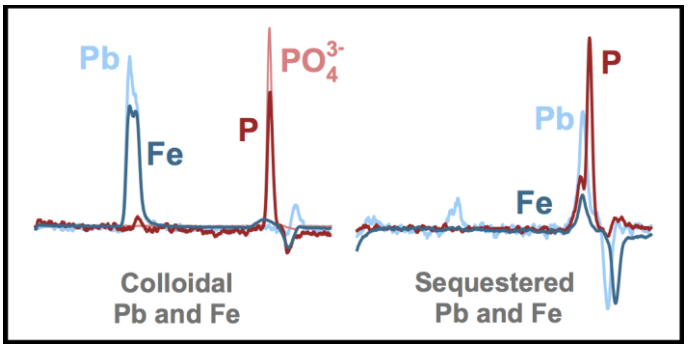

Figure 29 The presence of polyphosphate in distributed water appeared to sequester lead and iron in solution. In the absence of significant polyphosphate, lead and iron were present as colloidal particles.

Lead is a potent neurotoxin and drinking water represents an important route of exposure, especially where legacy lead pipe is widespread. Polyphosphates are often added to drinking water to sequester iron and calcium, but they may form coordination complexes with lead, increasing its solubility. This risk is not well characterized in practice: the prevalence of lead-polyphosphate complexes in drinking water systems is not known. We used size-exclusion chromatography (SEC) with multi-element detection to compare the speciation of lead below 0.45 µm in two water systems dosing phosphate-based corrosion inhibitors at different ortho:poly ratios and doses. In one system dosing polyphosphate at 0.05 mg P L^{-1} (3:1 ratio), it reverted almost completely to orthophosphate during distribution. In another system dosing polyphosphate at 0.20 mg P L^{-1} (1:1 ratio), it was detectable at points of use. Under the influence of polyphosphate, lead and iron were present as dissolved species strongly associated with phosphorus. Moreover, experiments with sodium hexametaphosphate confirmed our ability to detect lead as a coordination complex using SEC. In the absence of polyphosphate, lead and iron were present as colloidal particles. Orthophosphate on its own also appeared to reduce lead solubility, as estimated using paired sample profiles collected at seventeen single-unit residences. Increasing orthophosphate from 0.5 to 1.0 mg PO_4 L^{-1} accompanied decreases in lead levels of 38% (95% CI: 15 – 51%) within eight months.

Analysis of recovered lead pipe corrosion scale was consistent with the presence of an insoluble lead phosphate compound: hydroxypyromorphite ($Pb_5(PO_4)_3OH$).

6.2 Introduction

Lead service lines (LSLs) were installed widely throughout the first half of the twentieth century; in the United States, millions remain in place.[1] Legacy lead pipe is a significant public health concern because lead in drinking water is a risk factor for elevated blood lead.[2-4] High blood lead in childhood is strongly associated with lasting deficits in cognitive and academic skills.[5-8] The effect of childhood lead exposure is non-linear: at lower levels, increases in blood lead accompany steeper declines in cognitive performance.[5,6,8]

Orthophosphate is added to drinking water to limit corrosion and release of lead from distribution networks.[9] Orthophosphate inhibits lead release by forming insoluble lead phosphate compounds: possibilities include hydroxypyromorphite ($Pb_5(PO_4)_3OH$), chloropyromorphite ($Pb_5(PO_4)_3Cl$), and tertiary lead phosphate ($Pb_3(PO_4)_2$).[10,11] Orthophosphate may also inhibit dissolution of lead carbonates or other lead compounds by adsorbing to and passivating mineral surfaces,[12] as has been suggested in the case of calcite.[13] However, certain chemical species can interfere with these mechanisms. Successful formation of a phosphate-rich corrosion scale requires lead-phosphate supersaturation: species that form soluble complexes with lead—including carbonate and natural organic matter (NOM)[14,15]—can increase the equilibrium solubility of lead-phosphates (e.g., hydroxypyromorphite solubility increases with increasing dissolved inorganic carbon).[12] Furthermore, precipitation of other metal-phosphates (e.g., hydroxyapatite, $Ca_5(PO_4)_3OH$, in hard waters) may interfere with lead solubility control.[10]

Orthophosphate has been shown to inhibit lead release to drinking water in both laboratory and pilot studies.[16,17] Field data have provided additional confirmation—using random daytime,[18-20] 30 m stagnant,[21] or 6 h stagnant sampling[22,23]—that orthophosphate is effective in limiting lead release under at least some conditions (e.g., alkalinity less than 30 mg L^{-1} as $CaCO_3$). In other circumstances (e.g., at higher alkalinity), orthophosphate-based inhibitors have yielded ambiguous, insignificant, or adverse results

with respect to lead corrosion control.[22,24] Nevertheless, orthophosphate treatment has been an important aspect of the response to severe instances of drinking water lead contamination, including those that occurred in Washington, DC (2001 – 2004)[25] and Flint, MI (2014 – 2016).[26] After orthophosphate dosing had been initiated, lead pipe corrosion scale recovered from the Washington, DC distribution system was dominated by hydroxypyromorphite.[27]

As well as reducing lead solubility, orthophosphate may be used to control copper and iron release.[9,28] Orthophosphate has been shown in laboratory studies to reduce iron release from corroded iron pipes.[29,30] In other cases (e.g., under extended stagnant conditions), it has increased or had little effect on iron levels in water.[31] Orthophosphate may inhibit iron release via formation of sparingly soluble films composed of iron-phosphates (e.g., vivianite, $Fe_3(PO_4)_2 \cdot 8H_2O$).[32] Such films may act as diffusion barriers or may reduce the solubility of ferrous iron.[30,33] Adsorption of orthophosphate ions may also inhibit reductive and non-reductive ligand-promoted dissolution of ferric (oxyhydr)oxides.[34,35] Orthophosphate can reduce copper release by promoting formation of relatively insoluble copper-phosphates, such as $Cu_3(PO_4)_2$, over the more soluble cupric hydroxide ($Cu(OH)_2$).[36-38] However, copper-phosphates have higher equilibrium solubility than malachite ($Cu_2CO_3(OH)_2$) or tenorite (CuO), compounds that evolve slowly from newly precipitated cupric hydroxide. Since malachite and tenorite formation is inhibited by orthophosphate, natural aging of corrosion scale may eventually lower copper concentrations further than orthophosphate treatment.[37,38]

Orthophosphate is frequently dosed with polyphosphate as a blended formulation.[9] Polyphosphates form strong complexes with many metals and are useful as sequestering agents for the prevention of coloured water and scaling due to iron oxidation and calcium carbonate precipitation, respectively.[9,39,40] Polyphosphates may form soluble complexes with lead or copper, increasing solubility by maintaining low activity of the metal cation and undersaturation of the solubility-controlling phase.[39] Polyphosphates have been shown to enhance metal release from lead and copper pipes in laboratory studies.[16,41] These have been corroborated by observations of elevated lead in systems dosing polyphosphates.[22,42] Nevertheless, polyphosphates revert to orthophosphate over time, and blends could be effective in systems where reversion is relatively fast or where

metals other than lead are preferentially complexed.[41] Inhibition of copper release by polyphosphates in previous work has been attributed to orthophosphate reversion.[43]

We evaluated the effect of polyphosphate on lead speciation and the effect of orthophosphate on lead solubility. Data were collected in three separate water distribution systems via point-of-use sampling. These systems were characterized by several risk factors for elevated lead release: (1) distributed water pH in the circumneutral range (pH 7.2 – 7.3), (2) distribution by unlined cast iron mains,[44,45] and (3) in two systems, a chloride-to-sulfate mass ratio above the critical threshold of 0.5 – 0.77 identified in previous work as a driver of galvanic corrosion.[46,47]

6.3 Materials And Methods

6.3.1 Study Area

The study area comprised both single-unit residences and non-residential buildings that were known or suspected to be at risk for high lead levels in drinking water. Residential study sites were supplied by one of two water systems, denoted A and B. Non-residential sites were supplied by system C. Participating residences supplied by system A had full (12 sites) or partial LSLs (6 sites, including one site with a public LSL and a private line of unknown composition). Among the sites with partial LSLs, none had recently undergone replacement. In system B, service line configurations at participating residences were not known. However, based on a threshold of 1 μg Pb L^{-1} in flushed samples collected at near-peak water temperatures,[48] six sites were suspected to have service lines composed at least partially of lead. Non-residential outlets in system C included fountains and faucets but none of the service line configurations were known.

Sample sites in system A were supplied by cast iron distribution mains. In system B, two sites were supplied by cast iron, and the rest were supplied by either cement-mortar-lined mains or those of unknown composition. While unlined cast iron mains were common in system C, the composition of distribution mains supplying study sites was not known. Sample sites in systems A and B received distributed water from facilities described elsewehere.[49] These facilities employ enhanced coagulation by alum and free chlorine disinfection. System C was supplied by a facility employing enhanced coagulation, membrane microfiltration, and free chlorine disinfection. Treated water

quality is summarized in Table 8 for systems A – C.[50] All three systems applied blended ortho/polyphosphate corrosion inhibitors (Systems A and B dosed a 3:1 and system C a 1:1 ortho:poly formulation). In September 2015 A and B switched to formulations that did not include polyphosphate, and in April 2016, A and B increased the orthophosphate dose from 0.5 to 1.0 mg PO_4 L^{-1}.

Table 8 Typical values for treated water quality parameters, pre-distribution.

Parameter	System A	System B	System C[a]
Alkalinity (*as* $CaCO_3$)	22.5 mg L^{-1}	19.0 mg L^{-1}	13 mg L^{-1}
Free chlorine	1.2 mg L^{-1}	1.3 mg L^{-1}	<0.5 mg L^{-1}
Hardness (*as* $CaCO_3$)	10.1 mg L^{-1}	32.0 mg L^{-1}	5.0 mg L^{-1}
Total organic carbon	1.6 mg L^{-1}	1.8 mg L^{-1}	1.9 mg L^{-1}
pH	7.3	7.2	7.4
Chloride	8.9 mg L^{-1}	7.5 mg L^{-1}	7 mg L^{-1}
Sulfate	7.9 mg L^{-1}	25.0 mg L^{-1}	3 mg L^{-1}
Turbidity	<0.10 NTU	<0.04 NTU	0.5 NTU
Iron	<0.05 mg L^{-1}	<0.05 mg L^{-1}	<0.05 mg L^{-1}
Lead	<0.5 µg L^{-1}	<0.5 µg L^{-1}	<0.5 µg L^{-1}
Total phosphorus	-[b]	-[b]	0.34 mg L^{-1}
Orthophosphate (*as* P)	-[b]	-[b]	0.19 mg L^{-1}

[a]values represent flushed samples collected at a central location within the distribution system
[b]concentrations are discussed within the text

6.3.2 Sample Collection

Following a random daytime protocol,[18] we collected 250 mL samples at non-residential buildings in system C. Residents supplied by systems A and B collected profiles of six sequential 1L samples (L1− L6) from kitchen cold-water taps. These began with the first draw following a minimum 6 h standing period and were followed by a 10-minute flush of each outlet. Immediately after flushing, a seventh 1L sample (L7) was collected. Profiles were collected in April 2016 at an orthophosphate dose of 0.5 mg PO_4 L^{-1}, in June 2016 at an orthophosphate dose of 1.0 mg L^{-1}, and at approximate two-month intervals through April 2017. Residents were instructed to record exact stagnation times, to sample at maximum flow, and not to remove faucet aerators. Data were excluded from analysis when these instructions were not followed; sample sizes differ by round for this reason and also due to incomplete resident participation. Polyethylene (HDPE) bottles and caps were immersed in 2 M reagent-grade HNO_3 for a minimum of 24 h and rinsed thoroughly with ultrapure water prior to use.

6.3.3 Size-exclusion Chromatography With UV And ICP-MS Detection

The size-exclusion chromatography ICP-MS (SEC-ICP-MS) and SEC-UV

methods applied for the separation of field and experimental samples have been detailed in previous work.[51] All paired SEC-UV and SEC-ICP-MS separations were performed on an agarose-dextran stationary phase (Superdex 200, 10 × 300 mm, 13 µm nominal bead size, GE Healthcare) with a 50 mM tris-HCl mobile phase (pH 7.3) at a flow rate of 0.5 mL min^{-1}. Thyroglobulin (monitored as ^{127}I) and ovalbumin (^{31}P) were purchased from GE Healthcare and the humic isolate (monitored as ^{208}Pb) from Alfa Aesar. Injection volumes for SEC-UV and SEC-ICP-MS were 180 and 212 µL, respectively. All samples were filtered at 0.45 µm prior to size-separation.

6.3.4 Scale Analysis

Crystalline phases in lead pipe scale recovered from system A were identified using an X-ray diffractometer (Siemens D500) equipped with Cu$K\alpha$ radiation (λ = 1.54 Å) at 35 kV and 30 mA. Scans were performed with a step size of 0.05˚ (2θ) and a count time of 10.0 s per step. Scale was collected as a single layer from the interior of a recovered LSL section. Samples were held in a desiccator for 24 h and then finely ground with a mortar and pestle prior to XRD analysis. To determine elemental composition, scale samples were digested according to EPA method 3050B,[52] with modifications to accommodate the available sample mass and equipment. Digested samples were centrifuged at 3000 rpm for 10 m prior to dilution and analysis.

6.3.5 Other Analytical Methods

Total lead, iron, copper, aluminum, and phosphorus were measured by ICP-MS (Thermofisher X Series II, *Standard Methods 3125 and 3030*).[53] Reporting limits were 0.4, 6.0, 0.7, 4.0, and 4.9 µg L^{-1}, respectively. Orthophosphate was measured in a subset of samples, over the first two sampling rounds only, using a colorimeter (*Standard Method 4500-P E*).[53] Distributed water temperature data were obtained from the monitoring stations nearest the study sites.

6.3.6 Data Analysis

System A and B profiles collected before and after the increase in orthophosphate were paired by civic address. Metals concentrations in each of the seven litres were summed, and total masses over each profile were compared using two-tailed signed rank tests by follow-up round.[54] Natural log transformations were applied to the paired data to

promote symmetry in the distribution of differences. Multiplicative differences in lead levels were quantified using a Hodges−Lehmann estimator, c, where c = median(A_{ij}) and $A_{ij} = (D_i + D_j) / 2$ for all $i = 1, \ldots, n$ and $j \geq i$. The variable $D = \ln(x_i) - \ln(y_i)$ denotes the set of pairwise (log-transformed) differences, where x and y represent lead levels at n sites before and after the increase in orthophosphate to 1.0 mg PO_4 L^{-1}. The quantity c estimates the ratio of lead levels, where $y = \exp(c)\, x$.[55]

6.3.7 Model Distribution System

A model of system A was operated primarily to assess the effect of upstream iron corrosion on lead release under the influence of orthophosphate, as described elsewhere.[56] For this study, the model system comprised two pipe loops (one unlined iron and one PVC) and two pairs of simulated LSLs configured such that each pipe loop supplied one of the two LSL pairs. LSL and cast iron pipe sections were recovered from system A. The model system was operated for 41 weeks at an orthophosphate dose of 0.5 mg PO_4 L^{-1} (data not shown) and then for 51 weeks at 1.0 mg L^{-1}. Over this period, orthophosphate was supplied as the blended zinc ortho-polyphosphate product dosed in systems A and B before Sept. 2015 (75% orthophosphate, 25% polyphosphate). Finally, the model system was operated for 23 weeks at 1.0 mg PO_4 L^{-1} with orthophosphate supplied instead as phosphoric acid. Lead was quantified in 0.45 μm filtrate from 24 h-stagnant LSL effluent; filtration was performed using cellulose nitrate membrane filters mounted in syringe filter cartridges, as described previously.[51,56]

6.4 Results And Discussion

6.4.1 Lead Sequestration By Polyphosphate

The presence of polyphosphate—in a formulation intended specifically for sequestration—influenced the size distributions of lead and iron considerably. Figure 30 displays size-exclusion chromatograms representing typical separations of field samples collected in two separate water systems. In system A (Figure 30*a*), these metals consistently eluted together in a colloidal fraction at high apparent molecular weight. Colloidal lead and iron in system A may have originated from corrosion scale or may represent adsorption of lead to suspended colloidal iron (oxyhydr)oxides.[51,56-58] Consistent with the presence of colloidal particles rich in both elements, filtration of

system A field samples at 0.1 or 0.05 µm altered high molecular weight lead and iron peaks significantly and in near-identical fashion.[51] Furthermore, high molecular weight lead and iron eluted consistently on stationary phases with opposite surface charges, while dissolved metal standards were retained completely at environmentally relevant concentrations.[51] In previous work, lead and iron elution profiles and peak areas were highly correlated ($R^2_{average}$ = 0.96 and R^2 = 0.82, respectively).[51]

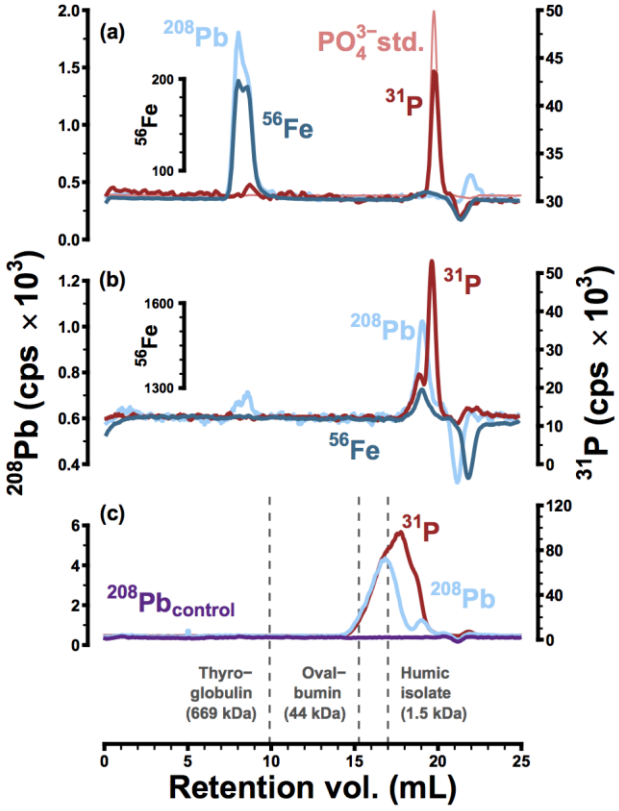

Figure 30 (a) In system A size-separations (pre-Sept. 2015), ^{208}Pb eluted in a high molecular weight (colloidal) fraction—along with ^{56}Fe—while ^{31}P eluted in the same retention volume as the orthophosphate anion. The peak retention volume of thyroglobulin is provided as a qualitative point of reference (hydrodynamic diameter: 17 nm). (b) In system C size-separations, ^{208}Pb and ^{56}Fe eluted in a low molecular weight (dissolved) fraction along with ^{31}P and consistent with sequestration by polyphosphate. (c) ^{208}Pb and ^{31}P coeluted at low apparent molecular weight in deionized water with sodium hexametaphosphate, a strong complexing agent for lead.

Size-separation provided little evidence of metal complexation within system A: lead, in particular, was never observed in a low apparent molecular weight fraction in anything more than trace quantities. Before Sept. 2015, the phosphate formulation added

to system A did include polyphosphate (dosed at 0.05 mg P L^{-1}), but it appeared to revert to orthophosphate during distribution: phosphorus in system A samples eluted consistently in the same retention volume as the orthophosphate anion (Figure 30). Previous work has demonstrated greater than 80% reversion of sodium hexametaphosphate in lead pipes at comparable pH and alkalinity, although reversion rates estimated from field data were lower.[40]

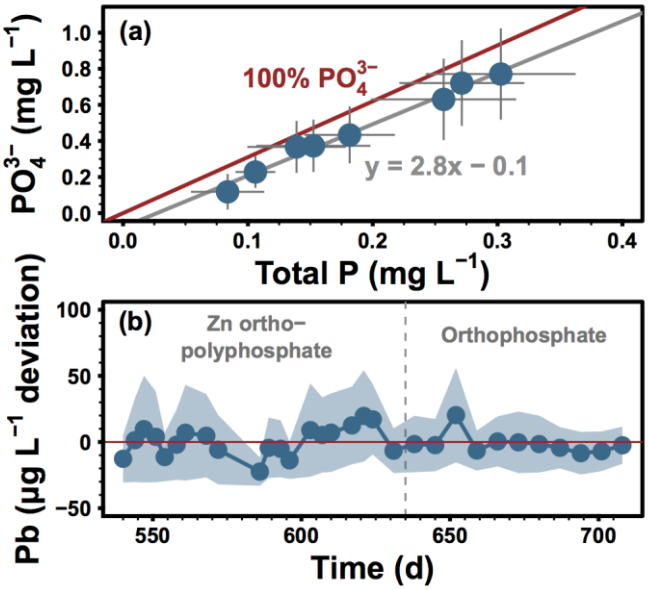

Figure 31 (a) Orthophosphate accounted for nearly all of the phosphorus present in effluent from eight LSL sections following simulated water distribution and a 24 h standing period within the LSLs. Points represent medians and error bars span the interquartile range. (b) After subtracting the global negative linear trend, mean lead in 0.45 µm-filtered effluent from four replicate LSL sections was not strongly influenced by switching from a blended zinc ortho-polyphosphate to phosphoric acid. Each point represents the mean of the four replicates, and the shaded region denotes one standard deviation about the mean.

Data from a model of system A were also consistent with the apparent reversion of polyphosphate in field samples (Figure 31*a*). As a linear predictor, phosphorus in LSL effluent explained 99% of the variation in orthophosphate ($\beta_1 = 2.8 \pm 0.3$, 95% CI). Under the assumption of complete reversion, the expected slope ($\beta_1 = 3.1$) was within the confidence bound of the linear model. SEC data provided additional assurance that polyphosphate complexation was not significant within the model system: lead eluted in an entirely separate fraction from phosphorus in typical size-separations.[56] Moreover, a change to phosphoric acid in the model system—from the zinc ortho-polyphosphate

applied at full-scale prior to Sept. 2015—did not appear to substantially influence lead solubility (Figure 31*b*). Lead release exhibited a negative trend that spanned—and was not clearly influenced by—the inhibitor change. While a negative trend in the standard deviation of lead release might be attributable to removing polyphosphate or zinc from the system, standard deviation was most correlated with lead concentration ($r = 0.93$). That is, the negative trend in variance was attributed to the global trend in lead concentration and not to changing the inhibitor. Moreover, the effect of zinc in phosphate formulations has been found elsewhere to be minimal.[59,60]

Lead and iron in system C (0.20 mg P L^{-1} polyphosphate) were consistently observed at low molecular weight, strongly associated with phosphorus. An estimated 55% of total phosphorus was present in system C as orthophosphate (Table 8). The apparent size-distribution of phosphorus in this system was bimodal: lead and iron coeluted with the higher apparent molecular weight phosphorus peak. This was interpreted as a consequence of sequestration/complexation. Polyphosphates form stable coordination complexes with many metals, including lead,[39] and polyphosphates can increase lead solubility due to complexation.[16,39] Random daytime samples collected within system C had a 90th percentile lead concentration of 33 µg L^{-1} ($n = 14$).

The ability of SEC to detect lead-polyphosphate complexes was confirmed by separation of deionized water with sodium bicarbonate (60 mg L^{-1}), lead nitrate (65 µg Pb L^{-1}), and sodium hexametaphosphate (2 mg P L^{-1}), a strong complexing agent for lead. After 16 h at pH 7.9, lead and phosphorus coeluted at low apparent molecular weight (Figure 30*c*). Without sodium hexametaphosphate, lead was retained on the stationary phase as expected. While lead only eluted in the presence of polyphosphate, lead and phosphorus peaks did not correspond entirely. This may have been due to the complex speciation of sodium hexametaphosphate[40] (i.e., the ^{31}P signal may represent multiple poorly resolved peaks, only one of which was associated with ^{208}Pb).

Complexation of lead by humic or fulvic acids can also increase lead solubility by maintaining undersaturation of the solubility-controlling phase (e.g., hydrocerussite or hyroxypyromorphite).[14] SEC with UV and multi-element detection has been used previously to characterize complexation of lead with NOM, and a strong correspondence between lead and UV absorption is typical in the presence of lead-NOM complexes.[44,61,62]

Previous size-separation of a humic acid solution that contacted metallic lead over 48 h was consistent with formation of an organic lead complex.[44] System A field data, in contrast, suggest that the strongest complexing fractions of NOM were removed during coagulation and filtration.[63] In separations of system A samples, lead never eluted in the same fraction as the principal UV_{254} signal at appreciable signal-to-noise ratios (Figure 32). Complexation of lead by NOM within system C was considered unlikely as well: as in system A, removal of complexing NOM fractions via enhanced coagulation/filtration was expected. NOM may, however, have influenced lead mobility by promoting colloidal dispersion of lead-rich particles.[64] This possibility is consistent with system A size-separations: colloidal lead and NOM (as UV_{254}) consistently eluted together at high apparent molecular weight (Figure 32).

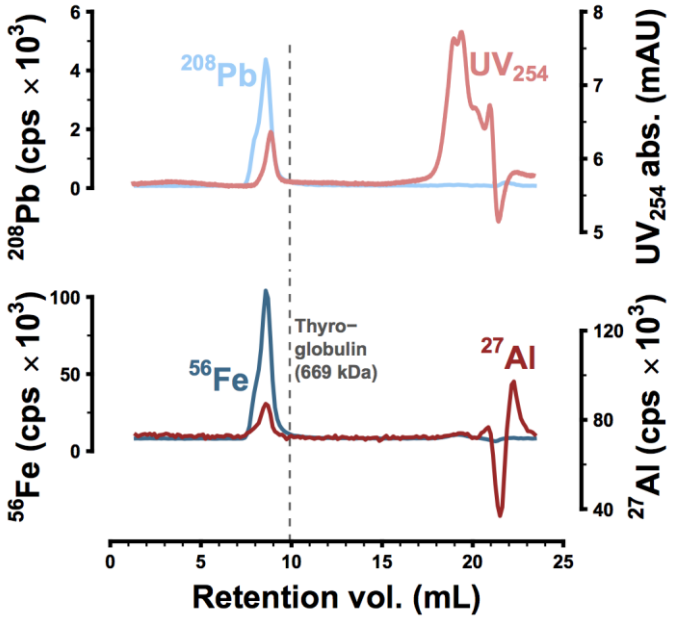

Figure 32 In system A size-separations, ^{208}Pb never eluted along with the principal NOM (UV_{254}) peak in anything more than trace quantities. Instead, ^{208}Pb eluted with the principal ^{56}Fe peak and a secondary, high molecular weight NOM peak in a colloidal fraction, as indicated in the typical chromatogram presented here. The peak retention volume of thyroglobulin is provided as a qualitative point of reference (hydrodynamic diameter 17 nm).

6.4.2 Controlling Lead And Copper Solubility With Orthophosphate

While polyphosphate in system C appeared to sequester/complex lead in solution, orthophosphate may have had the opposite effect in systems A and B by reducing lead solubility. Seven months after switching to an inhibitor formulation that did not include

polyphosphate, the orthophosphate dose in these water systems was increased from 0.5 to 1.0 mg PO_4 L^{-1}. This increase accompanied significant decreases in lead and copper release.

At the initial dose of 0.5 mg L^{-1}, lead and copper levels over the sample profile differed according to service line configuration (Figure 33). At sites with full LSLs, peak lead typically occurred in L4 or L5 (L5 median: 32.0 µg L^{-1}, range: 2.4 – 58.8 µg L^{-1}). At sites with partial LSLs, peak lead occurred in L3 (L3 median: 19.0 µg L^{-1}, range: <0.4 – 38.2 µg L^{-1}). These data are consistent with expected premises plumbing volumes of 2 – 3 litres.[65] At sites with unknown service line configurations, peak lead occurred in L4, although the distribution of lead across the sample profile was more uniform (L4 median: 0.6 µg L^{-1}, range: <0.4 – 13.8 µg L^{-1}).

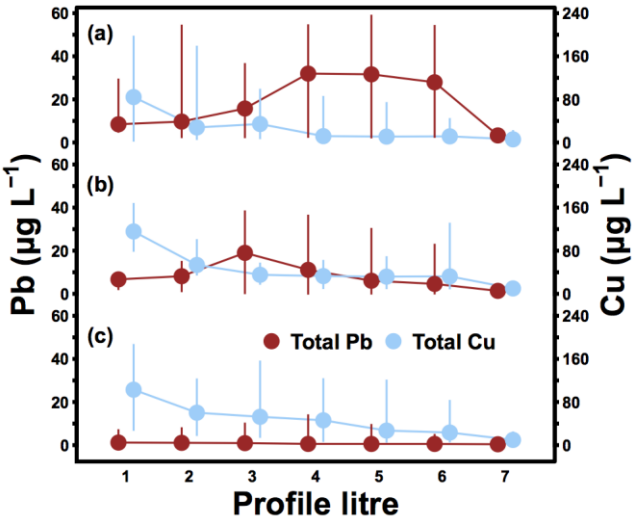

Figure 33 System A and B lead and copper levels at 0.5 mg PO_4 L^{-1} differed according to service line configuration: (a) full LSLs, (b) legacy partial LSLs, and (c) unknown service line configurations. Points represent medians and error bars denote ranges.

Phosphorus declined during stagnation, in agreement with the expected precipitation of lead/copper and phosphate or the adsorption of phosphate to corrosion scale. Orthophosphate demand at each study site was estimated as the largest difference between phosphorus in the flushed sample (L7) and the standing samples (L1 – L6). By this estimate, median phosphorus demand at 0.5 mg PO_4 L^{-1} was 13.3 µg L^{-1}. As expected, the dominant phosphorus species was orthophosphate: as a linear predictor, phosphorus concentration explained 97% of the variation in orthophosphate ($\beta_1 = 2.8 \pm$

0.1, 95% CI). Were all phosphorus present as orthophosphate, the expected value of β_1 would be 3.1, and the discrepancy may be attributed to a small fraction of total phosphorus present as other species.

Iron levels at 0.5 mg PO_4 L^{-1} differed most notably according to distribution main composition. At the initial orthophosphate level—and throughout the study—samples collected at sites supplied by cast iron distribution mains had higher iron than those collected at sites with lined ductile iron mains (median 8 µg L^{-1}, interquartile range (IQR) <6.0 – 34 µg L^{-1} and median <6 µg L^{-1}, IQR <6 – <6 µg L^{-1}, respectively). This was attributed to the fact that at least some of the cast iron mains were corroded and unlined. Iron release appeared to be temperature dependent: median iron in flushed samples was moderately correlated with distributed water temperature (r = 0.64). Moreover, the highest iron levels were observed at near-peak water temperatures: median iron in August was 22 µg L^{-1} (IQR: 8 – 53 µg L^{-1}) and 10 µg L^{-1} (7 – 28 µg L^{-1}) at sites with cast iron and ductile iron mains, respectively. Positive correlation between temperature and iron corrosion byproduct release has also been reported previously.[66]

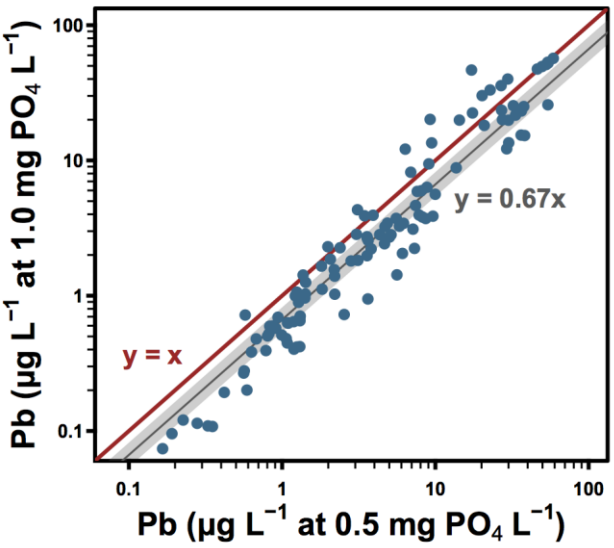

Figure 34 System A and B lead concentrations at 1.0 mg PO_4 L^{-1} were an estimated 67% of concentrations at 0.5 mg PO_4 L^{-1} (paired measurements at 17 residences comparing Apr. 2016 with an average of Dec., Mar., and Apr. 2017). The gray shaded region represents the 95% CI around the group difference estimate of 0.67.

Lead levels decreased following the increase to 1.0 mg PO_4 L^{-1} (Figure 34). Increasing orthophosphate also accompanied higher median phosphorus demand, from

13.3 µg L^{-1} at 0.5 mg PO_4 L^{-1} to 59 µg L^{-1} in June, at 1.0 mg L^{-1}. By April 2017, median phosphorus demand had dropped to 35 µg L^{-1}. Available data suggest that lead release was a strong positive linear function of temperature within system A at 0.5 mg L^{-1} ($r_{average}$ = 0.88).[67] Accordingly, a significant reduction in point-of-use lead was observed over the shortest interval for which temperature was approximately constant. December 2016 lead levels, at 1.0 mg PO_4 L^{-1}, were 62% of paired observations at 0.5 mg PO_4 L^{-1} the previous April (Table 2, 95% CI: 49 – 85%). Lead levels in March and April 2017 were lower than paired observations in April 2016 by similar magnitudes: 68 and 71%, respectively. Averaging by site over the last three sampling rounds, lead levels at 1.0 mg PO_4 L^{-1} were 67% of those observed at 0.5 mg L^{-1} (Figure 34 and Table 9, *final row*, 95% CI: 54 – 82%). Despite the probable influence of seasonally varying water quality, variation in lead release over the 6 sampling rounds at 1.0 mg PO_4 L^{-1} was generally low: standard deviations by site ranged from median 0.5 (L7) to 3.3 µg L^{-1} (L3) (systems A and B).

Table 9 Fraction of initial (2016-04) lead and copper levels remaining after increasing orthophosphate from 0.5 to 1.0 mg L^{-1}.

	% of initial Pb remaining			% of initial Cu remaining		
Date (*yyyy - mm*)	**Estimate[a]**	**95% CI**	**Distributed water temp. (˚C)**	**Estimate**	**95% CI**	**Paired sample size**
2016-04	-	-	9.6	-	-	-
2016-06	91	67 – 120	15.1	**79^{y}**	**71 – 87**	19
2016-08	89	64 – 130	21.8	**73^{z}**	**58 – 85**	19
2016-10	79	43 – 110	16.7	**73^{z}**	**62 – 83**	14
2016-12	**62^{y}**	**49 – 85**	9.4	**68^{z}**	**57 – 80**	16
2017-03	**68^{y}**	**55 – 87**	6.4	**67^{y}**	**55 – 88**	14
2017-04	**71^{y}**	**52 – 84**	8.1	**79^{y}**	**65 – 93**	15
Average[b]	**67^{z}**	**54 – 82**	8.0	**71^{z}**	**62 – 84**	17

[a]Statistical significance: ***x***: $p < 0.05$, ***y***: $p < 0.01$, ***z***: $p < 0.001$

[b]Average of last three sampling rounds (if a study site was only sampled once over this period, this profile replaced the average in the calculation)

While increasing orthophosphate to 1.0 mg L^{-1} accompanied a decrease in lead release over the study sites as a group, peak lead levels remained high. The highest concentration at 0.5 mg PO_4 L^{-1} was 58.8 µg L^{-1} and the highest at 1.0 mg L^{-1} was 60.3 µg L^{-1}. At comparable pH and alkalinity levels to those characterizing systems A and B, equilibrium lead solubility has been predicted at approximately 30 and 20 µg L^{-1} at 0.5 and 1.0 mg PO_4 L^{-1}, respectively.[10] Excess lead may be attributed to the presence of

particles: particulate and colloidal lead in system A were predominant.[51,67] Orthophosphate, while effective in lowering equilibrium solubility, may be less effective in controlling particulate lead release.[68] That is, where legacy lead pipe remains, orthophosphate provides no guarantee of protection from lead exposure.

In addition to its apparent effect on lead levels, increasing orthophosphate accompanied lower copper release. Data collected previously within system A showed that copper release and water temperature were moderately correlated at 0.5 mg PO_4 L^{-1} ($r_{average} = 0.73$).[67] Nevertheless, copper levels after just two months at 1.0 mg PO_4 L^{-1} were 79% of those at 0.5 mg PO_4 L^{-1} (95% CI: 71 – 87%). This interval spanned a 5.5 ˚C increase in mean water temperature. Copper levels in December were lower still: an estimated 67% of those observed the previous April. Averaging by site over the last three sampling rounds—approximating a constant temperature comparison—copper levels at 1.0 mg PO_4 L^{-1} were 71% of those observed at 0.5 mg PO_4 L^{-1} (95% CI: 62 – 84%). Increasing orthophosphate to 1.0 mg L^{-1} did not accompany significant reductions in iron release ($\alpha = 0.05$).

6.4.3 Identification Of Elements And Crystalline Phases In Lead Corrosion Scale

Lead pipe corrosion scale collected from system A was characterized by a primary and a secondary crystalline phase: hydrocerussite and hydroxypyromorphite, respectively ($Pb_3(CO_3)_2(OH)_2$ and $Pb_5(PO_4)_3OH$) (Figure 35). The former phase is thermodynamically favoured under the expected distributed water conditions and the latter is expected under orthophosphate control of lead solubility. Elemental analysis was consistent with the presence of hydroxypyromorphite as a secondary phase: phosphorus represented 2.6% of scale mass while the theoretical phosphorus content of hydroxypyromorphite is 6.9%.

The irregular baseline of the XRD pattern may be attributed to the amorphous content of the sample: iron, aluminum, manganese, zinc, and calcium were detected in amounts ranging from 0.4 – 5.5% (by mass) but were not present as distinct crystalline phases. Rather, these elements—especially Fe and Mn—probably occurred as poorly crystalline (oxyhydr)oxides.[69] The presence of zinc at a median concentration of 0.6% was attributable to the phosphate formulation: zinc was present in distributed water at a

median concentration of 65 µg L^{-1}. Traces of vanadium, copper, nickel, barium, chromium, arsenic, and cadmium in scale samples are consistent with previous reports.[69]

While scale layers were aggregated for analysis, in place they were visually consistent with descriptions offered elsewhere: a layer composed predominantly of hydrocerussite beneath a surface layer of amorphous iron or manganese (oxyhydr)oxides.[69] This stratification may explain the near-universal occurrence of colloidal particles rich in lead and iron in system A samples.

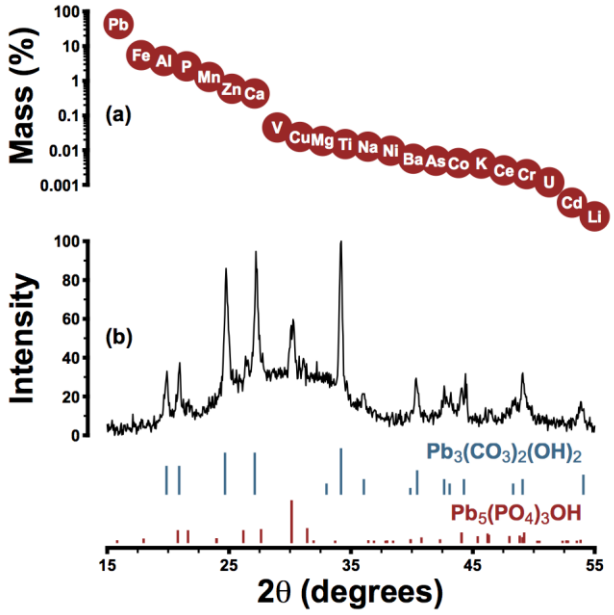

Figure 35 (a) Median mass fraction by element for triplicate scale samples representing an LSL recovered from system A. (b) XRD analysis was consistent with the presence of hydrocerussite, $Pb_3(CO_3)_2(OH)_2$, and hydroxypyromorphite, $Pb_5(PO_4)_3OH$.

6.4.4 Potential Influence Of Aluminum On Lead Release

Aluminum is a potential determinant of lead levels.[70] While median aluminum in system B was low and relatively constant at 8.3 µg L^{-1} (IQR: 7.1 – 9.3 µg L^{-1}), aluminum in system A varied seasonally, with higher levels occurring in winter (IQR: 37.8 – 125.3 µg L^{-1}). At 0.5 mg PO_4 L^{-1}, median lead in system A first-draw samples was greater by 1.3 µg L^{-1} at the higher winter aluminum levels (signed rank test, paired data, $n = 32$ sites, 95% CI: 0.6 – 2.7 µg L^{-1}).[71] At these sites, first-draw sample temperatures were lower in winter by 0.7 – 4.3˚C (IQR).

While the role of aluminum is not well characterized, colloidal aluminum and lead in system A field samples—as determined by SEC-ICP-MS—were often present in a common size fraction (Figure 32).[51] This may be explained by adsorption of lead to suspended colloidal iron and aluminum or to simultaneous release of these metals from corrosion scale. Lead adsorption to suspended particles could promote scale dissolution by reducing the activity of the lead cation in solution, prolonging undersaturation of the dissolving phase.

Despite the apparent effect of aluminum on lead release from premises plumbing, aluminum did not exert a primary influence on lead release over the full sample profile in this study. After controlling for changes in phosphorus, temperature, and iron via linear regression, aluminum was only weakly correlated with lead ($r = 0.15$). Nonetheless, relevant comparisons of lead release over time were structured to minimize aluminum variation: the mass of aluminum over system A profiles in April 2017 (1.0 mg PO_4 L^{-1}) was 87% of the same mass measured in April 2016 (0.5 mg PO_4 L^{-1}, 95% CI: 78 – 96%).

In light of these comparisons, field data from systems A and B add to a body of literature on the effective use of orthophosphate alone to control lead solubility. Data from system C, however, were consistent with previous experimental, theoretical, and observational work highlighting the risks of polyphosphate use in systems with legacy lead plumbing.[22,39,42] Elemental speciation by SEC-ICP-MS may represent a means of understanding the potential for lead sequestration—by polyphosphate or NOM—in drinking water distribution systems.

6.5 References

(1) Cornwell, D. A.; Brown, R. A.; Via, S. H. National survey of lead service line occurrence. *J. Am. Water Works. Assoc.* **2016***, 108* (4), E182 – E191.
(2) Watt, G. C.; Britton, A.; Gilmour, W. H.; Moore, M. R.; Murray, G. D.; Robertson, S. J.; Womersley, J. Is lead in tap water still a public health problem? An observational study in Glasgow. *BMJ* **1996**, *313* (7063), 979-981.
(3) Edwards, M.; Triantafyllidou, S.; Best, D. Elevated blood lead in young children due to lead-contaminated drinking water: Washington, DC, 2001− 2004. *Environ. Sci. Technol.* **2009**, *43* (5), 1618-1623.
(4) Hanna-Attisha, M.; LaChance, J.; Sadler, R. C.; Champney Schnepp, A. Elevated blood lead levels in children associated with the Flint drinking water crisis: a spatial analysis of risk and public health response. *Am. J. Public Health* **2016**, *106* (2), 283-290.
(5) Canfield, R. L.; Henderson Jr., C. R.; Cory-Slechta, D. A.; Cox, C.; Jusko, T. A.; Lanphear, B. P. Intellectual impairment in children with blood lead concentrations below 10 μg per deciliter. *N. Engl. J. Med.* **2003**, *348* (16), 1517-1526.

(6) Lanphear, B. P.; Dietrich, K.; Auinger, P.; Cox, C. Cognitive deficits associated with blood lead concentrations< 10 µg/dL in US children and adolescents. *Public Health Rep.* **2000**, *115* (6), 521-529.
(7) Miranda, M. L.; Kim, D.; Galeano, M. A. O.; Paul, C. J.; Hull, A. P.; Morgan, S. P. The relationship between early childhood blood lead levels and performance on end-of-grade tests. *Environ. Health Perspect.* **2007**, *115* (8), 1242-1247.
(8) Evens, A.; Hryhorczuk, D.; Lanphear, B. P.; Rankin, K. M.; Lewis, D. A.; Forst, L.; Rosenberg, D. The impact of low-level lead toxicity on school performance among children in the Chicago public Schools: a population-based retrospective cohort study. *Environ. Health* **2015**, *14* (21), 1−9.
(9) McNeill, L. S.; Edwards, M. Phosphate inhibitor use at US utilities. *J. Am. Water Works Assoc.* **2002**, *94* (7), 57-63.
(10) Schock, M. R. Understanding corrosion control strategies for lead. *J. Am. Water Works Assoc.* **1989**, *81* (7), 88−100.
(11) Hopwood, J. D.; Davey, R. J.; Jones, M. O.; Pritchard, R. G.; Cardew, P. T.; Booth, A. Development of chloropyromorphite coatings for lead water pipes. *J. Mater. Chem.* **2002**, *12* (6), 1717-1723.
(12) Noel, J. D.; Wang, Y.; Giammar, D. E. Effect of water chemistry on the dissolution rate of the lead corrosion product hydrocerussite. *Water Res.* **2014**, *54*, 237-246.
(13) Svensson, U.; Dreybrodt, W. Dissolution kinetics of natural calcite minerals in CO2-water systems approaching calcite equilibrium. *Chem. Geol.* **1992** *100* (1-2), 129-145.
(14) Debela, F.; Arocena, J. M.; Thring, R. W.; Whitcombe, T. Organic acids inhibit the formation of pyromorphite and Zn-phosphate in phosphorous amended Pb-and Zn-contaminated soil. *J. Environ. Manage.* **2013**, *116*, 156-162.
(15) Martinez, C. E.; Jacobson, A. R.; McBride, M. B. Lead phosphate minerals: solubility and dissolution by model and natural ligands. *Environ. Sci. Technol.* **2004**, *38*, 5584-5590.
(16) Edwards, M.; McNeill, L. S. Effect of phosphate inhibitors on lead release from pipes. *J. Am. Water Works Assoc.* **2002**, *94* (1), 79-90.
(17) Cartier, C.; Doré, E.; Laroche, L.; Nour, S.; Edwards, M.; Prévost, M. Impact of treatment on Pb release from full and partially replaced harvested lead service lines (LSLs). *Water Res.* **2013**, *47* (2), 661-671.
(18) Hayes, C. R.; Incledion, S.; Balch, M. Experience in Wales (UK) of the optimisation of orthophosphate dosing for controlling lead in drinking water. *J. Water Health* **2008**, *6* (2), 177-185.
(19) Cardew, P. T. A method for assessing the effect of water quality changes on plumbosolvency using random daytime sampling. *Water Res.* **2003**, *37* (12), 2821-2832.
(20) Richards, W. N.; Moore, M. R. Lead hazard controlled in Scottish water systems. *J. Am. Water Works Assoc.* **1984**, *76* (8), 60-67.
(21) Colling, J. H.; Croll, B. T.; Whincup, P. A. E.; Harward, C. Plumbosolvency effects and control in hard waters. *Water Environ. J.* **1992**, *6* (4), 259-268.
(22) Dodrill, D. M.; Edwards, M. Corrosion control on the basis of utility experience. *J. Am. Water Works Assoc.* **1995**, *87* (7), 74-85.
(23) Lee, R. G.; Becker, W. C.; Collins, D. W. Lead at the tap: Sources and control. *J. Am. Water Works Assoc.* **1989**, *81* (7), 52-62.
(24) Karalekas Jr., P. C.; Ryan, C. R.; Taylor, F. B. Control of lead, copper, and iron pipe corrosion in Boston. *J. Am. Water Works Assoc.* **1983**, *75* (2), 92-95.
(25) Edwards, M.; Triantafyllidou, S.; Best, D. Elevated blood lead in young children due to lead-contaminated drinking water: Washington, DC, 2001 – 2004. *Environ. Sci. Technol.* **2009**, *43*, 1618–1623
(26) Pieper, K. J.; Tang, M.; Edwards, M. A. Flint water crisis caused by interrupted corrosion control: investigating “ground zero” home. *Environ. Sci. Technol.* **2017**, *51* (4), 2007-2014.
(27) Wang, Y.; Mehta, V.; Welter, G. J.; Giammar, D. E. Effect of connection methods on lead release from galvanic corrosion. *J. Am. Water Works Assoc.* **2013**, *105* (7), E337-E351.
(28) Appenzeller, B. M. R.; Batté, M.; Mathieu, L.; Block, J. C.; Lahoussine, V.; Cavard, J.; Gatel, D. Effect of adding phosphate to drinking water on bacterial growth in slightly and highly corroded pipes. *Water Res.* **2001**, *35* (4), 1100-1105.
(29) Sarin, P.; Clement, J. A.; Snoeyink, V. L.; Kriven, W. M. Iron release from corroded, unlined cast-iron pipe. *J. Am. Water Works Assoc.* **2003**, *95* (11), 85-96.
(30) Lytle, D. A.; Sarin, P.; Snoeyink, V. L. The effect of chloride and orthophosphate on the release of iron from a cast iron pipe section. *J. Water Supply Res. T.* **2005**, *54* (5), 267-281.

(31) McNeill, L. S.; Edwards, M. Phosphate inhibitors and red water in stagnant iron pipes. *J. Environ. Eng.* **2000**, *126* (12), 1096-1102.
(32) Benjamin, M. M.; Sontheimer, H.; Leroy, P. Corrosion of iron and steel. In *Internal corrosion of water distribution systems*; AWWA Research Foundation: Denver, CO, 1996; pp. 29-70.
(33) Melendres, C. A.; Camillone, N.; Tipton, T. Laser Raman spectroelectrochemical studies of anodic corrosion and film formation on iron in phosphate solutions. *Electrochim. Acta* **1989**, *34* (2), 281-286.
(34) Biber, M. V.; dos Santos Afonso, M.; Stumm, W. The coordination chemistry of weathering: IV. Inhibition of the dissolution of oxide minerals. *Geochim. Cosmochim. Acta* **1994**, *58* (9), 1999-2010.
(35) Bondietti, G.; Sinniger, J.; Stumm, W. The reactivity of Fe (III)(hydr) oxides: effects of ligands in inhibiting the dissolution. *Colloids Surf., A* **1993**, *79* (2-3), 157-167.
(36) Reiber, S. H. Copper plumbing surfaces: an electrochemical study. *J. Am. Water Works Assoc.* **1989**, *81* (7), 114-122.
(37) Edwards, M.; Hidmi, L.; Gladwell, D. Phosphate inhibition of soluble copper corrosion by-product release. *Corros. Sci.* **2002**, *44* (5), 1057-1071.
(38) Schock, M. R.; Sandvig, A. M. Long-term effects of orthophosphate treatment on copper concentration. *J. Am. Water Works Assoc.* **2009**, *101* (7), 71-82.
(39) Holm, T. R.; Schock, M. R. Potential effects of polyphosphate products on lead solubility in plumbing systems. *J. Am. Water Works Assoc.* **1991**, *83* (7), 76-82.
(40) Holm, T. R.; Edwards, M. Metaphosphate reversion in laboratory and pipe-rig experiments. *J. Am. Water Works Assoc.* **2003**, *95* (4), 172-178.
(41) Cantor, A. F.; Denig-Chakroff, D.; Vela, R. R.; Oleinik, M. G.; Lynch, D. L. Use of polyphosphate in corrosion control. *J. Am. Water Works Assoc.* **2000**, *92* (2), 95-102.
(42) Ramaley, B.L. Monitoring and control experience under the lead and copper rule. *J. Am. Water Works Assoc.* **1993**, *85* (2), 64-67.
(43) Edwards, M.; Hidmi, L.; Gladwell, D. Phosphate inhibition of soluble copper corrosion by-product release. *Corros. Sci.* **2002**, *44* (5), 1057-1071.
(44) Trueman, B.F.; Sweet, G.A.; Harding, M.D.; Estabrook, H.; Bishop, D.P.; Gagnon, G.A. Galvanic corrosion of lead by iron (oxyhydr)oxides: potential impacts on drinking water quality. *Environ. Sci. Technol.* **2017**, *51* (12), 6812–6820.
(45) Camara, E.; Montreuil, K. R.; Knowles, A. K.; Gagnon, G. A. Role of the water main in lead service line replacement: A utility case study. *J. Am. Water Works Assoc.* **2013**, *105* (8), E423-E431.
(46) Edwards, M.; Triantafyllidou, S. Chloride-to-sulfate mass ratio and lead leaching to water. *J. Am. Water Works Assoc.* **2007**, *99* (7), 96−109.
(47) Nguyen, C. K.; Clark, B. N.; Stone, K. R.; Edwards, M. A. Role of chloride, sulfate, and alkalinity on galvanic lead corrosion. *Corrosion* **2011**, *67* (6), 065005-1−065005-9.
(48) Deshommes, E.; Bannier, A.; Laroche, L.; Nour, S.; Prevost, M. Monitoring-based framework to detect and manage lead water service lines. *J. Am. Water Works Assoc.* **2016**, *108* (11), E555-E570.
(49) Anderson, L. E.; Krkosek, W. H.; Stoddart, A. K.; Trueman, B. F.; Gagnon, G. A. Lake Recovery Through Reduced Sulfate Deposition: A New Paradigm for Drinking Water Treatment. *Environ. Sci. Technol.* **2017**, *51* (3), 1414-1422.
(50) *2015/2016 Annual Report*; Halifax Regional Water Comission: Halifax, Canada, 2016; https://www.halifax.ca/sites/default/files/documents/home-property/water/HalifaxWaterAnnualReport2016.pdf.
(51) Trueman, B. F.; Gagnon, G. A. A new analytical approach to understanding nanoscale lead-iron interactions in drinking water distribution systems. *J. Hazard. Mater.* **2016**, *311*, 151-157.
(52) U.S. EPA SW-846 Test Method 3050B: Acid Digestion of Sediments, Sludges, and Soils. https://www.epa.gov/sites/production/files/2015-12/documents/3050b.pdf
(53) American Public Health Association, American Waterworks Association, Water Pollution Control Federation. *Standard Methods For the Examination of Water and Wastewater*, 22nd ed.; American Public Heath Association: Washington, DC, 2012.
(54) *R: A language and environment for statistical computing*; R Foundation for Statistical Computing: Vienna, Austria, 2014; https://www.r-project.org.

(55) Helsel, D. R.; Hirsch, R. M. *Statistical Methods in Water Resources*; Elsevier: Amsterdam, 1992.
(56) Trueman, B. F.; Gagnon, G. A. Understanding the role of particulate iron in lead release to drinking water. *Environ. Sci. Technol.* **2016**, *50* (17), 9053-9060.
(57) Masters, S.; Edwards, M. Increased lead in water associated with iron corrosion. *Environ. Eng. Sci.* **2015**, *32* (5), 361-369.
(58) McFadden, M.; Giani, R.; Kwan, P.; Reiber, S. H. Contributions to drinking water lead from galvanized iron corrosion scales. *J. Am. Water Works Assoc.* **2011**, *103* (4), 76-89.
(59) Schneider, O. D.; LeChevallier, M. W.; Reed, H. F.; Corson, M. J. A comparison of zinc and nonzinc orthophosphate-based corrosion control. *J. Am. Water Works Assoc.* **2007**, *99* (11), 103-113.
(60) McNeill, L. S.; Edwards, M. Importance of Pb and Cu particulate species for corrosion control. *J. Environ. Eng.* **2004**, *130* (2), 136-144.
(61) Rottmann, L.; Heumann, K. G. Determination of heavy metal interactions with dissolved organic materials in natural aquatic systems by coupling a high-performance liquid chromatography system with an inductively coupled plasma mass spectrometer. *Anal. Chem.* **1994**, *66* (21), 3709-3715.
(62) Laborda, F.; Bolea, E.; Górriz, M. P.; Martín-Ruiz, M. P.; Ruiz-Beguería, S.; Castillo, J. R. A speciation methodology to study the contributions of humic-like and fulvic-like acids to the mobilization of metals from compost using size exclusion chromatography–ultraviolet absorption–inductively coupled plasma mass spectrometry and deconvolution analysis. *Anal. Chim. Acta* **2008**, *606* (1), 1-8.
(63) Korshin, G. V.; Ferguson, J. F.; Lancaster, A. N.; Wu, H. *Corrosion and metal release for lead-containing materials: influence of NOM*; AWWA Research Foundation: USA, 1999.
(64) Korshin, G. V.; Ferguson, J. F.; Lancaster, A. N. Influence of natural organic matter on the morphology of corroding lead surfaces and behavior of lead-containing particles. *Water Res.* **2005**, *39*, 811−818.
(65) Cartier, C.; Laroche, L.; Deshommes, E.; Nour, S.; Richard, G.; Edwards, M.; Prévost, M. Investigating dissolved lead at the tap using various sampling protocols. *J. Am. Water Works Assoc.* **2011**, *103* (3), 55-67.
(66) Imran, S. A.; Dietz, J. D.; Mutoti, G.; Taylor, J. S.; Randall, A. A.; Cooper, C. D. Red water release in drinking water distribution systems. *J. Am. Water Works Assoc.* **2005**, *97* (9), 93-100.
(67) Trueman, B. F.; Camara, E.; Gagnon, G. A. Evaluating the effects of full and partial lead service line replacement on lead levels in drinking water. *Environ. Sci. Technol.* **2016**, *50* (14), 7389-7396.
(68) Xie, Y.; Giammar, D. E. Effects of flow and water chemistry on lead release rates from pipe scales. *Water Res.* **2011**, *45* (19), 6525-6534.
(69) Schock, M. R.; Hyland, R. N.; Welch, M. M. Occurrence of contaminant accumulation in lead pipe scales from domestic drinking-water distribution systems. *Environ. Sci. Technol.* **2008**, *42* (12), 4285-4291.
(70) Knowles, A. D.; Nguyen, C. K.; Edwards, M. A.; Stoddart, A.; McIlwain, B.; Gagnon, G. A. Role of iron and aluminum coagulant metal residuals and lead release from drinking water pipe materials. *J. Environ. Sci. Health A Tox. Hazard. Subs.t Environ. Eng.* **2015**, *50* (4), 414-423.
(71) McIlwain, B. Investigating sources of elevated lead in drinking water. M.A.Sc. Dissertation, Dalhousie University, Halifax, Canada, 2013.

Chapter 7 Conclusions

7.1 Concluding Remarks

This work explored three general approaches to controlling lead exposure via drinking water: lead service line replacement (LSLR), orthophosphate treatment, and control of complexing or adsorbing species. A brief summary of key findings follows.

Partial LSLR entails considerable risk and may be counterproductive to controlling lead exposure. While partial replacement is widely—and controversially—practiced, little field research is available on its effects. Much of what is available highlights serious concerns. At the time of publication, data reported here represented—to our knowledge—the largest study comparing full and partial LSLR via point-of-use sampling. These data show that, as expected, full LSLR reduced lead levels significantly and unambiguously, while partial LSLR did not accompany clear reductions in lead and was even associated with a greater frequency of elevated lead in the medium term (i.e., the first 6 mo.). That is, these data do not support partial LSLR as a reliable strategy for reducing lead levels in drinking water.

Iron corrosion was a significant predictor of lead at the point of use and the explanatory mechanisms may be more complex than previously thought. Corroded iron pipes distribute a significant fraction of North American drinking water, and lead and iron often occur together at points of use. An improved understanding of lead-iron interactions in drinking water systems could inform risk assessment and aid in prioritizing interventions intended to reduce lead exposure (e.g., by focusing replacement efforts on areas with corroding iron distribution infrastructure). This thesis offers new insights into lead-iron interactions via experimental electrochemical data and characterization of colloidal/nanosize lead and iron in environmental samples. Expermentally and observationally, upstream iron corrosion was a significant determinant of lead release. In a model system, lead release was elevated when a source of corroding iron was present upstream. This phenomenon may be linked with both iron deposition corrosion and co-mobilization of colloidal/nanosize lead and iron. In the field,

lead levels post-LSLR were substantially higher at study sites supplied by unlined—as opposed to lined—iron distribution pipe. This effect, while poorly characterized, was most pronounced following partial LSLR. As in the model system, it may be attributed to both adsorptive and electrochemical phenomena. In a field study reported here, colloidal/nanosize iron and lead— as determined by SEC-ICP-MS—were strongly correlated in point-of-use samples whenever a source of corroding iron was present upstream. Experiments showed that galvanic corrosion of lead by iron (oxyhydr)oxides could also be significant: to our knowledge, the potential for accelerated lead release via this mechanism has not been acknowledged previously. These galvanic effects seem plausible, given that previous research has repeatedly identified lead pipe scale composed predominantly of iron oxides at the water-scale interface. Furthermore, recent observations of potential reversal (i.e., lead as cathode) at lead-copper and lead-brass junctions provide an instructive analogue. Potential reversal appears to occur when lead scale contains electronically conductive PbO_2 as a significant crystalline phase. Zinc also reverses its potential—becoming noble to iron—with the formation on its surface of semiconducting ZnO that behaves as an oxygen electrode. Assuming that PbO_2 behaves similarly on lead, potential reversal implies electrical continuity between metallic lead and semiconducting PbO_2 phases at the water-scale interface. This is broadly consistent with the proposed mechanism of iron oxide deposition corrosion. From a practical standpoint, iron pipe rehabilitation and other interventions that reduce iron release to distributed water might lead to significant reductions in lead release as well. Moreover, partial LSLR may be entail particular risk when water is supplied via corroded iron distribution pipe.

Some natural organic matter fractions mobilize lead via complexation; this represents a risk to public health that could be diagnosed at the point of use. In electrochemical experiments described here, humic acid mobilized lead oxidized by galvanic interaction with iron (oxyhydr)oxides. This was attributed in part to complexation of lead in solution: size-exclusion chromatography data were consistent with the presence of an aqueous lead-humate complex in experimental samples. The presence of dissolved organics that form coordination complexes with lead could severely

exacerbate the effects of galvanic corrosion after partial LSLR by mobilizing lead that would have otherwise been stored as scale. While many systems distribute water with high levels of organic carbon, natural organic matter remains poorly characterized in many of these and the importance of metal complexation is not known. The size-exclusion chromatography method described in this thesis could serve as a diagnostic tool for identifying corrosion control problems related to natural organic matter complexation. This information could inform corrosion control programs as they are implemented for control of lead exposure.

Orthophosphate represents an important tool for minimizing lead release, but environmental measurements of aqueous lead complexation by polyphosphate are concerning. This research adds to a body of work showing that, under certain conditions, orthophosphate is effective for controlling lead release. However, other species—including colloidal iron and humic substances—may interfere with effective orthophosphate control. While orthophosphate decreased lead release in experimentally and residential field studies reported here, humic acid reduced this effect in lab experiments. Moreover, orthophosphate did not diminish the effect of upstream iron corrosion on lead release observed in a model distribution system. A high concentration of orthophosphate did, however, immobilize lead oxidized by (iron oxide-catalyzed) galvanic corrosion. This was attributed to formation of hydroxypyromorphite, an insoluble lead phosphate compound. Galvanic corrosion may be less of a concern in systems where lead is immobilized as insoluble crystalline minerals within corrosion scale.

Orthophosphate is often applied along with polyphosphate, despite warnings from several researchers that polyphosphates may increase lead release. Polyphosphate species have the potential to increase lead solubility via complexation reactions, but the extent of aqueous polyphosphate complexation with lead in the field is not known. We used size-exclusion chromatography to understand lead-polyphosphate complexation in both experimental and field samples, highlighting the potential of this method for identifying lead corrosion problems related to the presence of complexing organic and inorganic

species. In some cases, removing these from inhibitor formulations could be an important step towards reducing lead exposure via drinking water. Moreover, SEC-ICP-MS could be used as a diagnostic tool to identify— via environmental measurements— polyphosphate formulations that risk exacerbating lead-in-water issues.

7.2 Recommendations

Several recommendations follow from these key findings:

Given the risks of partial lead service line replacement, the practice should be avoided where possible. Data presented here show that partial replacement represents a lead exposure risk that is especially serious in the short term. Residences that do undergo partial LSLR should be monitored closely. Special consideration should also be given to potential risk factors for elevated lead release due to galvanic corrosion, including the presence of humic substances, polyphosphates, or unlined iron distribution mains.

Improved characterization of the mechanisms underlying iron particle-induced lead release is recommended. This may include size-fraction via filtration, size-exclusion chromatography, or field-flow fractionation to characterize co-mobilization of lead and iron. Additional validation of the latter two methods using standard nanoparticle materials would improve our ability to characterize apparent size distributions of suspended particles. Detailed analysis of corrosion scale from recovered pipe specimens may also elucidate the electrochemical role of electronically conductive scale deposits such as iron (oxyhydr)oxides and lead(IV) oxides.

A better understanding of the practical relevance of complexing natural organics and polyphosphates is needed. The significance of these complexing species is supported by theoretical and experimental work, but understanding the extent of the lead exposure risk would inform corrosion control strategies and health risk assessment. Given the complexity of natural organic matter (NOM), potential interactions between lead and organics have received little attention. Analytical methods that identify metal

complexation—including size-exclusion chromatography and field-flow fractionation with multielement detection—could be applied to identify corrosion control issues related to complexation. Combined with other tools for characterizing NOM, these methods could lead to a better understanding of the role of NOM in metal mobility.

References

2013/2014 Annual Report; Halifax Regional Water Comission: Halifax, Canada, 2014; http://www.halifax.ca/hrwc/documents/AnnualReportFinal-2014.pdf.

2015/2016 Annual Report; Halifax Regional Water Comission: Halifax, Canada, 2016; https://www.halifax.ca/sites/default/files/documents/home-property/water/HalifaxWaterAnnualReport2016.pdf.

A Guide to Assist Nova Scotia Municipal Water Works Prepare Annual Sampling Plans; Nova Scotia Environment: Halifax, Canada, 2010; https://www.novascotia.ca/nse/water/docs/GuideToAnnualSamplingPlans.pdf.

Allison, J. D.; Allison, T. L. *Partition coefficients for metals in surface water, soil, and waste*; EPA/600/R-05/0742005; U.S. Environmental Protection Agency, Office of Research and Development: Washington DC, 2005.

American Public Health Association, American Waterworks Association, Water Pollution Control Federation. *Standard Methods For the Examination of Water and Wastewater*, 22nd ed.; American Public Heath Association: Washington, DC, 2012.

Anderson, L. E.; Krkosek, W. H.; Stoddart, A. K.; Trueman, B. F.; Gagnon, G. A. Lake Recovery Through Reduced Sulfate Deposition: A New Paradigm for Drinking Water Treatment. *Environ. Sci. Technol.* **2017**, *51* (3), 1414-1422.

Appenzeller, B. M. R.; Batté, M.; Mathieu, L.; Block, J. C.; Lahoussine, V.; Cavard, J.; Gatel, D. Effect of adding phosphate to drinking water on bacterial growth in slightly and highly corroded pipes. *Water Res.* **2001**, *35* (4), 1100-1105.

Arnold Jr, R. B.; Edwards, M. Potential reversal and the effects of flow pattern on galvanic corrosion of lead. *Environ. Sci. Technol.* **2012**, *46* (20), 10941-10947.

Baalousha, M.; Manciulea, A.; Cumberland, S.; Kendall, K.; Lead, J. R. Aggregation and surface properties of iron oxide nanoparticles: influence of pH and natural organic matter. *Environ. Toxicol. Chem.* **2008**, *27* (9), 1875-1882.

Bajpai, I.; Balani, K.; Basu, B. Spark plasma sintered HA-Fe_3O_4-based multifunctional magnetic biocomposites. *J. Am. Ceram. Soc.* **2013**, *96* (7), 2100-2108.

Barkatt, A.; Pulvirenti, A. L.; Adel-Hadadi, M. A.; Viragh, C.; Senftle, F. E.; Thorpe, A. N.; Grant, J. R. Composition and particle size of superparamagnetic corrosion products in tap water. *Water Res.* **2009**, *43* (13), 3319−3325.

Benjamin, M. M.; Leckie, J. O. Multiple-site adsorption of Cd, Cu, Zn, and Pb on amorphous iron oxyhydroxide. *J. Colloid Interf. Sci.* **1981**, *79* (1), 209-221.

Benjamin, M. M.; Sontheimer, H.; Leroy, P. Corrosion of iron and steel. In *Internal corrosion of water distribution systems*; AWWA Research Foundation: Denver, CO, 1996; pp. 29-70.

Berthouex, P. M., Brown, L. C. *Statistics for Environmental Engineers*; CRC Press: Boca Raton, FL, 2002.

Biber, M. V.; dos Santos Afonso, M.; Stumm, W. The coordination chemistry of weathering: IV. Inhibition of the dissolution of oxide minerals. *Geochim. Cosmochim. Acta* **1994**, *58* (9), 1999-2010.

Bisogni, J. J.; Nassar, I. S.; Menegaux, A. M. Effect of calcium on lead in soft-water distribution systems. *J. Environ. Eng.* **2000**, *126* (5), 475-478.

Bondietti, G.; Sinniger, J.; Stumm, W. The reactivity of Fe (III)(hydr) oxides: effects of ligands in inhibiting the dissolution. *Colloids Surf., A* **1993**, *79* (2-3), 157-167.

Britton, A.; Richards, W. N. Factors Influencing Plumbosolvency in Scotland. *J. Inst. Water Eng. Sci.* **1981**, *35* (5), 349−364.

Brown, M. J.; Raymond, J.; Homa, D.; Kennedy, C.; Sinks, T. Association between children's blood lead levels, lead service lines, and water disinfection, Washington, DC, 1998−2006. *Environ. Res.* **2011**, *111* (1), 67−74.

Brown, R. A.; Cornwell, D. A. High-velocity household and service line flushing following LSL replacement. *J. Am. Water Works Assoc.* **2015**, *107* (3), E140−E151.

Camara, E.; Montreuil, K.R.; Knowles, A.K.; Gagnon, G.A. Role of the water main in lead service line replacement: A utility case study. *J. Am. Water Works Assoc.* **2013**, *105* (8) E423-E431.

Canfield, R. L.; Henderson Jr., C. R.; Cory-Slechta, D. A.; Cox, C.; Jusko, T. A.; Lanphear, B. P. Intellectual impairment in children with blood lead concentrations below 10 μg per deciliter. *N. Engl. J. Med.* **2003**, *348* (16), 1517-1526.

Cantor, A. F. Optimization of phosphorus-based corrosion control chemicals; *In Proceedings of the 2016 AWWA Water Quality Technology Conference*; AWWA: Indianapolis, IN, 2016.

Cantor, A. F.; Denig-Chakroff, D.; Vela, R. R.; Oleinik, M. G.; Lynch, D. L. Use of polyphosphate in corrosion control. *J. Am. Water Works Assoc.* **2000**, *92* (2), 95-102.

Cardew, P. T. A method for assessing the effect of water quality changes on plumbosolvency using random daytime sampling. *Water Res.* **2003**, *37* (12), 2821-2832.

Cartier, C.; Arnold, R. B.; Triantafyllidou, S.; Prevost, M.; Edwards, M. Effect of flow rate and lead/copper pipe sequence on lead release from service lines. *Water Res.* **2012**, *46* (13), 4142−4152.

Cartier, C.; Arnold, R. B.; Triantafyllidou, S.; Prévost, M.; Edwards, M. Effect of flow rate and lead/copper pipe sequence on lead release from service lines. *Water Res.* **2012**, *46* (13), 4142-4152.

Cartier, C.; Doré, E.; Laroche, L.; Nour, S.; Edwards, M.; Prévost, M. Impact of treatment on Pb release from full and partially replaced harvested lead service lines (LSLs). *Water Res.* **2013**, *47* (2), 661−671.

Cartier, C.; Laroche, L.; Deshommes, E.; Nour, S.; Richard, G.; Edwards, M.; Prévost, M. Investigating dissolved lead at the tap using various sampling protocols. *J. Am. Water Works Assoc.* **2011**, *103* (3), 55−67.

Clark, B.; Cartier, C.; St. Clair, J.; Triantafyllidou, S.; Prévost, M.; Edwards, M. Effect of connection type on galvanic corrosion between lead and copper pipes. *J. Am. Water Works Assoc.* **2013**, *105* (10), E576−E586.

Clark, B.; St. Clair, J.; Edwards, M. Copper deposition corrosion elevates lead release to potable water. *J. Am. Water Works. Assoc.* **2015**, *107* (11), E627-E637.

Clement, M., Seux, R., Rabarot, S. A practical model for estimating total lead intake from drinking water. *Water Res.* **2000**, *34* (5), 1533-1542.

Colling, J. H.; Croll, B. T.; Whincup, P. A. E.; Harward, C. Plumbosolvency effects and control in hard waters. *Water Environ. J.* **1992**, *6* (4), 259-268.

Colling, J. H.; Whincup, P. A. E.; Hayes, C. R. The measurement of plumbosolvency propensity to guide the control of lead in tapwaters. *Water Environ. J.* **1987**, *1* (3), 263-269.

Cornwell, D. A.; Brown, R. A.; Via, S. H. National survey of lead service line occurrence. *J. Am. Water Works. Assoc.* **2016***, 108* (4), E182 – E191.

Davis, J.R., Ed. *Corrosion of Aluminum and Aluminum Alloys*; ASM International: Ohio, 1999.

de Mora, S. J.; Harrison, R. M. The use of physical separation techniques in trace metal speciation studies. *Water Res.* **1983**, *17* (7), 723-733.

de Mora, S. J.; Harrison, R. M.; Wilson, S. J. The effect of water treatment on the speciation and concentration of lead in domestic tap water derived from a soft upland source. *Water Res.* **1987**, *21* (1), 83-94.

Debela, F.; Arocena, J. M.; Thring, R. W.; Whitcombe, T. Organic acids inhibit the formation of pyromorphite and Zn-phosphate in phosphorous amended Pb-and Zn-contaminated soil. *J. Environ. Manage.* **2013**, *116*, 156-162.

Del Toral, M. A.; Porter, A.; Schock, M. R. Detection and evaluation of elevated lead release from service lines: a field study. *Environ. Sci. Technol.* **2013**, *47* (16), 9300−9307.

DeSantis, M. K.; Welch, M.; Shock, M. Mineralogical evidence of galvanic corrosion in domestic drinking water pipes. In *Proceedings of the 2009 AWWA Water Quality Technology Conference*; AWWA, 2009.

Deshommes, E.; Bannier, A.; Laroche, L.; Nour, S.; Prevost, M. Monitoring-based framework to detect and manage lead water service lines. *J. Am. Water Works Assoc.* **2016**, *108* (11), E555-E570.

Deshommes, E.; Laroche, L.; Nour, S.; Cartier, C.; Prévost, M. Source and occurrence of particulate lead in tap water. *Water Res.* **2010**, *44* (12), 3734−3744.

Deshommes, E.; Zhang, Y.; Gendron, K.; Sauvé, S.; Edwards, M.; Nour, S.; Prévost, M. Lead removal from tap water using POU devices. *J. Am. Water Works Assoc.* **2010**, *102* (10), 91−105.

Desmarais, M.; Trueman, B.; Wilson, P.; Huggins, D.; Swertfeger, J.; Deshommes, E.; Prévost, M. Impact of partial lead service line replacements on water quality: Lead profiling sampling results in 6 North American utilities. In *Proceedings of the 2015 AWWA Water Quality Technology Conference*; AWWA, 2015.

Dodrill, D. M.; Edwards, M. Corrosion control on the basis of utility experience. *J. Am. Water Works Assoc.* **1995**, *87* (7), 74-85.

Dryer, D. J.; Korshin, G. V. Investigation of the reduction of lead dioxide by natural organic matter. *Environ. Sci. Technol.* **2007**, *41* (15), 5510-5514.

Edwards, M. Fetal death and reduced birth rates associated with exposure to lead contaminated drinking water. *Environ. Sci. Technol.* **2014**, *48* (1), 739−746.

Edwards, M.; Hidmi, L.; Gladwell, D. Phosphate inhibition of soluble copper corrosion by-product release. *Corros. Sci.* **2002**, *44* (5), 1057-1071.

Edwards, M.; McNeill, L. S. Effect of phosphate inhibitors on lead release from pipes. *J. Am. Water Works Assoc.* **2002**, *94* (1), 79-90.

Edwards, M.; Triantafyllidou, S. Chloride-to-sulfate mass ratio and lead leaching to water. *J. Am. Water Works Assoc.* **2007**, *99* (7), 96−109.

Edwards, M.; Triantafyllidou, S.; Best, D. Elevated blood lead in young children due to lead-contaminated drinking water: Washington, DC, 2001− 2004. *Environ. Sci. Technol.* **2009**, *43* (5), 1618−1623.

Eick, M. J.; Peak, J. D.; Brady, P. V.; Pesek, J. D. Kinetics of lead adsorption/desorption on goethite: residence time effect. *Soil Sci.* **1999**, *164* (1), 28-39.

El Mendili, Y.; Bardeau, J. F.; Randrianantoandro, N.; Grasset, F.; Greneche, J. M. Insights into the mechanism related to the phase transition from γ-Fe_2O_3 to α-Fe_2O_3 nanoparticles induced by thermal treatment and laser irradiation. *J. Phys. Chem. C* **2012**, *116* (44), 23785-23792.

Erel, Y.; Morgan, J. J. The relationships between rock-derived lead and iron in natural waters. *Geochim. Cosmochim. Acta* **1992**, *56* (12), 4157-4167.

Evens, A.; Hryhorczuk, D.; Lanphear, B. P.; Rankin, K. M.; Lewis, D.A.; Forst, L.; Rosenberg, D. The impact of low-level lead toxicity on school performance among children in the Chicago Public Schools: a population- based retrospective cohort study. *Environ. Health* **2015**, *14* (21), 1-9.

Fertmann, R.; Hentschel, S.; Dengler, D.; Janßen, U.; Lommel, A. Lead exposure by drinking water: an epidemiologial study in Hamburg, Germany. *Int. J. Hyg. Environ. Health* **2004**, *207* (3), 235−244.

Francis, R. *Bimetallic corrosion*; National Physical Laboratory: Teddington, U.K., 2000.

Friedman, M.; Hill, A.; Reiber, S.; Valentine, R.L.; Larsen, G.; Young, A.; Korshin, G.V.; Peng, C.Y. *Assessment of inorganics accumulation in drinking water system scales and sediments*; Water Research Foundation: Denver, CO, 2010.

Fujii, M.; Imaoka, A.; Yoshimura, C.; Waite, T. D. Effects of molecular composition of natural organic matter on ferric iron complexation at circumneutral pH. *Environ. Sci. Technol.* **2014**, *48* (8), 4414-4424.

Fushimi, K.; Yamamuro, T.; Seo, M. Hydrogen generation from a single crystal magnetite coupled galvanically with a carbon steel in sulfate solution. *Corros. Sci.* **2002**, *44* (3), 611-623.

Gagnon, G.A.; Doubrough, J. D. Lead release from premise plumbing: a profile of sample collection and pilot studies from a small system. *Can. J. Civil Eng.* **2011**, *38* (7), 741-750.

Garay, J. E. Current-activated, pressure-assisted densification of materials. *Annu. Rev. Mater. Res.* **2010**, *40*, 445-468.

Gaudisson, T.; Vázquez-Victorio, G.; Bañobre-López, M.; Nowak, S.; Rivas, J.; Ammar, S.; Mazaleyrat, F.; Valenzuela, R. The Verwey transition in nanostructured magnetite produced by a combination of chimie douce and spark plasma sintering. *J. Appl. Phys.* **2014**, *115*, 17E117.

Gerke, T.L.; Maynard, J.B.; Schock, M.R.; Lytle, D.L. Physiochemical characterization of five iron tubercles from a single drinking water distribution system: Possible new insights on their formation and growth. *Corros. Sci.* **2008**, *50*, 2030-2039.

Gialanella, S.; Girardi, F.; Ischia, G.; Lonardelli, I.; Mattarelli, M.; Montagna, M. On the goethite to hematite phase transformation. *J. Therm. Anal. Calorim.* **2010**, *102* (3), 867-873.

Gu, B.; Schmitt, J.; Chen, Z.; Liang, L.; McCarthy, J. F. Adsorption and desorption of different organic matter fractions on iron oxide. *Geochim. Cosmochim. Acta* **1995**, *59* (2), 219-229.

Guidance on Controlling Corrosion in Drinking Water Distribution Systems; Catalogue H128-1/09-595E; Health Canada: Ottawa, Canada, 2009; http://www.hcsc.gc.ca/ewh-semt/alt_formats/hecs-sesc/pdf/pubs/water-eau/corrosion/corrosion-eng.pdf.

Guidelines for Canadian Drinking Water Quality—Summary Table; Health Canada, Water, Air and Climate Change Bureau, Healthy Environments and Consumer Safety Branch: Ottawa, Canada, 2012; http://www.hc-sc.gc.ca/ewh-semt/pubs/water-eau/sum_guideres_recom/index-eng.php.

Hanna-Attisha, M.; LaChance, J.; Sadler, R. C.; Champney Schnepp, A. Elevated blood lead levels in children associated with the Flint drinking water crisis: a spatial analysis of risk and public health response. *Am. J. Public Health* **2016**, *106* (2), 283-290.

Harrison, R. M.; Laxen, D. P. H. Physicochemical speciation of lead in drinking water. *Nature* **1980***, 286*, 791-793.

Hassellöv, M.; von der Kammer, F. Iron oxides as geochemical nanovectors for metal transport in soil-river systems. *Elements* **2008**, *4* (6), 401-406.

Hayes, C. R.; Incledion, S.; Balch, M. Experience in Wales (UK) of the optimisation of orthophosphate dosing for controlling lead in drinking water. *J. Water Health* **2008**, *6* (2), 177-185.

Helsel, D. R.; Hirsch, R. M. *Statistical Methods in Water Resources*; Elsevier: Amsterdam, 1992.

Hill, D. M.; Aplin, A. C. Role of colloids and fine particles in the transport of metals in rivers draining carbonate and silicate terrains. *Limnol. Oceanogr.* **2001**, *46* (2), 331-344.

Holm, T. R.; Edwards, M. Metaphosphate reversion in laboratory and pipe-rig experiments. *J. Am. Water Works Assoc.* **2003**, *95* (4), 172-178.

Holm, T. R.; Schock, M. R. Potential effects of polyphosphate products on lead solubility in plumbing systems. *J. Am. Water Works Assoc.* **1991**, *83* (7), 76-82.

Hopwood, J. D.; Davey, R. J.; Jones, M. O.; Pritchard, R. G.; Cardew, P. T.; Booth, A. Development of chloropyromorphite coatings for lead water pipes. *J. Mater. Chem.* **2002**, *12* (6), 1717-1723.

Hu, J.; Gan, F.; Triantafyllidou, S.; Nguyen, C. K.; Edwards, M. A. Copper-induced metal release from lead pipe into drinking water. *Corrosion* **2012**, *68* (11), 1037-1048.

Hua, M.; Shujuan, Z.; Bingcai, P.; Weiming, Z.; Lu, L.; Quanxing, Z. Heavy metal removal from water/wastewater by nanosized metal oxides: a review. *J. Hazard. Mater.* **2012**, *211-212*, 317-331.

Huslmann, A. D. Particulate lead in water supplies. *Water Environ. J.* **1990**, *4* (1), 19-25.

Imran, S. A.; Dietz, J. D.; Mutoti, G.; Taylor, J. S.; Randall, A. A.; Cooper, C. D. Red water release in drinking water distribution systems. *J. Am. Water Works Assoc.* **2005**, *97* (9), 93-100.

Jackson, B. P.; Ranville, J. F.; Bertsch, P. M.; Sowder, A. G. Characterization of colloidal and humic-bound Ni and U in the "dissolved" fraction of contaminated sediment extracts. *Environ. Sci. Technol.* **2005**, *39* (8), 2478-2485.

Johnson, R.A.; Wichern, D.W. *Applied multivariate statistical analysis,* 6thed; Peason Education: New Jersey, 2007.

Jordan, K.; Cazacu, A.; Manai, G.; Ceballos, S. F.; Murphy, S.; Shvets, I. V. Scanning tunneling spectroscopy study of the electronic structure of Fe_3O_4 surfaces. *Phys. Rev. B* **2006**, *74*, 085416.

Karalekas Jr., P. C.; Ryan, C. R.; Taylor, F. B. Control of lead, copper, and iron pipe corrosion in Boston. *J. Am. Water Works Assoc.* **1983**, *75* (2), 92-95.

Karathanasis, A. D. Colloid-mediated transport of Pb through soil porous media. *Int. J. Environ. Stud.* **2000**, *57* (5), 579-596.

Kaste, J. M.; Bostick, B. C.; Friedland, A. J.; Schroth, A. W.; Siccama, T. G. Fate and speciation of gasoline-derived lead in organic horizons of the northeastern USA. *Soil Sci. Soc. Am. J.* **2006**, *70* (5), 1688-1698.

Kato, Y.; O'Donnell, J. K.; Fisher, J. Size exclusion chromatography using TSK-Gel columns and Toyopearl resins. In *Column Handbook for Size Exclusion Chromatography*; Wu, C.S., Ed.; Academic Press: San Diego 1999; pp. 93-158.

Kimbrough, D. E. Brass corrosion as a source of lead and copper in traditional and all-plastic distribution systems. *J. Am. Water Works Assoc.* **2007***, 99* (8), 70-76.

Knowles, A. D.; MacKay, J.; Gagnon, G. A. Pairing a pilot plant to a direct filtration water treatment plant. *Can. J. Civ. Eng.* **2012**, *39* (6), 689-700.

Knowles, A. D.; Nguyen, C. K.; Edwards, M. A.; Stoddart, A.; McIlwain, B.; Gagnon, G. A. Role of iron and aluminum coagulant metal residuals and lead release from drinking water pipe materials. *J. Environ. Sci. Health A Tox. Hazard. Subs.t Environ. Eng.* **2015**, *50* (4), 414-423.

Korshin, G. V.; Ferguson, J. F.; Lancaster, A. N. Influence of natural organic matter on the morphology of corroding lead surfaces and behavior of lead-containing particles. *Water Res.* **2005**, *39*, 811−818.

Korshin, G. V.; Ferguson, J. F.; Lancaster, A. N.; Wu, H. *Corrosion and metal release for lead-containing materials: influence of NOM*; AWWA Research Foundation: USA, 1999.

Kozai, N.; Ohnuki, T.; Iwatsuki, T. Characterization of saline groundwater at Horonobe, Hokkaido, Japan by SEC-UV-ICP-MS: Speciation of uranium and iodine. *Water Res.* **2013**, *47* (4), 1570-1584.

Kuch, A.; Wagner, I. A mass transfer model to describe lead concentrations in drinking water. *Water Res.* **1983**, *17* (10), 1303-1307.

Kuech, T. R.; Hamers, R. J.; Pedersen, J. A. Chemical transformations of metal, metal oxide, and metal chalcogenide nanoparticles in the environment. In *Engineered nanoparticles and the environment: Biophysicochemical processes and toxicity*; Xing, B., Vecitis, C. D., Senesi, N., Eds.; John Wiley & Sons: Hoboken, NJ 2016; pp 271.

Laborda, F.; Bolea, E.; Górriz, M. P.; Martín-Ruiz, M. P.; Ruiz-Beguería, S.; Castillo, J. R. A speciation methodology to study the contributions of humic-like and fulvic-like acids to the mobilization of metals from compost using size exclusion chromatography–ultraviolet absorption–inductively coupled plasma mass spectrometry and deconvolution analysis. *Anal. Chim. Acta* **2008**, *606* (1), 1-8.

Lanphear, B. P.; Dietrich, K.; Auinger, P.; Cox, C. Cognitive deficits associated with blood lead concentrations <10 microg/dL in US children and adolescents. *Public Health Rep.* **2000**, *115* (6), 521−529.

Lanphear, B. P.; Hornung, R.; Yolton, K.; Baghurst, P.; Bellinger, DC.; Canfield, R. L.; et al. Low-level environmental lead exposure and children's intellectual function: an international pooled analysis. *Environ. Health Persp.* **2005**, *113* (7), 894-899.

Lead in Drinking Water; Health Canada: Ottawa, Canada, 2016; http://www.healthycanadians.gc.ca/health-system-systeme-sante/consultations/lead-drinking-water-plomb-eau-potable/document-eng.php#purpose

Lead tips: Sources of lead in water; Centers for Disease Control and Prevention: Atlanta, GA, 2010; http://www.cdc.gov/nceh/lead/tips/water.htm.

Lee, R. G.; Becker, W. C.; Collins, D. W. Lead at the tap: Sources and control. *J. Am. Water Works Assoc.* **1989***, 81* (7), 52-62.

Lin, Y. P.; Valentine, R. L. The release of lead from the reduction of lead oxide (PbO_2) by natural organic matter. *Environ. Sci. Technol.* **2008**, *42*, 760-765.

Liu, C.; Huang, P. M. Pressure-jump relaxation studies on kinetics of lead sorption by iron oxides formed under the influence of citric acid. *Geoderma.* **2001**, *102* (1), 1-25.

Liu, J. F.; Zhao, Z. S.; Jiang, G. B. Coating Fe_3O_4 magnetic nanoparticles with humic acid for high efficient removal of heavy metals in water. *Environ. Sci. Technol.* **2008**, *42* (18), 6949−6954.

Loghman-Adham, M. Renal effects of environmental and occupational lead exposure. *Environ. Health Perspect.* **1997**, *105* (9), 928-938.

Lytle, D. A.; Sarin, P.; Snoeyink, V. L. The effect of chloride and orthophosphate on the release of iron from a cast iron pipe section. *J. Water Supply Res. T.* **2005**, *54* (5), 267-281.

Lytle, D. A.; Schock, M. R.; Scheckel, K. The inhibition of Pb(IV) oxide formation in chlorinated water by orthophosphate. *Environ. Sci. Technol.* **2009**, *43* (17), 6624-6631.

Lytle, D. A.; Sorg, T. J.; Muhlen, C.; Wang, L. Particulate arsenic release in a drinking water distribution system. *J. Am. Water Works Assoc.* **2010**, *102* (3), 87-98.

Lyvén, B.; Hassellöv, M.; Turner, D. R.; Haraldsson, C.; Andersson, K. Competition between iron-and carbon-based colloidal carriers for trace metals in a freshwater assessed using flow field-flow fractionation coupled to ICPMS. *Geochim. Cosmochim. Acta* **2003**, *67* (20), 3791-3802.

Magnuson, M. L.; Lytle, D. A.; Frietch, C. M.; Kelty, C. A. Characterization of submicrometer aqueous iron (III) colloids formed in the presence of phosphate by sedimentation field flow fractionation with multiangle laser light scattering detection. *Anal. Chem.* **2001**, *73* (20), 4815-4820.

Manceau, A.; Boisset, M. C.; Sarret, G.; Hazemann, J. L.; Mench, M.; Cambier, P.; Prost, R. Direct determination of lead speciation in contaminated soils by EXAFS spectroscopy. *Environ. Sci. Technol.* **1996**, *30*, 1540-1552.

Martinez, C. E.; Jacobson, A. R.; McBride, M. B. Lead phosphate minerals: solubility and dissolution by model and natural ligands. *Environ. Sci. Technol.* **2004**, *38*, 5584-5590.

Masters, S.; Edwards, M. A. Increased lead in water associated with iron corrosion. *Environ. Eng. Sci.* **2015**, 32 (5), 361-369.

Masters, S.; Welter, G. J.; Edwards, M. Seasonal variations in lead release to potable water. *Environ. Sci. Technol.* **2016**, *50* (10), 5269-5277.

Maximum contaminant level goals and national primary drinking water regulations for lead and copper. Final rule *Fed. Regist.*, **1991**, *56*, 26460.

McFadden M.; Giani, R.; Kwan, P.; Reiber, S.H. Contributions to drinking water lead from galvanized iron corrosion scales. *J. Am. Water Works Assoc.* **2011***, 103* (4), 76-89.

McIlwain, B. Investigating sources of elevated lead in drinking water. M.A.Sc. Dissertation, Dalhousie University, Halifax, Canada, 2013.

McKenzie, R. M. The adsorption of lead and other heavy metals on oxides of manganese and iron. *Soil Res.* **1980**, *18* (1), 61-73.

McNeill, L. S.; Edwards, M. Importance of Pb and Cu particulate species for corrosion control. *J. Environ. Eng.-ASCE*. **2004**, *130* (2), 136- 144.

McNeill, L. S.; Edwards, M. Iron pipe corrosion in distribution systems. *J. Am. Water Works Assoc.* **2001**, *93* (7), 88-100.

McNeill, L. S.; Edwards, M. Phosphate inhibitor use at US utilities. *J. Am. Water Works Assoc*. **2002**, *94* (7), 57-63.

McNeill, L. S.; Edwards, M. Phosphate inhibitors and red water in stagnant iron pipes. *J. Environ. Eng.* **2000**, *126* (12), 1096-1102.

Melendres, C. A.; Camillone, N.; Tipton, T. Laser Raman spectroelectrochemical studies of anodic corrosion and film formation on iron in phosphate solutions. *Electrochim. Acta* **1989**, *34* (2), 281-286.

Miranda, M. L.; Kim, D.; Galeano, M. A. O.; Paul, C. J.; Hull, A. P.; Morgan, S. P. The relationship between early childhood blood lead levels and performance on end-of grade tests. *Environ. Health Perspect.* **2007**, *115* (8), 1242−1247.

MPIF Standard 42. Determination of density of compacted or sintered metal powder products. In *Standard test methods for metal powders and powder metallurgy products*; Metal Powder Industries Federation: Princeton, NJ, 2000.

Muylwyk, Q.; Gilks, J.; Suffoletta, V.; Olesiuk, J. Lead occurrence and the impact of LSL replacement in a well buffered groundwater. In *Proceedings of the 2009 AWWA Water Quality Technology Conference*; AWWA, 2009.

Navas-Acien, A.; Guallar, E.; Silbergeld, E. K.; Rothenberg, S. J. Lead exposure and cardiovascular disease—a systematic review. *Environ. Health Perspect.* **2007**, *115* (3), 472-482.

Nelson, Y. M.; Lion, L. W.; Shuler, M. L.; Ghiorse, W. C. Effect of oxide formation mechanisms on lead adsorption by biogenic manganese (hydr) oxides, iron (hydr) oxides, and their mixtures. *Environ. Sci. Technol.* **2002**, *36* (3), 421-425.

Nguyen, C. K.; Clark, B. N.; Stone, K. R.; Edwards, M. A. Role of chloride, sulfate, and alkalinity on galvanic lead corrosion. *Corrosion* **2011**, *67* (6), 065005-1−065005-9.

Nguyen, C. K.; Stone, K. R.; Dudi, A.; Edwards, M. A. Corrosive microenvironments at lead solder surfaces arising from galvanic corrosion with copper pipe. *Environ. Sci. Technol.* **2010**, *44* (18), 7076-7081.

Nguyen, C. K.; Stone, K. R.; Edwards, M. A. Chloride-to-sulfate mass ratio: practical studies in galvanic corrosion of lead solder. *J. Am. Water Works Assoc.* **2011**, *103* (1), 81-92.

Nigg, J. T.; Knottnerus, G. M.; Martel, M. M.; Nikolas, M.; Cavanagh, K.; Karmaus, W.; Rappley, M. D. Low blood lead levels associated with clinically diagnosed attention-deficit/hyperactivity disorder and mediated by weak cognitive control. *Biol. Psychiatry* **2008**, *63* (3), 325-331.

Noel, J. D.; Wang, Y.; Giammar, D. E. Effect of water chemistry on the dissolution rate of the lead corrosion product hydrocerussite. *Water Res.* **2014**, *54*, 237-246.

Owen, D. M.; Chowdhury, Z. K.; Summers, R. S.; Hooper, S. M.; Solarik, G.; Gray, K. *Removal of DBP precursors by GAC adsorption*; AWWA Research Foundation: USA, 1998.

Peabody, A.W., Bianchetti, R.L., Eds. *Peabody's control of pipeline corrosion*, 2nd ed.; NACE International: Houston, 2001.

Peng, C. Y., Korshin, G. V., Valentine, R. L., Hill, A. S., Friedman, M. J., Reiber, S. H. Characterization of elemental and structural composition of corrosion scales and deposits formed in drinking water distribution systems. *Water Res.* **2010**, *44* (15), 4570-4580.

Pieper, K. J.; Tang, M.; Edwards, M. A. Flint water crisis caused by interrupted corrosion control: investigating "ground zero" home. *Environ. Sci. Technol.* **2017**, *51* (4), 2007-2014.

Pokrovsky, O. S.; Schott, J.; Dupré, B. Trace element fractionation and transport in boreal rivers and soil porewaters of permafrost-dominated basaltic terrain in Central Siberia. *Geochim. Cosmochim. Acta* **2006**, *70* (13), 3239-3260.

R: A language and environment for statistical computing; R Foundation for Statistical Computing: Vienna, Austria, 2014; https://www.r-project.org/.

Rahman, M. S.; Gagnon, G. A. Bench-scale evaluation of drinking water treatment parameters on iron particles and water quality. *Water Res.* **2014**, *48*, 137-147.

Rahman, M. S.; Whalen, M.; Gagnon, G. A. Adsorption of dissolved organic matter (DOM) onto the synthetic iron pipe corrosion scales (goethite and magnetite): Effect of pH. *Chem. Eng. J.* **2013**, *234*, 149-157.

Rahman, M. S.; Whalen, M.; Gagnon, G. A. Adsorption of dissolved organic matter (DOM) onto the synthetic iron pipe corrosion scales (goethite and magnetite): effect of pH. *Chem. Eng. J.* **2013**, *234*, 149–157.

Ramaley, B.L. Monitoring and control experience under the lead and copper rule. *J. Am. Water Works Assoc.* **1993**, *85* (2), 64-67.

Reiber, S. H. Copper plumbing surfaces: an electrochemical study. *J. Am. Water Works Assoc.* **1989**, *81* (7), 114-122.

Reuben, A.; Caspi, A.; Belsky, D. W.; Broadbent, J.; Harrington, H.; Sugden, K.; Houts, R. M.; Ramrakha, S.; Poulton, R.; Moffitt, T. E. Association of Childhood Blood Lead Levels With Cognitive Function and Socioeconomic Status at Age 38 Years and With IQ Change and Socioeconomic Mobility Between Childhood and Adulthood. *J. Am. Med. Assoc.* **2017**, *317* (12), 1244-1251.

Richards, W. N.; Moore, M. R. Lead hazard controlled in Scottish water systems. *J. Am. Water Works Assoc.* **1984**, *76* (8), 60-67.

Roberge, P.R. *Corrosion inspection and monitoring*; John Wiley & Sons: Hoboken, New Jersey, 2007.

Rodda, D. P.; Johnson, B. B.; Wells, J. D. The effect of temperature and pH on the adsorption of copper (II), lead (II), and zinc (II) onto goethite. *J. Colloid Interface Sci.* **1993**, *161* (1), 57−62.

Rottmann, L.; Heumann, K. G. Determination of heavy metal interactions with dissolved organic materials in natural aquatic systems by coupling a high-performance liquid chromatography system with an inductively coupled plasma mass spectrometer. *Anal. Chem.* **1994**, *66* (21), 3709-3715.

Sander, S.; Mosley, L. M.; Hunter, K. A. Investigation of interparticle forces in natural waters: Effects of adsorbed humic acids on iron oxide and alumina surface properties. *Environ. Sci. Technol.* **2004**, *38* (18), 4791-4796.

Sandvig, A.; Kwan, P.; Kirmeyer, G.; Maynard, B.; Mast, D.; Trussell, R.; Trussell, S.; Cantor, A. F.; Prescott, A. *Contribution of Service Line and Plumbing Fixtures to Lead and Copper Rule Compliance Issues, 91229*; American Water Works Association Research Foundation and U.S. Environmental Protection Agency: Denver, CO, 2008.

Sarin, P.; Clement, J. A.; Snoeyink, V. L.; Kriven, W. M. Iron release from corroded, unlined cast-iron pipe. *J. Am. Water Works Assoc.* **2003**, *95* (11), 85-96.

Sarin, P.; Snoeyink, V. L.; Bebee, J.; Jim, K. K.; Beckett, M. A.; Kriven, W. M.; Clement, J. A. Iron release from corroded iron pipes in drinking water distribution systems: effect of dissolved oxygen. *Water Res.* **2004**, *38* (5), 1259-1269.

Sarin, P.; Snoeyink, V. L.; Bebee, J.; Kriven, W. M.; Clement, J. A. Physico-chemical characteristics of corrosion scales in old iron pipes. *Water Res.* **2001**, *35* (12), 2961-2969.

Schaumlöffel, D.; Ouerdane, L.; Bouyssiere, B.; Łobiński, R. Speciation analysis of nickel in the latex of a hyperaccumulating tree *Sebertia acuminata* by HPLC and CZE with ICP MS and electrospray MS-MS detection. *J. Anal. At. Spectrom.* **2003**, *18* (2), 120-127.

Schmitt, D.; Müller, M. B.; Frimmel, F. H. Metal distribution in different size fractions of natural organic matter. *Acta Hydroch. Hydrob.* **2001**, *28* (7), 400-410.

Schneider, O. D.; LeChevallier, M. W.; Reed, H. F.; Corson, M. J. A comparison of zinc and nonzinc orthophosphate-based corrosion control. *J. Am. Water Works Assoc.* **2007**, *99* (11), 103-113.

Schock, M. R. Causes of temporal variability of lead in domestic plumbing systems. *Environ. Monit. Assess.* **1990**, *15* (1), 59-82.

Schock, M. R. Understanding corrosion control strategies for lead. *J. Am. Water Works Assoc.* **1989**, *81* (7), 88−100.

Schock, M. R.; Cantor, A. F.; Triantafyllidou, S.; Desantis, M. K.; Scheckel, K. G. Importance of pipe deposits to Lead and Copper Rule compliance. *J. Am. Water Works Assoc.* **2014**, *106* (7), E336−E349.

Schock, M. R.; Hyland, R. N.; Welch, M. M. Occurrence of contaminant accumulation in lead pipe scales from domestic drinking water distribution systems. *Environ. Sci. Technol.* **2008**, *42* (12), 4285−4291.

Schock, M. R.; Neff, C. H. Trace metal contamination from brass fittings. *J. Am. Water Works Assoc.* **1988**, *80* (11), 47-56.

Schock, M. R.; Sandvig, A. M. Long-term effects of orthophosphate treatment on copper concentration. *J. Am. Water Works Assoc.* **2009**, *101* (7), 71-82.

Schock, M. R.; Wagner, I.; Oliphant, R. J. Corrosion and solubility of lead in drinking water. In *Internal corrosion of water distribution systems*; AWWA Research Foundation: Denver, CO, 1996; pp. 131-230.

Science Advisory Board Evaluation of the Effectiveness of Partial Lead Service Line Replacements; EPA-SAB-11e015; US Environmental Protection Agency (US EPA): Washington, DC, 2011; https://www.epa.gov/sites/production/files/2015-09/documents/sab_evaluation_partial_lead_service_lines_epa-sab-11-015.pdf.

Senftle, F. E.; Thorpe, A. N.; Grant, J. R.; Barkatt, A. Superparamagnetic nanoparticles in tap water. *Water Res.* **2007**, *41* (13), 3005-3011.

Shih, R. A.; Hu, H.; Weisskopf, M. G.; Schwartz, B. S. Cumulative lead dose and cognitive function in adults: a review of studies that measured both blood lead and bone lead. *Environ. Health Perspect.* **2007**, *115* (3), 483-492.

Stansbury, E.E.; Buchanan, R.A. *Fundamentals of electrochemical corrosion*; ASM International: Ohio, 2000.

Stoddart, A.K.; Gagnon, G.A. Full-scale pre-chlorine removal: impact on filter performance and water quality. *J. Am. Water Works Assoc.* **2015**, *107* (12), E638-E647.

Svensson, U.; Dreybrodt, W. Dissolution kinetics of natural calcite minerals in CO2-water systems approaching calcite equilibrium. *Chem. Geol.* **1992** *100* (1-2), 129-145.

Swertfeger, J.; Hartman, D. J.; Shrive, C.; Metz, D. H.; DeMarco, J. Water quality effects of partial lead line replacement. In *Proceedings of the 2006 AWWA Annual Conference*; AWWA, 2006.

Triantafyllidou, S.; Edwards, M. Galvanic corrosion after simulated small-scale partial lead service line replacements. *J. Am. Water Works Assoc.* **2011**, *103* (9), 85−99.

Triantafyllidou, S.; Edwards, M. Lead (Pb) in tap water and in blood: implications for lead exposure in the United States. *Crit. Rev. Environ. Sci. Technol.* **2012**, *42* (13), 1297−1352.

Triantafyllidou, S.; Schock, M. R.; DeSantis, M. K.; White, C. Low contribution of PbO_2-coated lead service lines to water lead contamination at the tap. *Environ. Sci. Technol.* **2015**, *49* (6), 3746−3754.

Trueman, B. F.; Camara, E.; Gagnon, G. A. Evaluating the effects of full and partial lead service line replacement on lead levels in drinking water. *Environ. Sci. Technol.* **2016**, *50* (14), 7389-7396.

Trueman, B. F.; Gagnon, G. A. A new analytical approach to understanding nanoscale lead-iron interactions in drinking water distribution systems. *J. Hazard. Mater.* **2016**, *311*, 151-157.

Trueman, B. F.; Gagnon, G. A. Understanding the role of particulate iron in lead release to drinking water. *Environ. Sci. Technol.* **2016**, *50* (17), 9053-9060.

Trueman, B.F.; Sweet, G.A.; Harding, M.D.; Estabrook, H.; Bishop, D.P.; Gagnon, G.A. Galvanic corrosion of lead by iron (oxyhydr)oxides: potential impacts on drinking water quality. *Environ. Sci. Technol.* **2017**, *51* (12), 6812–6820.

U.S. EPA SW-846 Test Method 3050B: Acid Digestion of Sediments, Sludges, and Soils. https://www.epa.gov/sites/production/files/2015-12/documents/3050b.pdf

Vadasarukkai, Y. S.; Gagnon, G. A. Application of low-mixing energy input for the coagulation process. *Water Res.* **2015**, *84*, 333-341.

Vago, E. R.; Calvo, E. J. Electrocatalysis of oxygen reduction at Fe_3O_4 oxide electrodes in alkaline solutions. *J. Electroanal. Chem.* **1992**, *339*, 41−67.

Vago, E. R.; Calvo, E. J.; Stratmann, M. Electrocatalysis of oxygen reduction at well-defined iron oxide electrodes. *Electrochim. Acta* **1994**, *39* (11), 1655-1659.

Veselý, J.; Majer, V.; Kučera, J.; Havránek, V. Solid–water partitioning of elements in Czech freshwaters. *Appl. Geochem.* **2001**, *16* (4), 437-450.

Violante, A.; Ricciardella, M.; Pigna, M. Adsorption of heavy metals on mixed Fe-Al oxides in the absence or presence of organic ligands. *Water Air Soil Poll.* **2003**, *145*, 289-306.

Vogl, J.; Heumann, K. G. Determination of heavy metal complexes with humic substances by HPLC/ICP-MS coupling using on-line isotope dilution technique. *Fresenius. J. Anal. Chem.* **1997**, *359* (4-5), 438-441.

Vu, H. P.; Shaw, S.; Brinza, L.; Benning, L. G. Partitioning of Pb (II) during goethite and hematite crystallization: Implications for Pb transport in natural systems. *Appl. Geochem.* **2013**, *39*, 119-128.

Wang, Y.; Jing, H.; Mehta, V.; Welter, G. J.; Giammar, D. E. Impact of galvanic corrosion on lead release from aged lead service lines. *Water Res.* **2012**, *46* (16), 5049-5060.

Wang, Y.; Jing, H.; Mehta, V.; Welter, G.J.; Giammar, D.E. Impact of galvanic corrosion on lead release from aged lead service lines. *Water Res.* **2012**, *46*, 5049-5060.

Wang, Y.; Mehta, V.; Welter, G. J.; Giammar, D. E. Effect of connection methods on lead release from galvanic corrosion. *J. Am. Water Works Assoc.* **2013**, *105* (7), E337-E351.

Watt, G. C. M.; Britton, A.; Gilmour, H. G.; Moore, M. R.; Murray, G. D.; Robertson, S. J. Public health implications of new guidelines for lead in drinking water: a case study in an area with historically high water lead levels. *Food Chem. Toxicol.* **2000**, *38*, S73−S79.

Watt, G. C.; Britton, A.; Gilmour, W. H.; Moore, M. R.; Murray, G. D.; Robertson, S. J.; Womersley, J. Is lead in tap water still a public health problem? An observational study in Glasgow. *Br. Med. J.* **1996**, *313* (7063), 979−981.

Weng, L.; Temminghoff, E. J.; Lofts, S.; Tipping, E.; Van Riemsdijk, W. H. Complexation with dissolved organic matter and solubility control of heavy metals in a sandy soil. *Environ. Sci. Technol.* **2002**, *36* (22), 4804-4810.

Wilhelm, S.M. Galvanic corrosion caused by corrosion products. In *Galvanic Corrosion.* ASTM STP 978. Hack, H.P., Ed.; American Society for Testing and Materials: Philadelphia, 1988.

Winning, L. D.; Gorczyca, B.; Brezinski, K. Effect of total organic carbon and aquatic humic substances on the occurrence of lead at the tap. *Water Qual. Res. J.* **2017**, *52* (1), 2-10.

Woszczynski, M.; Bergese, J.; Gagnon, G. A. Comparison of chlorine and chloramines on lead release from copper pipe rigs. *J. Environ. Eng- ASCE*. **2013**, *139* (8), 1099-1107.

Xia, K.; Bleam, W.; Helmke, P. A. Studies of the nature of Cu^{2+} and Pb^{2+} binding sites in soil humic substances using X-ray absorption spectroscopy. *Geochim. Cosmochim. Acta* **1997**, *61*(11), 2211-2221.

Xie, L.; Giammar, D. E. Equilibrium solubility and dissolution rate of the lead phosphate chloropyromorphite. *Environ. Sci. Technol.* **2007**, *41*, 8050–8055.

Xie, Y.; Giammar, D. E. Effects of flow and water chemistry on lead release rates from pipe scales. *Water Res.* **2011**, *45*, 6525-6534.

Xu, Y.; Thipnakarin, B.; Lisa, A.; Sungmin, M.; Trevor, T. Surface complexation of Pb (II) on amorphous iron oxide and manganese oxide: spectroscopic and time studies. *J. Colloid Interf. Sci.* **2006**, *299*, 28-40.

Yang, F.; Shi, B.; Gu, J.; Wang, D.; Yang, M. Morphological and physicochemical characteristics of iron corrosion scales formed under different water source histories in a drinking water distribution system. *Water Res.* **2012**, *46*, 5423-5433.

Zhang, Y.; Chen, Y.; Westerhoff, P.; Crittenden, J. Impact of natural organic matter and divalent cations on the stability of aqueous nanoparticles. *Water Res.* **2009**, *43* (17), 4249-4257.

Appendix A: Supporting Data For Chapter 2

Table 10 Slopes and R^2 values for separate regressions of total lead release on 5 min. flushed sample temperature for sites A and B (Figure 3).

	Site A		Site B	
Profile litre	Slope (µg L^{-1} °C^{-1})	R-squared	Slope (µg L^{-1} °C^{-1})	R-squared
1	0.82	0.81	0.25	0.72
2	0.81	0.72	0.32	0.89
3	0.79[a]	0.59	0.33	0.81
4	1.21[a]	0.72	0.34	0.84
5	1.18[a]	0.74	0.34	0.85
6	1.13[a]	0.71	0.36	0.77
7	0.95[a]	0.46	0.31	0.82
8	1.48[a]	0.76	0.32	0.84
9	1.36[a]	0.90	0.61[a]	0.74
10	0.85	0.91	0.99[a]	0.69
11	0.71	0.94	1.07[a]	0.71
12	0.68	0.91	1.06[a]	0.72
13 (flushed)	0.72	0.98	0.33	0.89

[a]profile litres with apparent LSL contact during stagnation, based on lead and copper levels

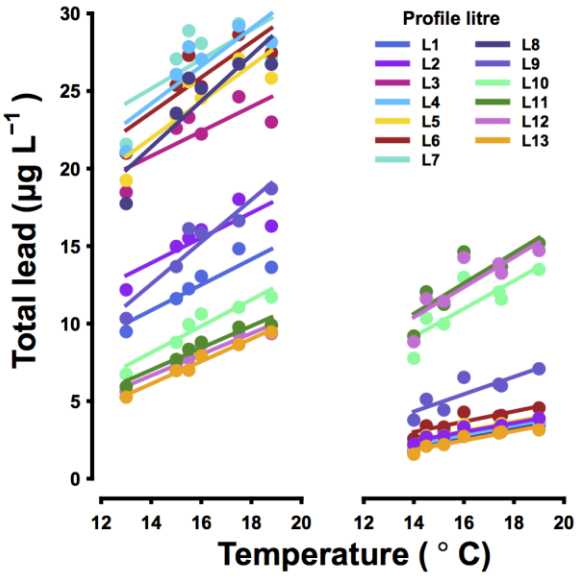

Figure 36 Total lead release over a 13 × 1L sample profile (sites A and B, left and right panels respectively) as a function of 5-min. flushed sample temperature. For a given profile liter, temperature explained 46 – 98% of variation in lead release (79% on average).

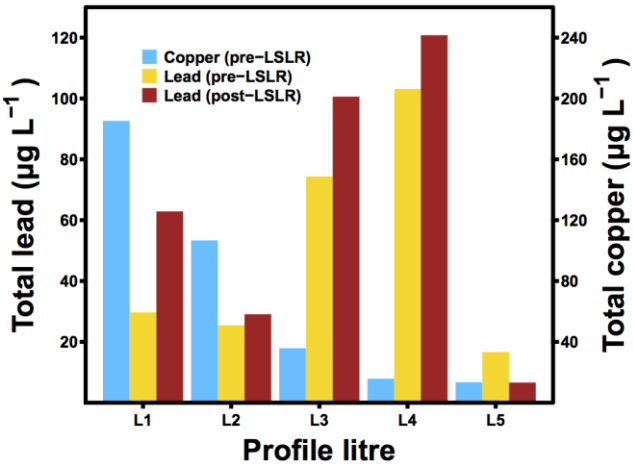

Figure 37 Lead and copper levels pre-LSLR and lead levels 3 months after partial LSLR. Based on lead and copper levels pre-replacement, L3-4 appear to have contacted the LSL during stagnation. Despite a drop in water temperature from August to December, L3-4 lead levels at the 3-month follow-up are still elevated above their pre-replacement counterparts.

Sampling instructions provided to residents.

Preparation

Do not use any water in your house for at least 6 hours before collecting water samples. The period of no water use should be no longer than 24 hours. Since 6 hours of no water use is required, the best time for collecting water samples is usually first thing in the morning or upon returning home at the end of the work day. No water use for at least 6 hours is required to ensure that concentrations of lead reflect worse case stagnation conditions and to ensure that any possible lead occurrence in your home can be accurately identified.

No Water Use: NO running taps, flushing toilets, showering, dishwashing, laundry or any other household water use. Be sure appliances, such as icemakers, lawn sprinkler systems and HVAC humidifiers, are shut off.

Following 6 hours of no water use, water samples will be collected from the kitchen COLD water tap. All samples must be collected from the same faucet. If a water treatment unit or filter is attached to your plumbing system or faucet, remove or bypass this system before sampling. If this is not possible, collect the water sample from a bathroom or other cold water tap.

If, for any given reason, water has been used in your home within the past 6 hours, please do not proceed with the sampling procedure below. Please wait to collect samples at a time when water has been allowed to sit for at least 6 hours.

1. Write the date and time you last used any water in your home.

   Date: _____ Time: _____

Sampling Instructions

Sample Bottles 1, 2, 3 and 4

1. Locate sample bottles 1, 2, 3 and 4. Remove the caps and arrange the bottles in sequence from 1 through 4 on the counter near the sink, taking care to place the caps on a clean surface to avoid sample contamination.
2. Hold bottle 1 under the cold water faucet. Open the cold water tap and begin to fill bottle 1.
3. When bottle 1 is filled approximately 1cm from top, remove it from the flow and quickly replace it with bottle 2, without adjusting the faucet.
4. Repeat Step 3 for bottles 3 and 4.
5. After collecting the bottle 4 sample, immediately turn off the cold water tap and tightly cap all 4 of the sample bottles.
6. Note the date, time and faucet location below and then proceed to the sampling procedure for bottle 5.

Date: _____ Time: _____ Faucet Location: _____

Sample Bottle 5

1. Open the cold water faucet fully and allow water to flow for a minimum of 5 minutes. Hold bottle 5 under the faucet until it is completely filled, and then cap.
2. Note the date, time and faucet location below.

Date: _____ Time: _____ Faucet Location: _____

Please take a few minutes to fill out all fields on each sample bottle label: Collection Date, Collection Time, Collector (your name).

Appendix B: Supporting Data For Chapter 3

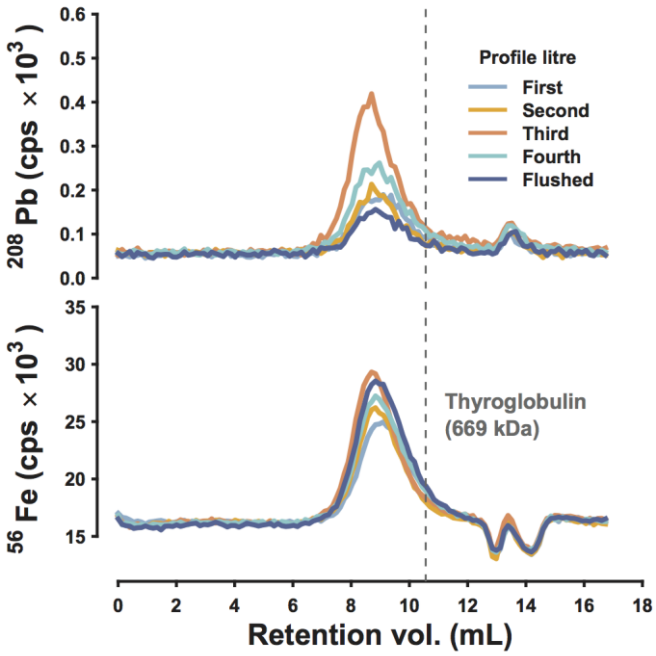

Figure 38 ^{208}Pb and ^{56}Fe chromatograms for a 5 × 1L point-of-use sample profile, collected 3 days after full lead service line replacement and separated on polymethacrylate. Iron and lead in 0.45 µm filtrate ranged from 28.0 – 39.0 and < 0.4 – 0.7 µg L^{-1}, respectively.

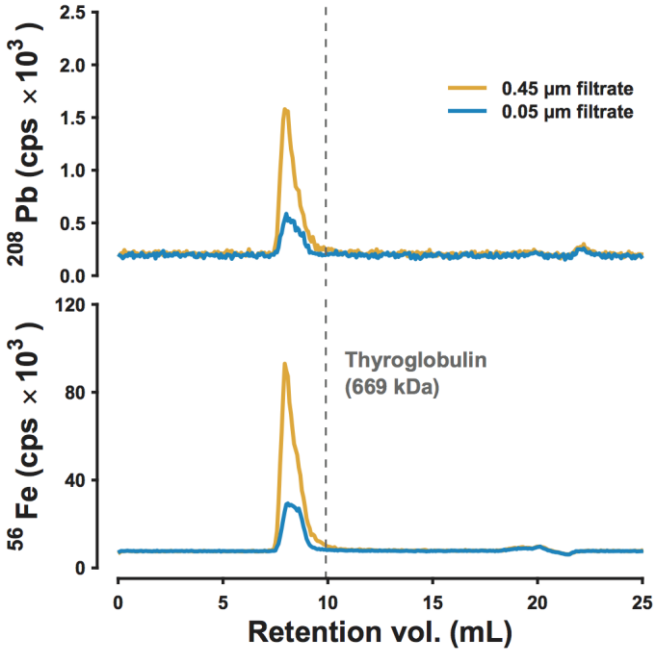

Figure 39 ^{208}Pb and ^{56}Fe chromatograms representing a distributed water sample

Appendix C: Supporting Data For Chapter 4

Table 11 Medians (Med.) and interquartile ranges (IQR) for orthophosphate residual, free chlorine residual, and pH in LSL influent.

	Orthophosphate[a] (mg L^{-1} as PO_4^{3-})		Orthophosphate[b] (mg L^{-1} as PO_4^{3-})		Free chlorine (mg L^{-1} Cl_2)		pH	
Material	**Med.**	**IQR**	**Med.**	**IQR**	**Med.**	**IQR**	**Med.**	**IQR**
PVC	0.59	0.39, 0.80	1.04	0.91, 1.15	0.94	0.84, 1.14	7.44	7.16, 7.67
	0.49	0.28, 0.65	1.04	0.90, 1.15	0.98	0.83, 1.14	7.36	7.18, 7.64
Iron	0.56	0.46, 0.65	1.03	0.93, 1.17	0.98	0.82, 1.15	7.44	7.24, 7.62
	0.46	0.41, 0.62	1.03	0.89, 1.17	0.98	0.85, 1.13	7.44	7.25, 7.60

[a]baseline phase; [b]test phase

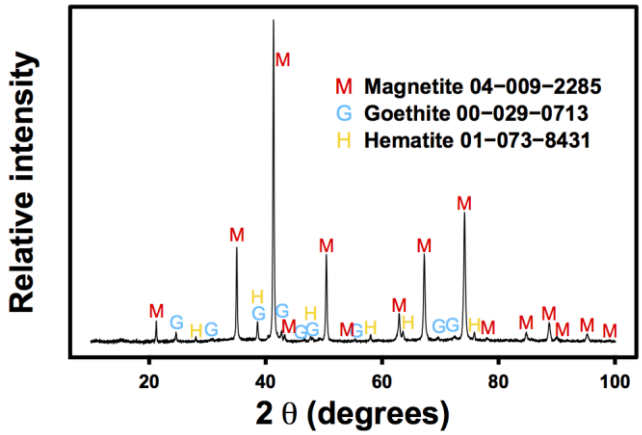

Figure 40 X-ray diffraction pattern for magnetite (Fe_3O_4) powder (pre-densification). Peaks associated with magnetite, as well as trace secondary phases goethite (α-FeOOH) and hematite (α-Fe_2O_3), are labelled (ICDD PDF numbers are provided for each phase).

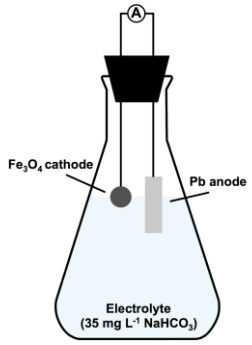

Figure 41 Simplified diagram of a galvanic cell.

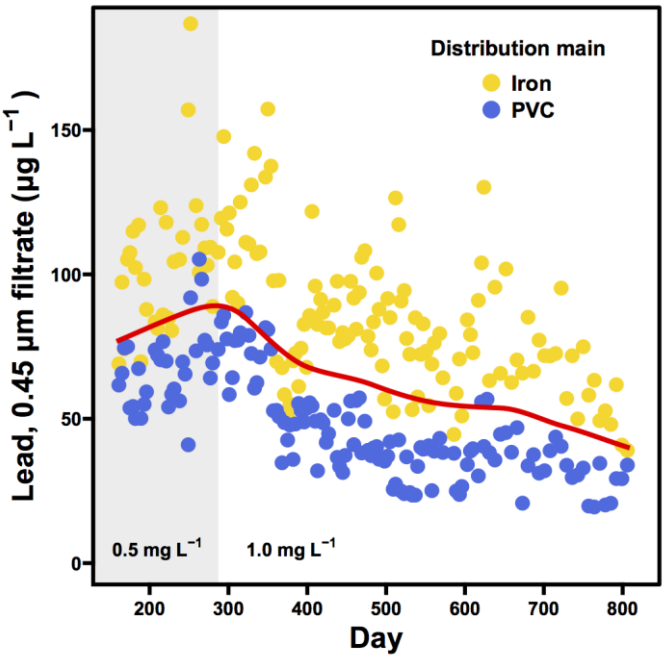

Figure 42 Mean lead in LSL effluent (N = 145 per section), aggregated at each point in time by distribution main material. Orthophosphate doses (0.5 and 1.0 mg L^{-1}) are separated by background shading, and a local linear smooth is superimposed to represent the overall trend.

Appendix D: Supporting Data For Chapter 5

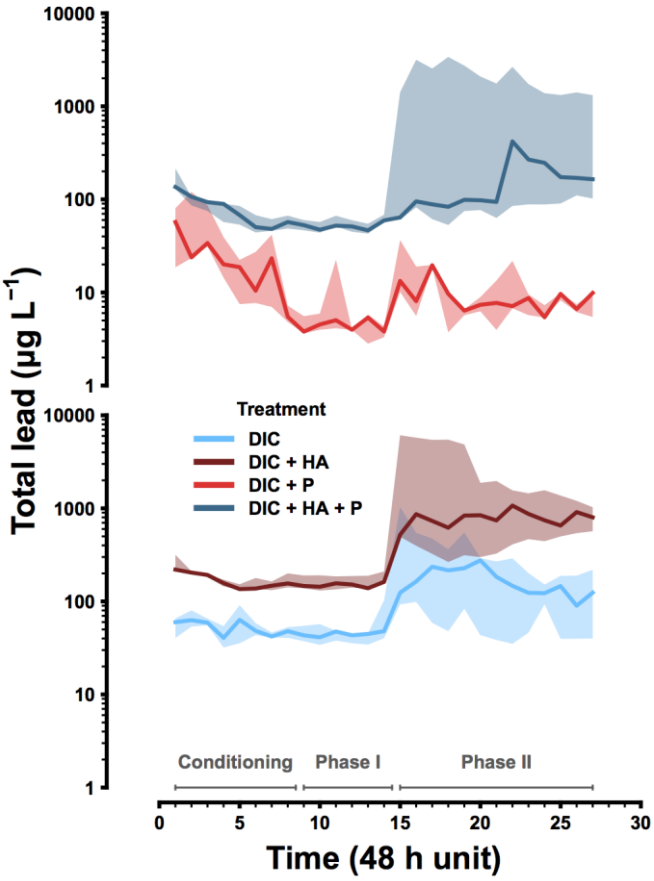

Figure 43 Median lead release from anodes over the conditioning phase and the two experimental phases (phases I and II); the error envelope represents the range in lead release from the triplicate cells with each electrolyte composition (DIC = dissolved inorganic carbon, HA = humic acid, P = orthophosphate).

Table 12 Linear model coefficients and p-values for effects on lead release over phase I alone (R^2 = 0.95).

Effect	Effect size (µg L^{-1})	P-value
Humic acid (HA)	81	**1.61e-05**
Orthophosphate (P)	-74	**3.06e-05**
HA:P interaction	-33	**0.0058**

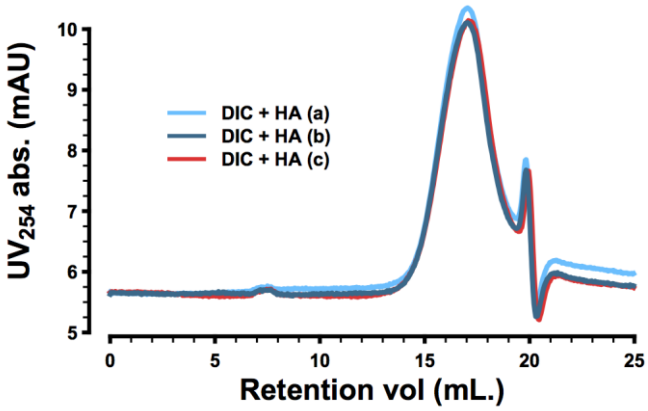

Figure 44 SEC-UV chromatograms representing 48 h effluent from triplicate galvanic cells dosed with humic acid and separated on agarose/dextran (DIC = dissolved inorganic carbon, HA = humic acid, a, b, and c are replicates).

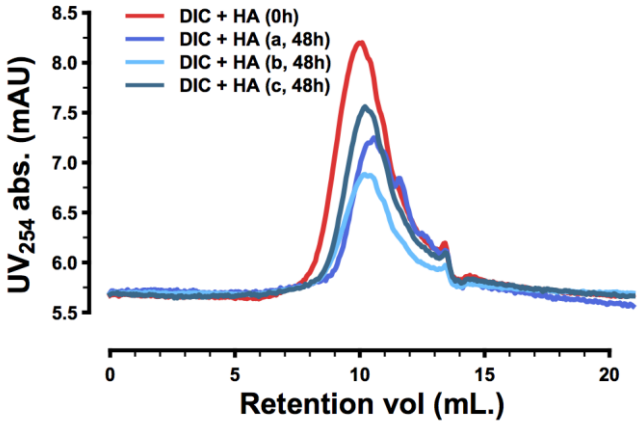

Figure 45 SEC chromatograms representing decreases in humic acid between 0 and 48 h during phase II (silica stationary phase, DIC = dissolved inorganic carbon, HA = humic acid, *a*,*b*, and *c* represent the three cathode materials).

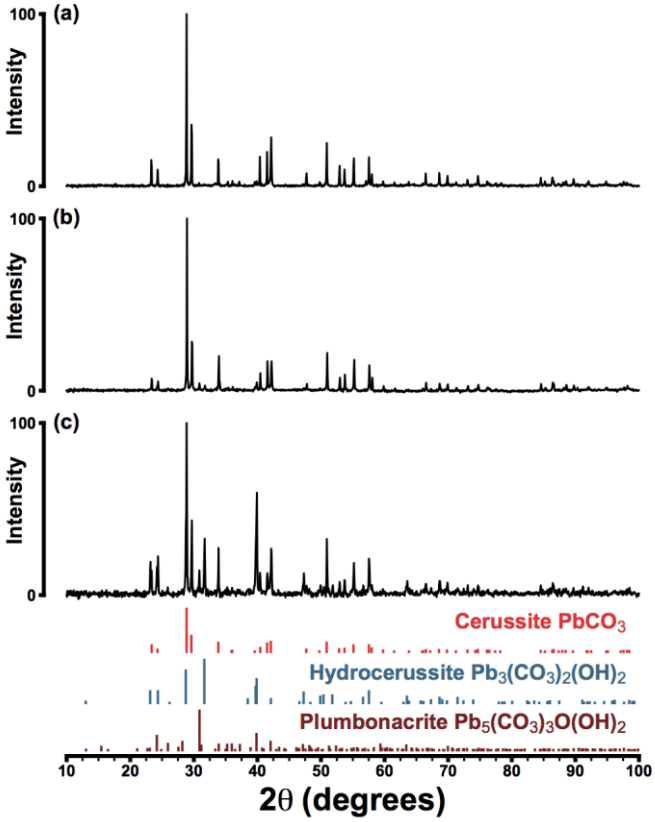

Figure 46 X-ray diffraction patterns for lead anodes exposed to dissolved inorganic carbon alone (panels a, b, and c represent sintered magnetite, sintered hematite, and field-extracted magnetite/goethite cathodes, respectively). Cerussite (ICDD PDF 00-047-1734), hydrocerussite (04-016-7055), and plumbonacrite (04-017-4336) standards are included.

Table 13 Linear model coefficients and p-values for effects on lead release over phase I and II together (R2 = 0.45).

Effect	Effect size (µg L^{-1})	P-value[a]
Humic acid (HA)	536	**3.99e-06**
Orthophosphate (P)	-245	**3.91e-05**
Iron oxyhydroxide (FeO*x*)	531	**0.000656**
HA:P interaction	-132	0.059284
HA:FeO*x* interaction	455	0.210304
P:FeO*x* interaction	-171	0.594378
HA:P:FeO*x* interaction	-99	0.720337

[a]p-values calculated for a log-transformed response variable, while effects were calculated on the untransformed response

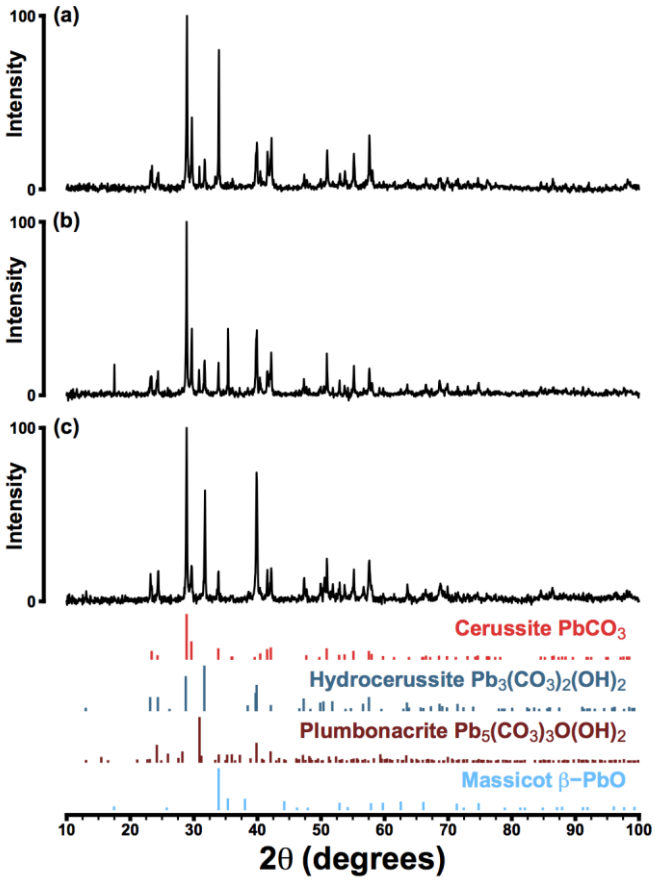

Figure 47 X-ray diffraction patterns for lead anodes exposed to dissolved inorganic carbon with humic acid (panels a,b, and c represent sintered magnetite, sintered hematite, and field-extracted magnetite/goethite cathodes, respectively). Cerussite (ICDD PDF 00-047-1734), hydrocerussite (04-016-7055), plumbonacrite (04-017-4336) and massicot (00-038-1477) standards are included.

Table 14 Linear model coefficients and p-values for effects on lead release over phase II alone (R2 = 0.35).

Effect	Effect size (µg L^{-1})	P-value[a]
Humic acid (HA)	990	**0.00322**
Orthophosphate (P)	-416	**0.01390**
HA:P interaction	-230	0.25718

[a]p-values calculated for a log-transformed response variable, while effects were calculated on the untransformed response

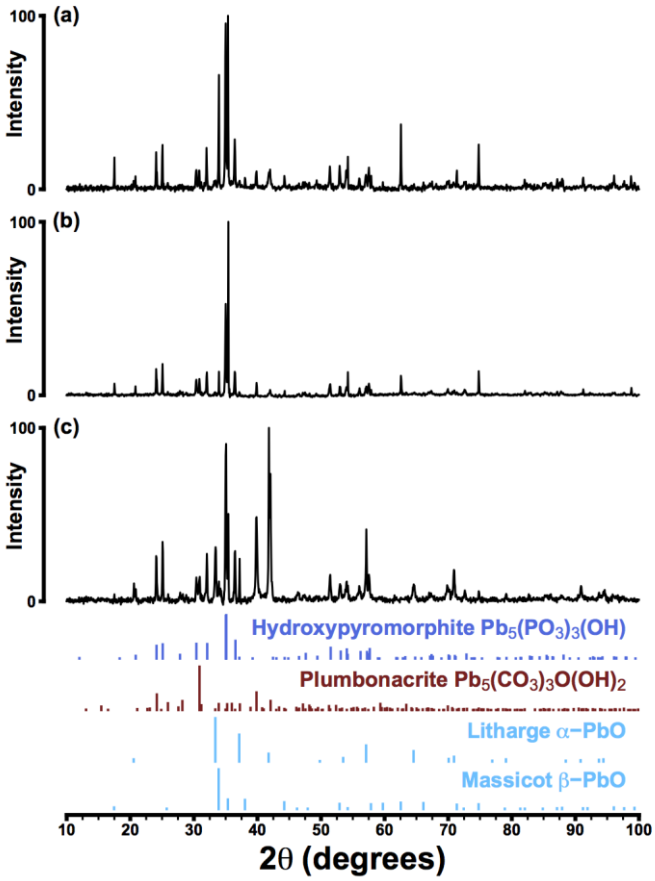

Figure 48 X-ray diffraction patterns for lead anodes exposed to dissolved inorganic carbon with orthophosphate (panels a,b, and c represent sintered magnetite, sintered hematite, and field-extracted magnetite/goethite cathodes, respectively). Hydroxypyromorphite (ICDD PDF 04-014-1328), plumbonacrite (04-017-4336) massicot (00-038-1477), and litharge (00-005-0561) standards are included.

Table 15 Linear model coefficients and p-values for effects on iron release over phase II alone (R^2 = 0.49).

Effect	Effect size (µg L^{-1})	P-value
Humic acid (HA)	85	**0.030304**
Orthophosphate (P)	11	0.742635
HA:P interaction	24	0.475054

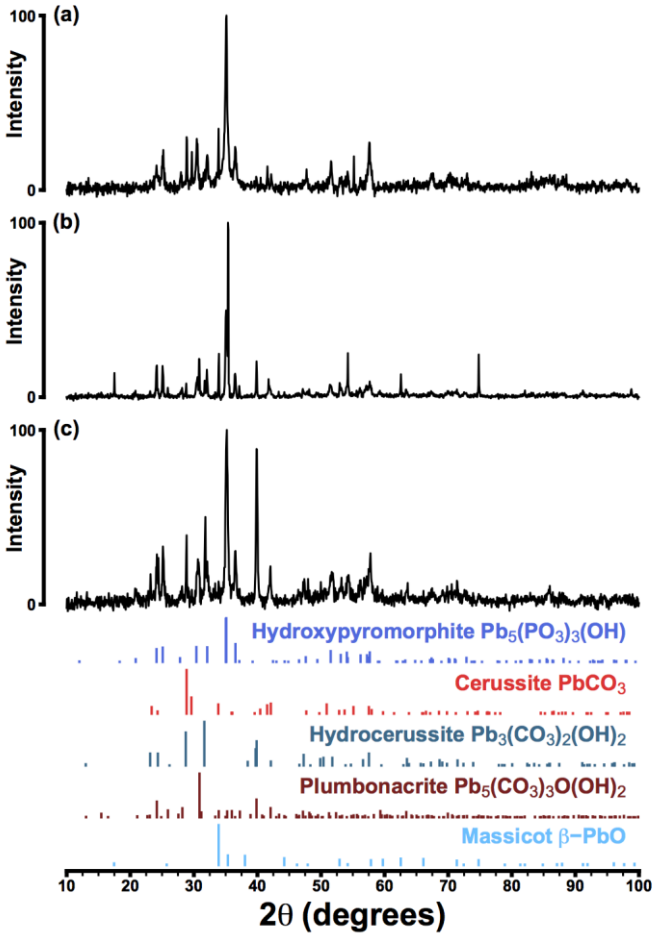

Figure 49 X-ray diffraction patterns for lead anodes exposed to dissolved inorganic carbon with orthophosphate and humic acid (panels a,b, and c represent sintered magnetite, sintered hematite, and field-extracted magnetite/goethite cathodes, respectively). Hydroxypyromorphite (ICDD PDF 04-014-1328), cerussite (00-047-1734), hydrocerussite (04-016-7055), plumbonacrite (04-017-4336) and massicot (00-038-1477) standards are included.

Appendix E: Copyright Permissions

Title: Evaluating the Effects of Full and Partial Lead Service Line Replacement on Lead Levels in Drinking Water

Author: Benjamin F. Trueman, Eliman Camara, Graham A. Gagnon

Publication: Environmental Science & Technology

Publisher: American Chemical Society

Date: Jul 1, 2016

LOGIN

If you're a copyright.com user, you can login to RightsLink using your copyright.com credentials. Already **a RightsLink user** or want to learn more?

PERMISSION/LICENSE IS GRANTED FOR YOUR ORDER AT NO CHARGE

This type of permission/license, instead of the standard Terms & Conditions, is sent to you because no fee is being charged for your order. Please note the following:

- Permission is granted for your request in both print and electronic formats, and translations.
- If figures and/or tables were requested, they may be adapted or used in part.
- Please print this page for your records and send a copy of it to your publisher/graduate school.
- Appropriate credit for the requested material should be given as follows: "Reprinted (adapted) with permission from (COMPLETE REFERENCE CITATION). Copyright (YEAR) American Chemical Society." Insert appropriate information in place of the capitalized words.
- One-time permission is granted only for the use specified in your request. No additional uses are granted (such as derivative works or other editions). For any other uses, please submit a new request.

BACK CLOSE WINDOW

ELSEVIER LICENSE
TERMS AND CONDITIONS

Aug 30, 2017

This Agreement between Mr. Benjamin Trueman ("You") and Elsevier ("Elsevier") consists of your license details and the terms and conditions provided by Elsevier and Copyright Clearance Center.

License Number	4178821007553
License date	Aug 30, 2017
Licensed Content Publisher	Elsevier
Licensed Content Publication	Journal of Hazardous Materials
Licensed Content Title	A new analytical approach to understanding nanoscale lead-iron interactions in drinking water distribution systems
Licensed Content Author	Benjamin F. Trueman,Graham A. Gagnon
Licensed Content Date	Jul 5, 2016
Licensed Content Volume	311
Licensed Content Issue	n/a
Licensed Content Pages	7
Start Page	151
End Page	157
Type of Use	reuse in a thesis/dissertation
Portion	full article
Format	both print and electronic
Are you the author of this Elsevier article?	Yes
Will you be translating?	No
Title of your thesis/dissertation	Controlling Lead Release To Drinking Water: Impacts Of Iron Oxides, Complexing Species, Orthophosphate, And Lead Pipe Replacement
Expected completion date	Dec 2017
Estimated size (number of pages)	150
Requestor Location	Mr. Benjamin Trueman 2-2118 Robie St. Halifax, NS B3K4M4 Canada Attn: Mr. Benjamin Trueman
Total	0.00 USD

Title: Understanding the Role of Particulate Iron in Lead Release to Drinking Water

Author: Benjamin F. Trueman, Graham A. Gagnon

Publication: Environmental Science & Technology

Publisher: American Chemical Society

Date: Sep 1, 2016

PERMISSION/LICENSE IS GRANTED FOR YOUR ORDER AT NO CHARGE

This type of permission/license, instead of the standard Terms & Conditions, is sent to you because no fee is being charged for your order. Please note the following:

- Permission is granted for your request in both print and electronic formats, and translations.
- If figures and/or tables were requested, they may be adapted or used in part.
- Please print this page for your records and send a copy of it to your publisher/graduate school.
- Appropriate credit for the requested material should be given as follows: "Reprinted (adapted) with permission from (COMPLETE REFERENCE CITATION). Copyright (YEAR) American Chemical Society." Insert appropriate information in place of the capitalized words.
- One-time permission is granted only for the use specified in your request. No additional uses are granted (such as derivative works or other editions). For any other uses, please submit a new request.

BACK CLOSE WINDOW

Dr. Trueman,

Your permission requested is granted and there is no fee for this reuse. In your planned reuse, you must cite the ACS article as the source, add this direct link <http://pubs.acs.org/doi/abs/10.1021/acs.est.7b01671>, and include a notice to readers that further permissions related to the material excerpted should be dire

If you need further assistance, please let me know.

Jawwad Saeed

ACS Customer Services & Information

https://help.acs.org

Your help request has been resolved. If you have further issues regarding this matter, please let us know by responding to this email. Please note that this request will auto-close in 14 days. If you need to contact us after 14 days regarding this matter please submit a new help request and refer to this help request number.

How are we doing? Let us know!
Please click on your selection below to begin our two-question survey.

Based on this support interaction, how satisfied were you with the help provided?

Not at all satisfied *Completely satisfied*

0 1 2 3 4 5 6 7 8 9 10

E-mail Information:

Attachments

cc bn767932@dal.ca

Request Information:

Request # 9131-7748509

Date Created 8/30/2017 10:03 AM EDT

Summary FW: thesis reproduction of ES&T author's choice manuscript

From: Benjamin Trueman [mailto:bn767932@dal.ca]

Sent: Wednesday, August 30, 2017 10:02 AM
To: Darla Henderson <D_Henderson@acs.org>
Subject: thesis reproduction of ES&T author's choice manuscript

Dear Dr. Henderson,

I am preparing my PhD thesis for submission to the Faculty of Graduate Studies at Dalhousie University, Halifax, Nova Scotia, Canada. I am seeking your permission to include a manuscript version of the following Author's Choice paper as a chapter in the thesis:

Trueman, B.F.; Sweet, G.A.; Harding, M.D.; Estabrook, H.; Bishop, D.P.; Gagnon, G.A. Galvanic corrosion of lead by iron (oxyhydr)oxides: potential impacts on drinking water quality. Environ. Sci. Technol. 2017, 51 (12), 6812–6820.

http://pubs.acs.org/doi/abs/10.1021/acs.est.7b01671

Details GALVANIC
CORROSION OF LEAD BY IRON (OXYHYDR)OXIDES ...

pubs.acs.org

galvanic corrosion of lead by iron (oxyhydr)oxides: potential impacts on drinking water quality

Canadian graduate theses are reproduced by the Library and Archives of Canada (formerly National Library of Canada) through a non-exclusive, world-wide license to reproduce, loan, distribute, or sell theses. I am also seeking your permission for the material described above to be reproduced and distributed by the LAC(NLC). Further details about the LAC(NLC) thesis program are available on the LAC(NLC) website (http://www.nlc-bnc.ca). Full publication details and a copy of this permission letter will be included in the thesis.

I would appreciate it if you could include the following in your reply:

Permission is granted for: a) the inclusion of the material described above in your thesis. b) for the material described above to be included in the copy of your thesis that is sent to the Library and Archives of Canada (formerly National Library of Canada) for reproduction and distribution.

Sincerely,
Benjamin Trueman